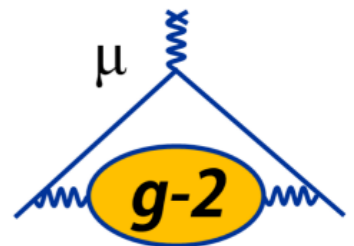




# Experimental Review of Muon $g-2$

Esra Barlas-Yucel  
 on behalf of the Muon  $g-2$  Collaboration  
 FPCP - University of Mississippi  
 25 May 2022

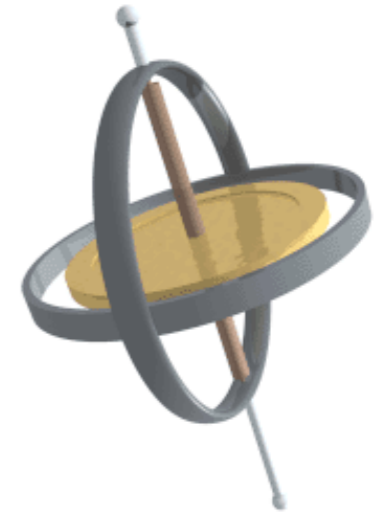


# Muon Magnetic Moment and Defining the Anomaly

## Magnetic Moment of Muon

$$\vec{\mu} = g_{\mu} \frac{e}{2m} \vec{s}$$

$g$ : Proportionality constant between spin and magnetic moment



## Anomalous Magnetic Moment of Muon

$$a_{\mu} = \frac{g_{\mu} - 2}{2}, \quad \vec{\mu} = (1 + a_{\mu}) \frac{e}{m} \vec{s}$$



Shows how much  $g$  differs fractionally from 2!

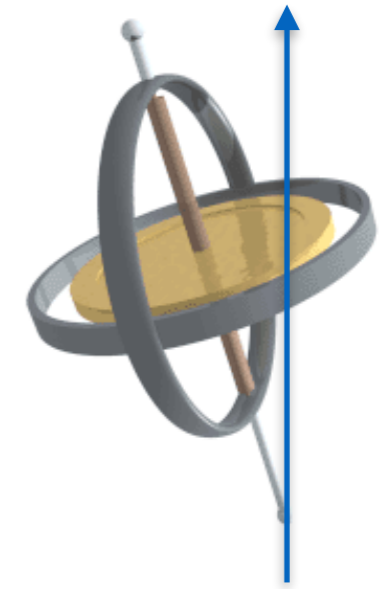
Measuring this anomaly could tell us if there are new particles or even forces that contribute to  $a_{\mu}$

# Muon Magnetic Moment and Defining the Anomaly

## Magnetic Moment of Muon

$$\vec{\mu} = g_{\mu} \frac{e}{2m} \vec{s}$$

$g$ : Proportionality constant between spin and magnetic moment



Magnetic Field

## Anomalous Magnetic Moment of Muon

$$a_{\mu} = \frac{g_{\mu} - 2}{2}, \quad \vec{\mu} = (1 + a_{\mu}) \frac{e}{m} \vec{s}$$



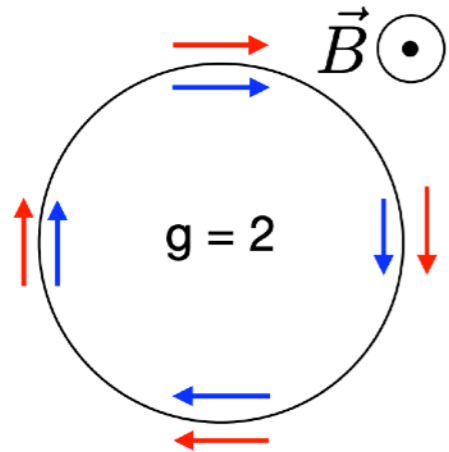
Shows how much  $g$  differs fractionally from 2!

Measuring this anomaly could tell us if there are new particles or even forces that contribute to  $a_{\mu}$

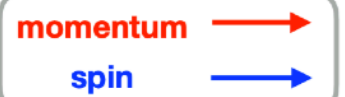
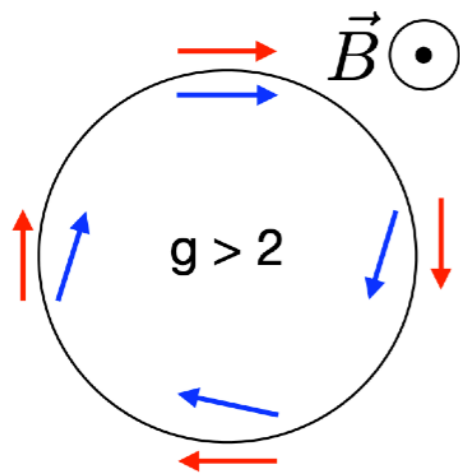
# Muon Magnetic Moment and Measuring the Anomaly

polarized muons in a magnetic field

$$\text{If } g = 2 \Rightarrow \vec{\omega}_a = 0$$



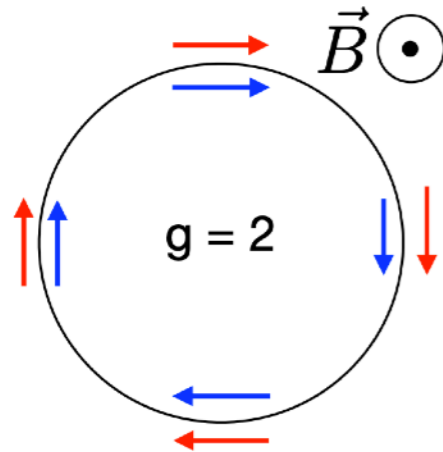
$$g \neq 2 \Rightarrow \vec{\omega}_a \cong a_\mu \frac{e}{m} \vec{B}$$



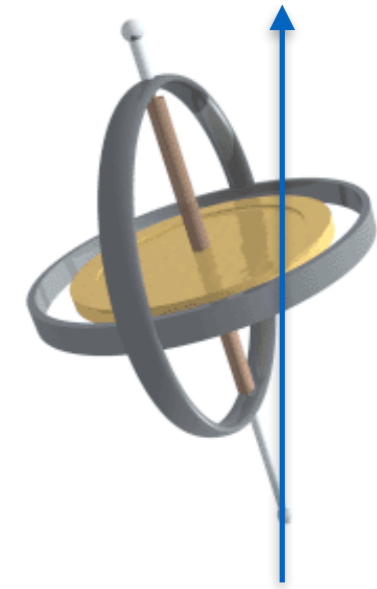
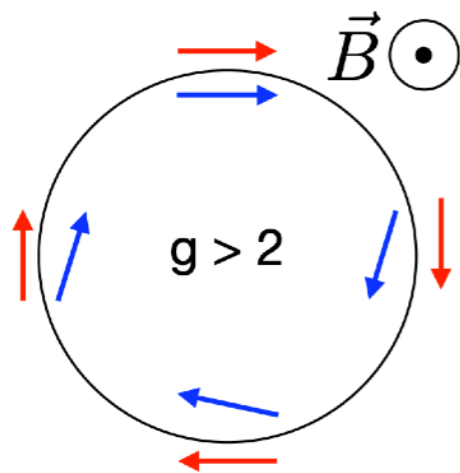
# Muon Magnetic Moment and Measuring the Anomaly

polarized muons in a magnetic field

$$\text{If } g = 2 \Rightarrow \vec{\omega}_a = 0$$



$$g \neq 2 \Rightarrow \vec{\omega}_a \cong a_\mu \frac{e}{m} \vec{B}$$



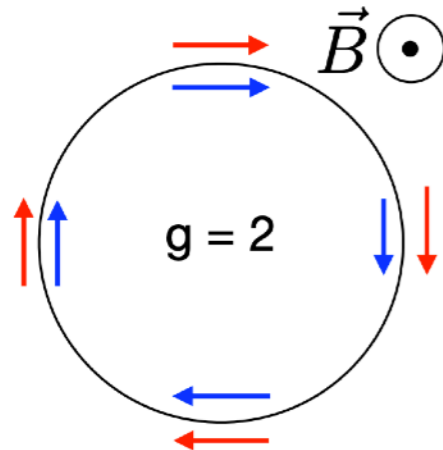
Magnetic Field

$$\vec{\omega}_c = -\frac{e}{\gamma m} \vec{B}, \text{ cyclotron frequency (freq. of charged particle under magnetic field)}$$

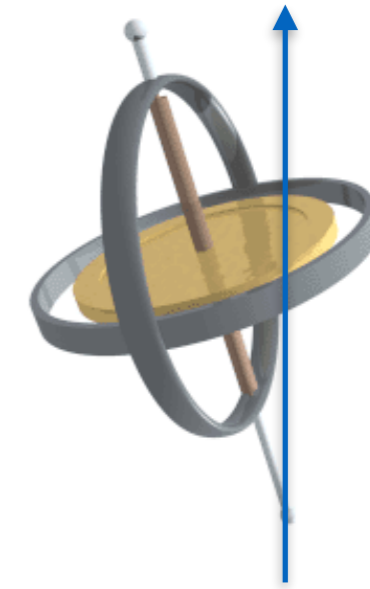
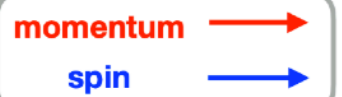
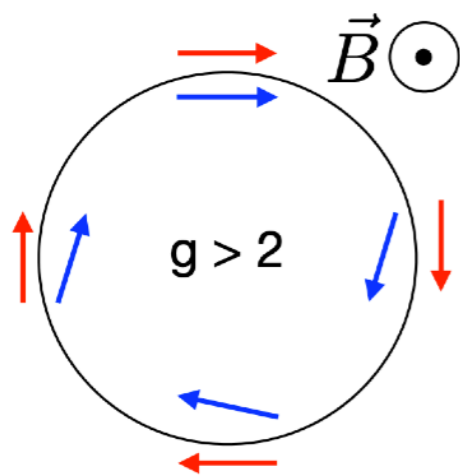
# Muon Magnetic Moment and Measuring the Anomaly

polarized muons in a magnetic field

$$\text{If } g = 2 \Rightarrow \vec{\omega}_a = 0$$



$$g \neq 2 \Rightarrow \vec{\omega}_a \cong a_\mu \frac{e}{m} \vec{B}$$



Magnetic Field

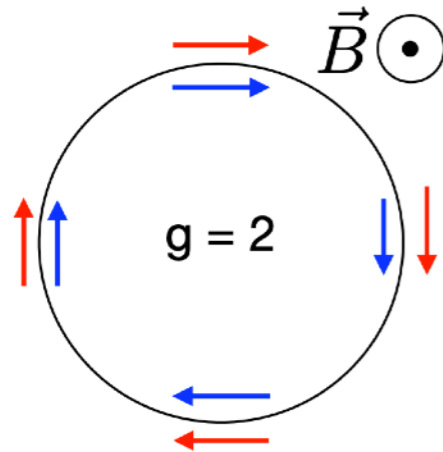
$$\vec{\omega}_c = -\frac{e}{\gamma m} \vec{B}, \text{ cyclotron frequency (freq. of charged particle under magnetic field)}$$

$$\vec{\omega}_s = -\frac{e}{\gamma m} \vec{B} (1 + \gamma a_\mu), \text{ Larmor precession frequency (total spin precession freq.)}$$

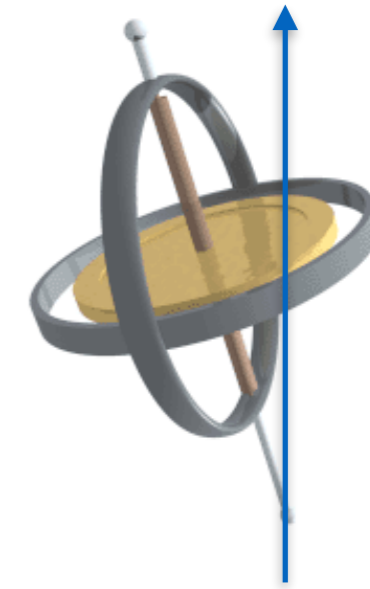
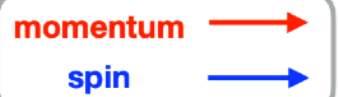
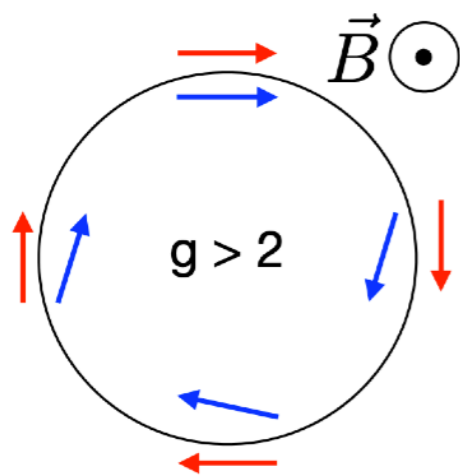
# Muon Magnetic Moment and Measuring the Anomaly

polarized muons in a magnetic field

$$\text{If } g = 2 \Rightarrow \vec{\omega}_a = 0$$



$$g \neq 2 \Rightarrow \vec{\omega}_a \cong a_\mu \frac{e}{m} \vec{B}$$



Magnetic Field

$$\vec{\omega}_c = -\frac{e}{\gamma m} \vec{B}, \text{ cyclotron frequency (freq. of charged particle under magnetic field)}$$

$$\vec{\omega}_s = -\frac{e}{\gamma m} \vec{B} (1 + \gamma a_\mu), \text{ Larmor precession frequency (total spin precession freq.)}$$

$$\vec{\omega}_a \cong \vec{\omega}_s - \vec{\omega}_c, \text{ anomalous precession frequency}$$

$$\vec{\omega}_a \cong a_\mu \frac{e}{m} \vec{B}$$

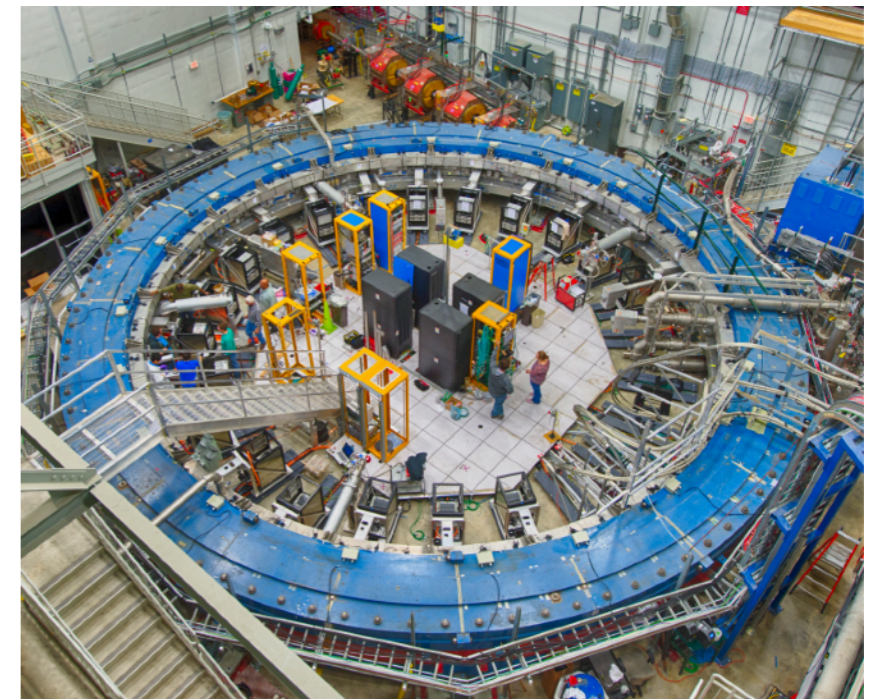
Measure them to extract anomaly

# CERN and BNL g-2 Experiments

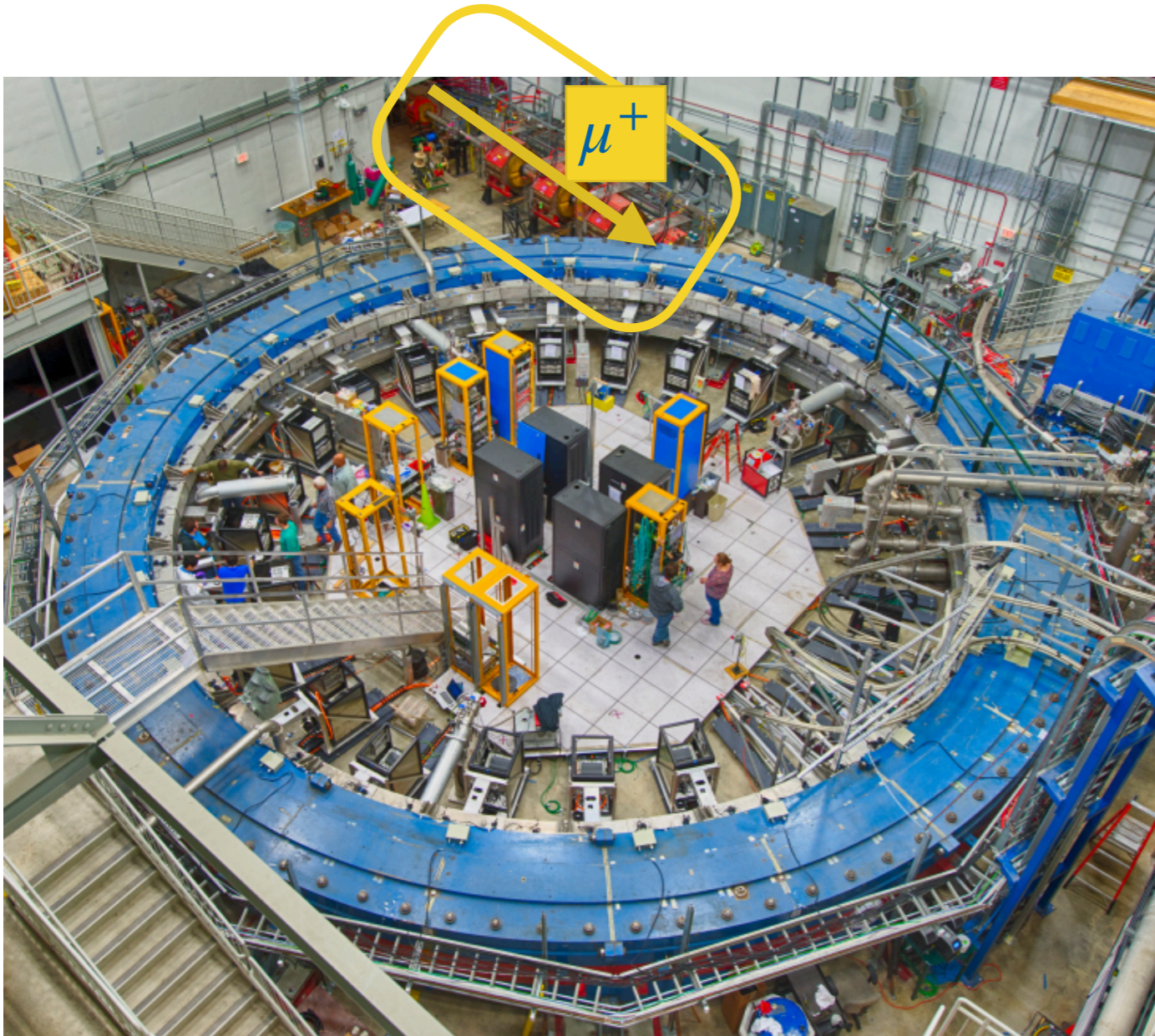
- Muon g-2 experiments were launched at CERN to measure  $a_\mu$ 
  - Launched a measurement( with a long dipole magnet) with precision of 2% and finally **0.4%** (1961,1962)
  - Second measurement with a storage ring-> x25 more precise- **270ppm**-> Revealed a quantitative discrepancy with the theory (1966)
  - Third measurement with a storage ring + electrostatic quadrupole field-> **7.3 ppm** precision (1969-1979)
- BNL took over the effort on measuring the anomaly more precisely (1997-2001)
  - Storage ring magnet + electrostatic quadrupole field + Fast Kickers +24 calorimeters
  - $\mu^+$  and  $\mu^-$  running
  - A factor of 14 improvement on precision after latest CERN measurement - **0.54ppm**



# Fermilab Muon g-2 Experiment

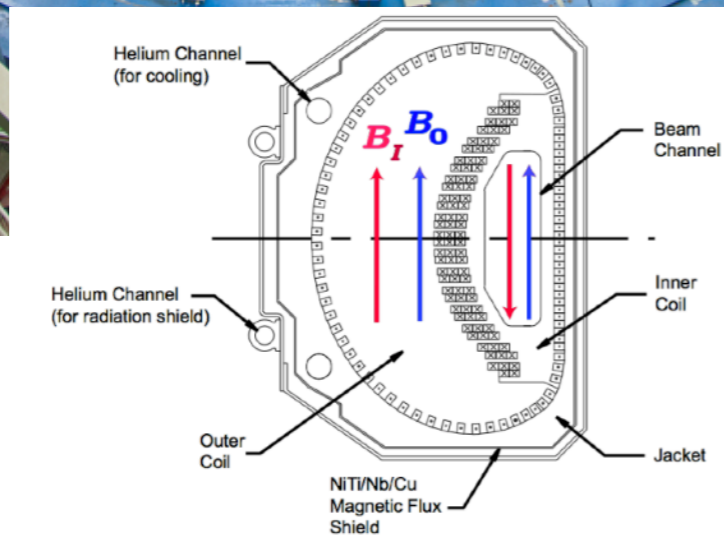
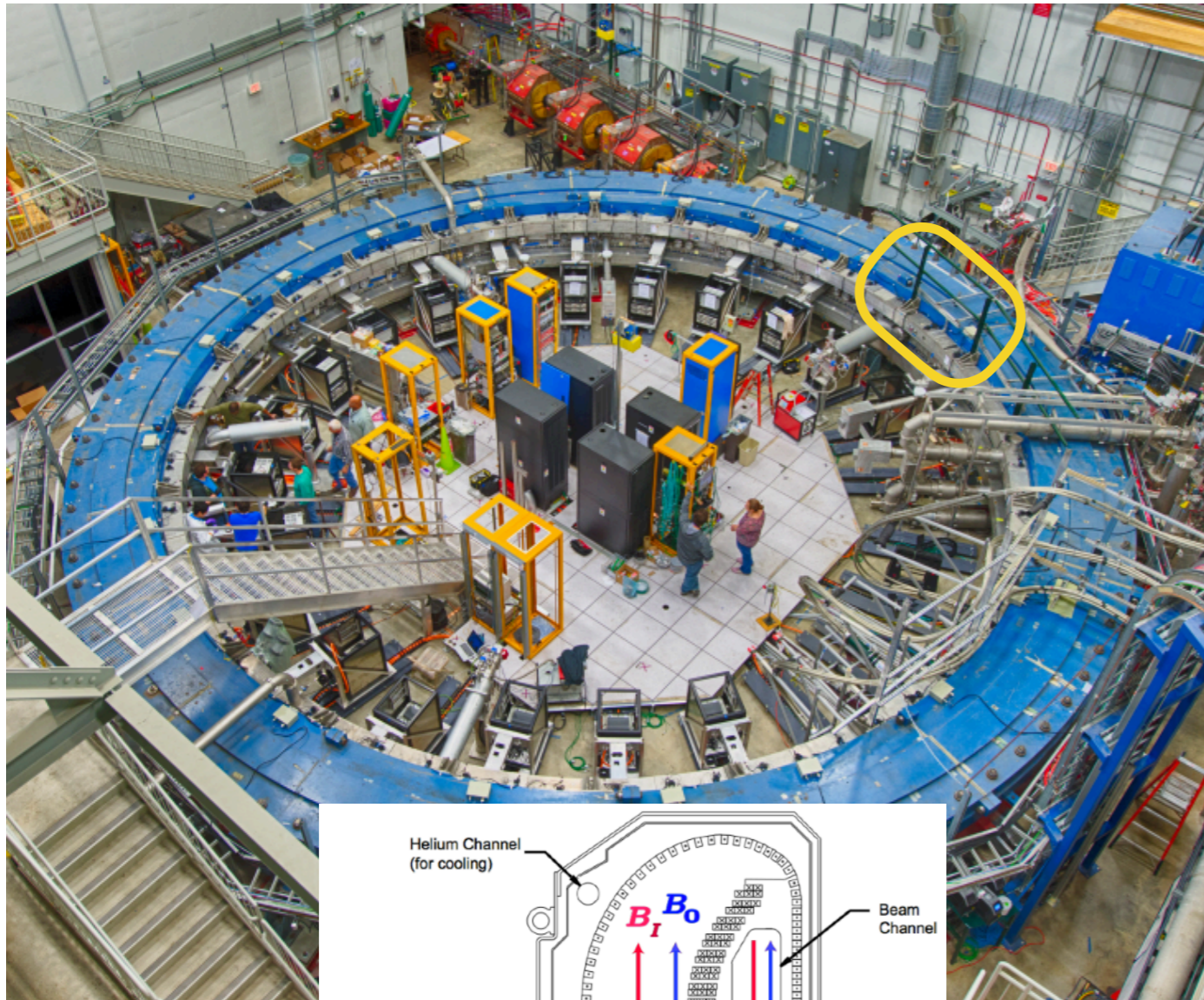


# Muons at the Experimental Hall !



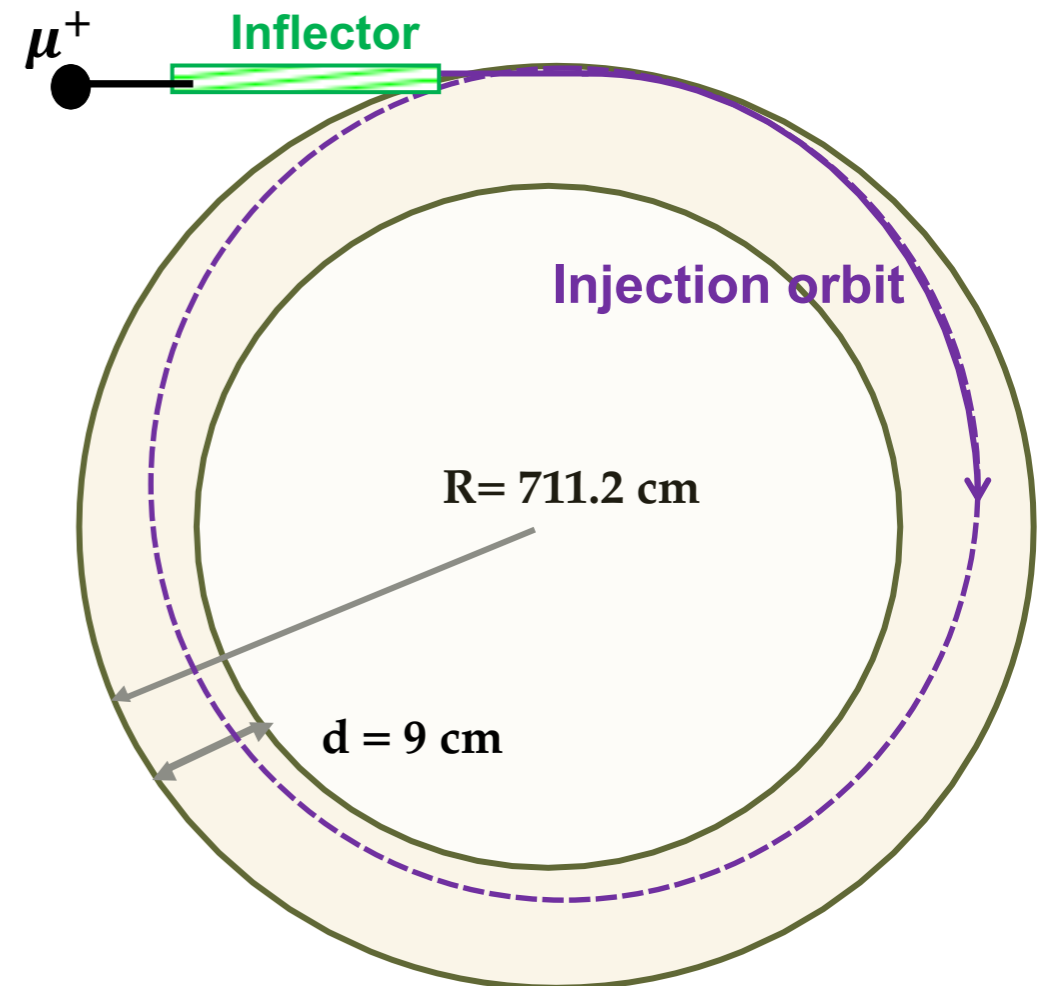
- 8 GeV protons are delivered to Recycler Ring from Booster
- Split the proton bunch into four bunches with RF system.
- Direct the proton punches to pion production target and obtain pions.
- Muons produced by pion decays circulate in the delivery ring until proton contamination is removed.
- Deliver 3.1 GeV polarized muons to g-2 storage ring .

# Storing the Muons : **Inflector** and Kickers



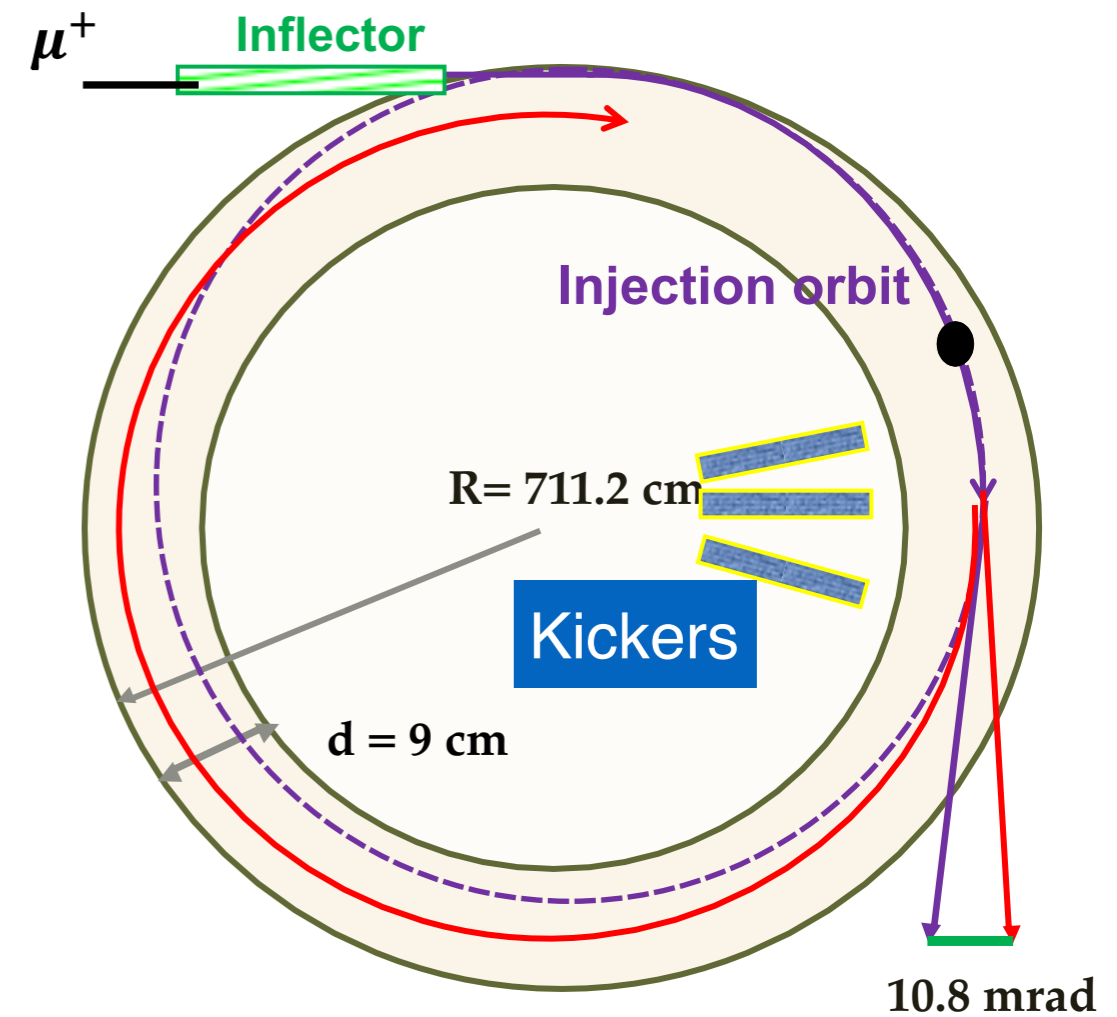
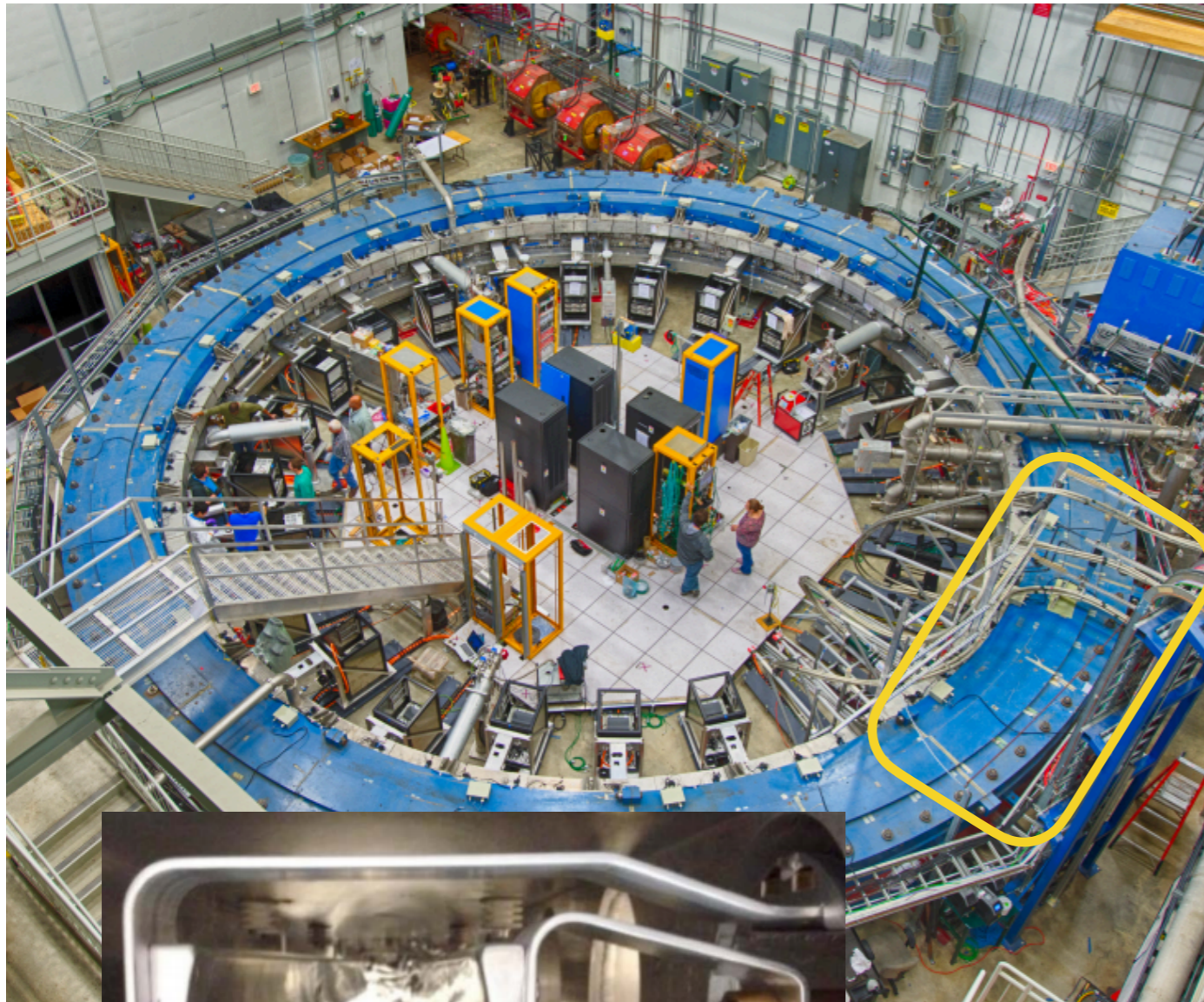
- **Inflector**

- Super conducting magnet
- Cancels B field(1.45T) in the magnet gap and let the beam enter the storage ring without being deflected.
- They are at  $r=77\text{mm}$  outside central closed orbit

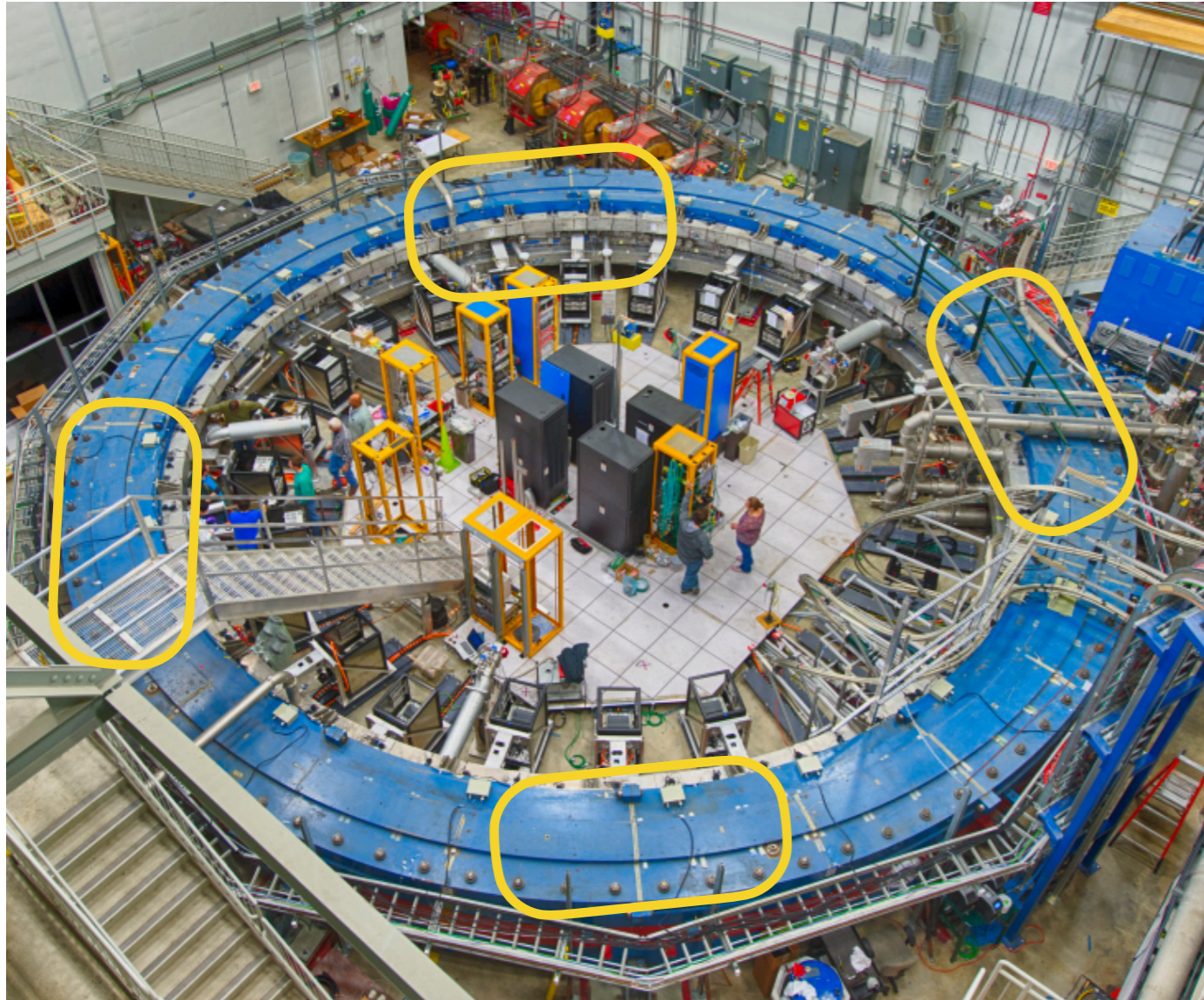


# Storing the Muons : Inflector and Kickers

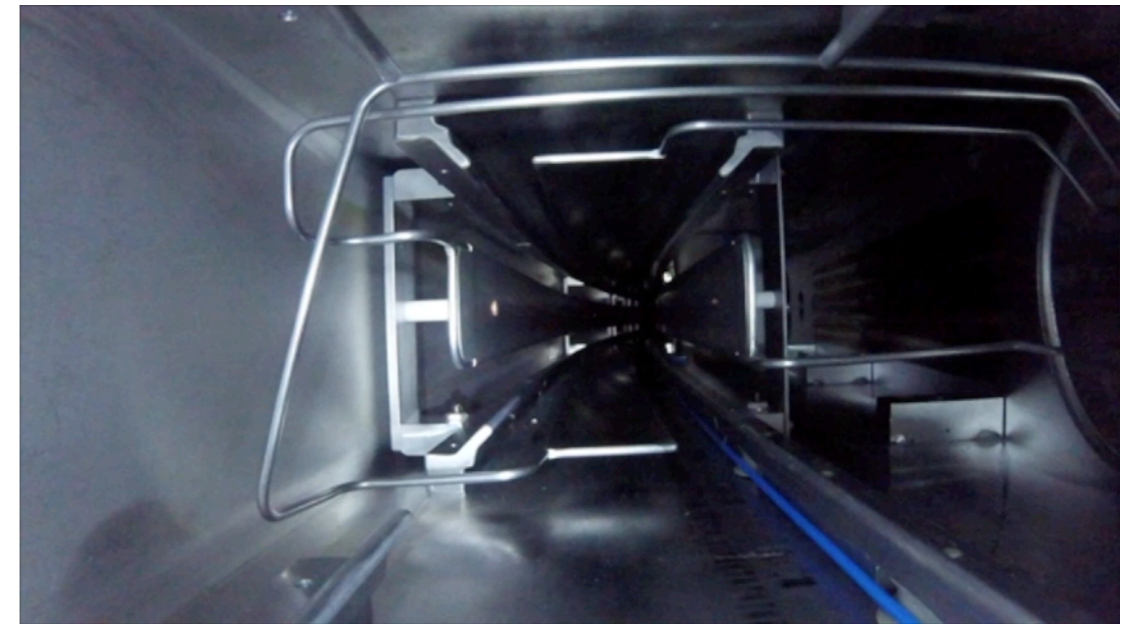
- **Magnetic Kickers**
  - Kick some more to direct the muons into ideal orbit.
  - Use 10.8 mrad pulsed kicks (<149 ns)



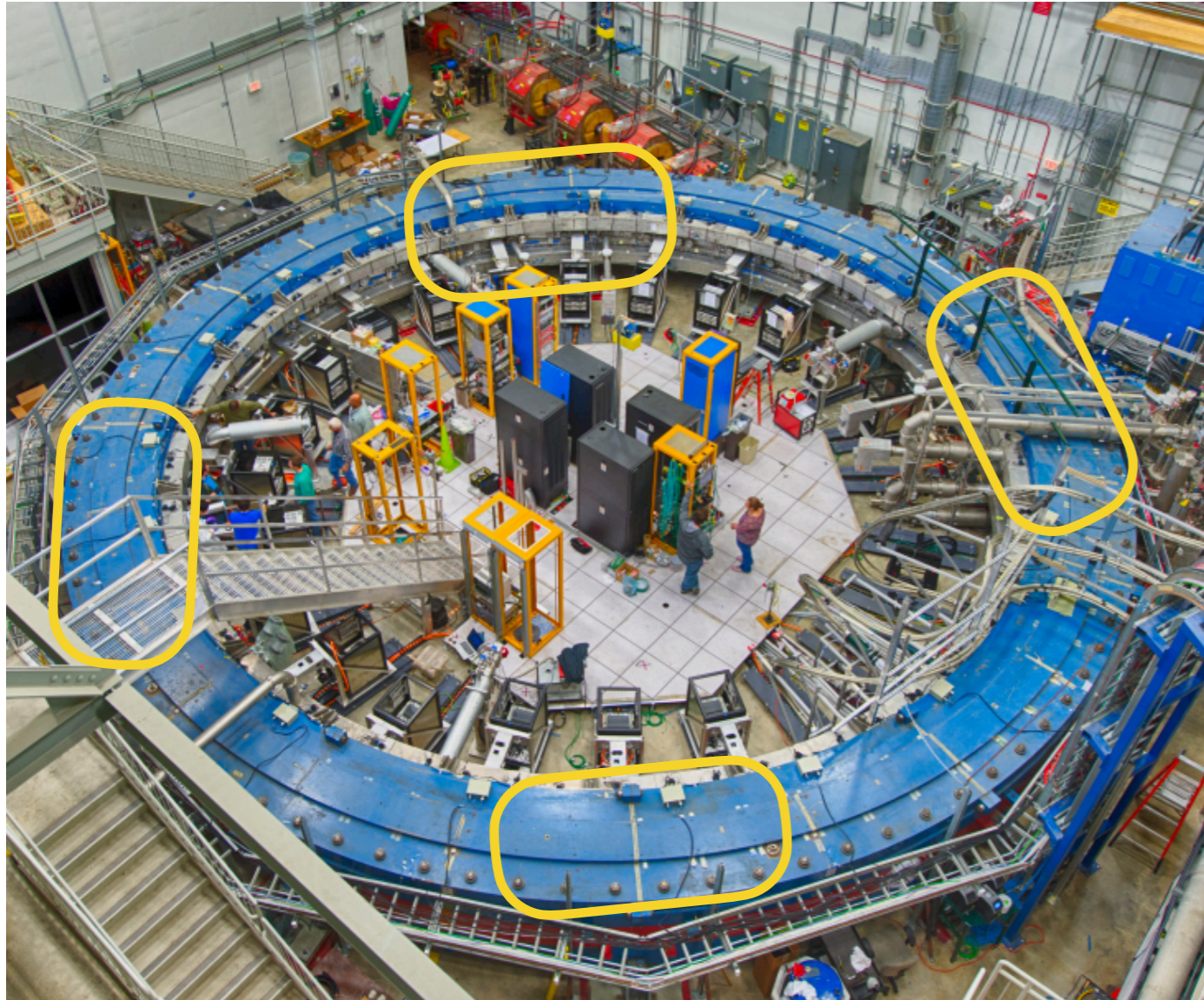
# Storing the Muons: **Electrostatic Quadrupoles**



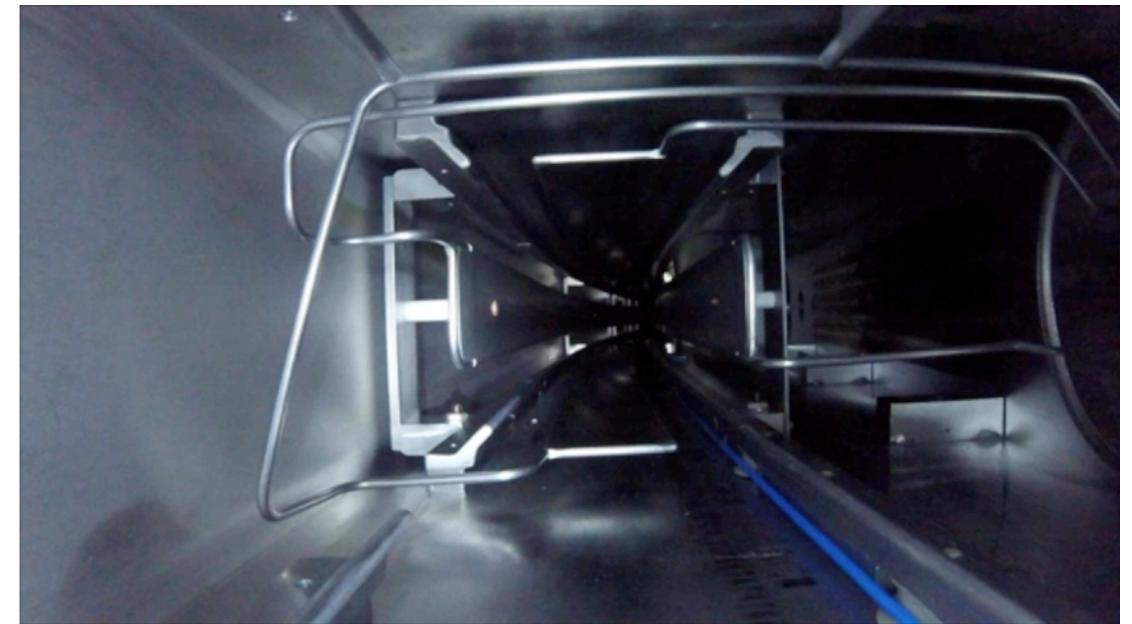
- **Electrostatic Quadrupoles**
  - 4 sets of quads which cover 43% of the ring
  - Electrostatic quadrupoles are used to focus the beam vertically while the storage ring field provides horizontal focusing
  - Cancels out leading order of electric field contribution running at magic momentum  $p = 3.094 \text{ GeV}/c$



# Storing the Muons: **Electrostatic Quadrupoles**



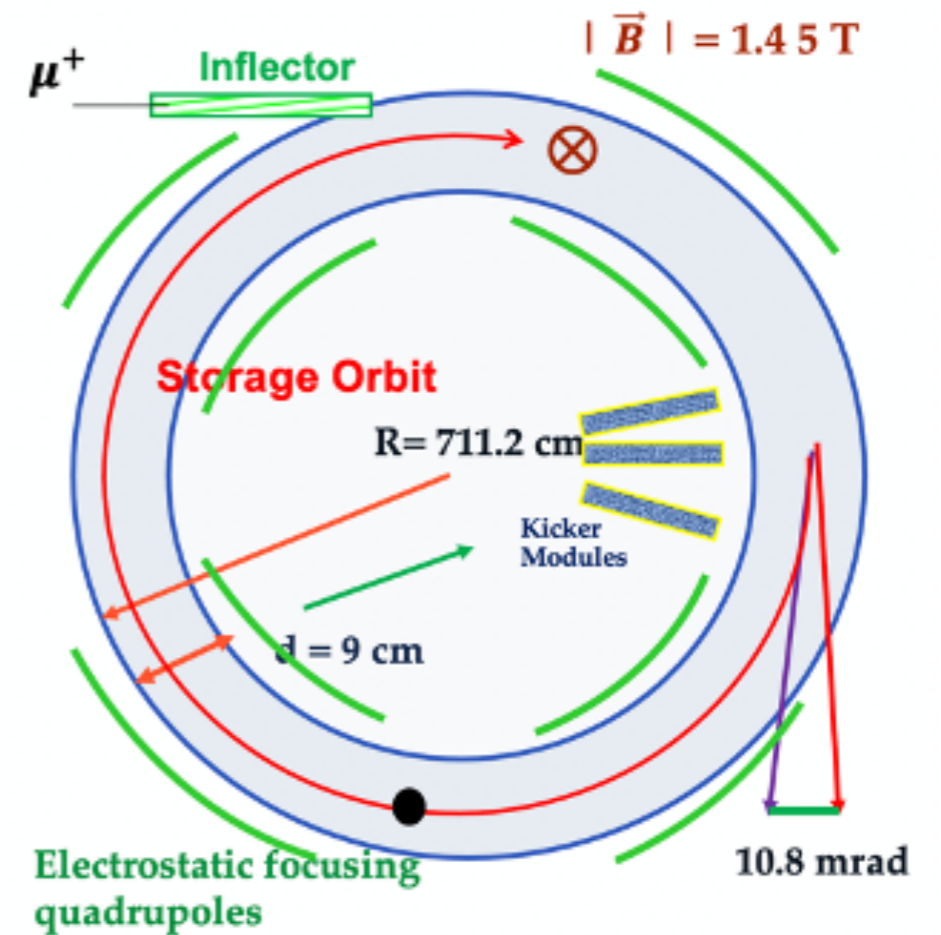
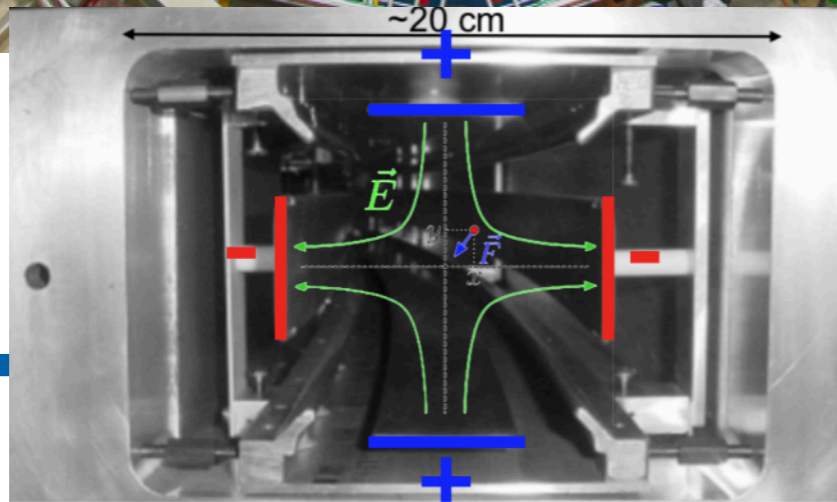
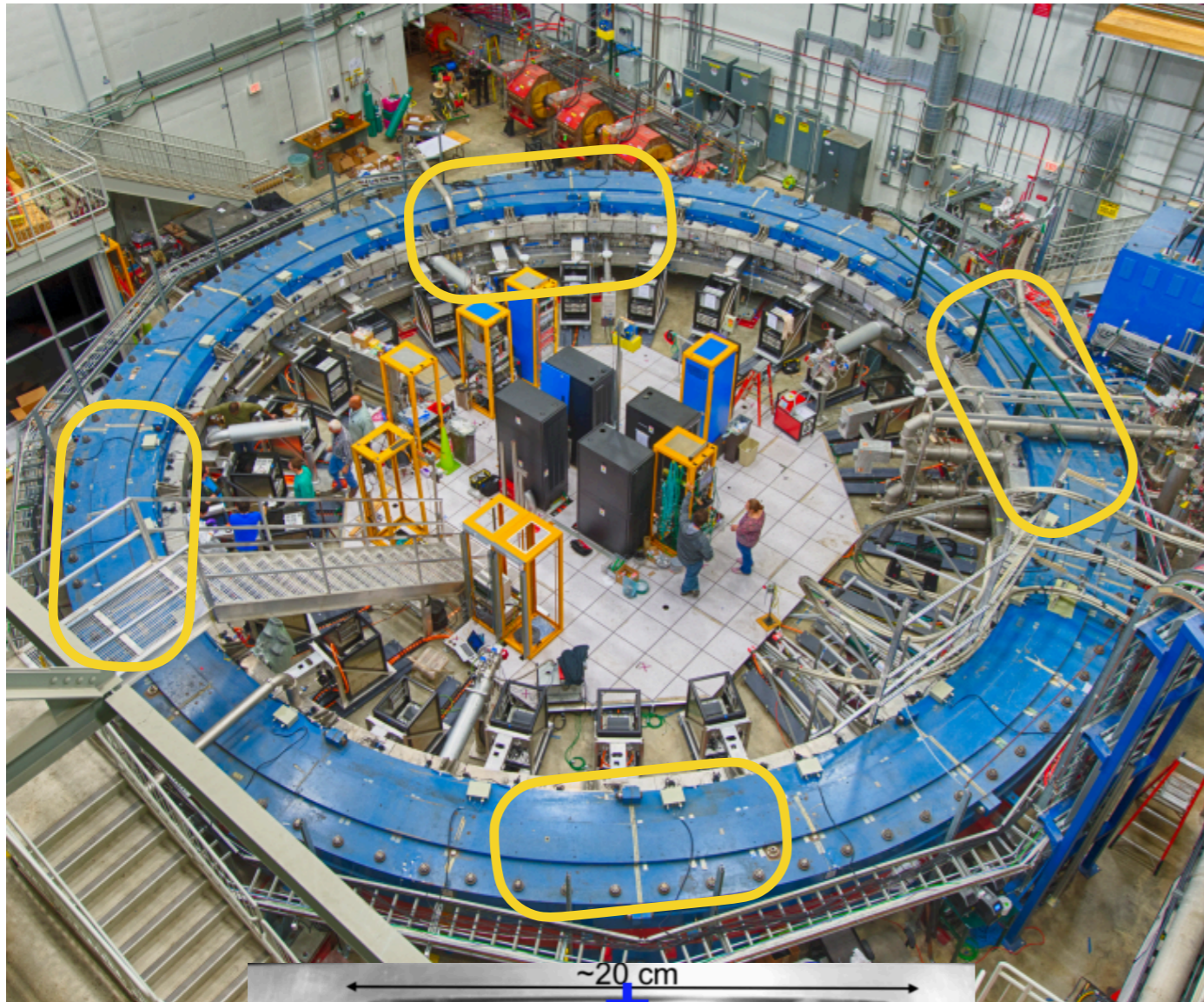
- **Electrostatic Quadrupoles**
  - 4 sets of quads which cover 43% of the ring
  - Electrostatic quadrupoles are used to focus the beam vertically while the storage ring field provides horizontal focusing
  - Cancels out leading order of electric field contribution running at magic momentum  $p = 3.094 \text{ GeV}/c$



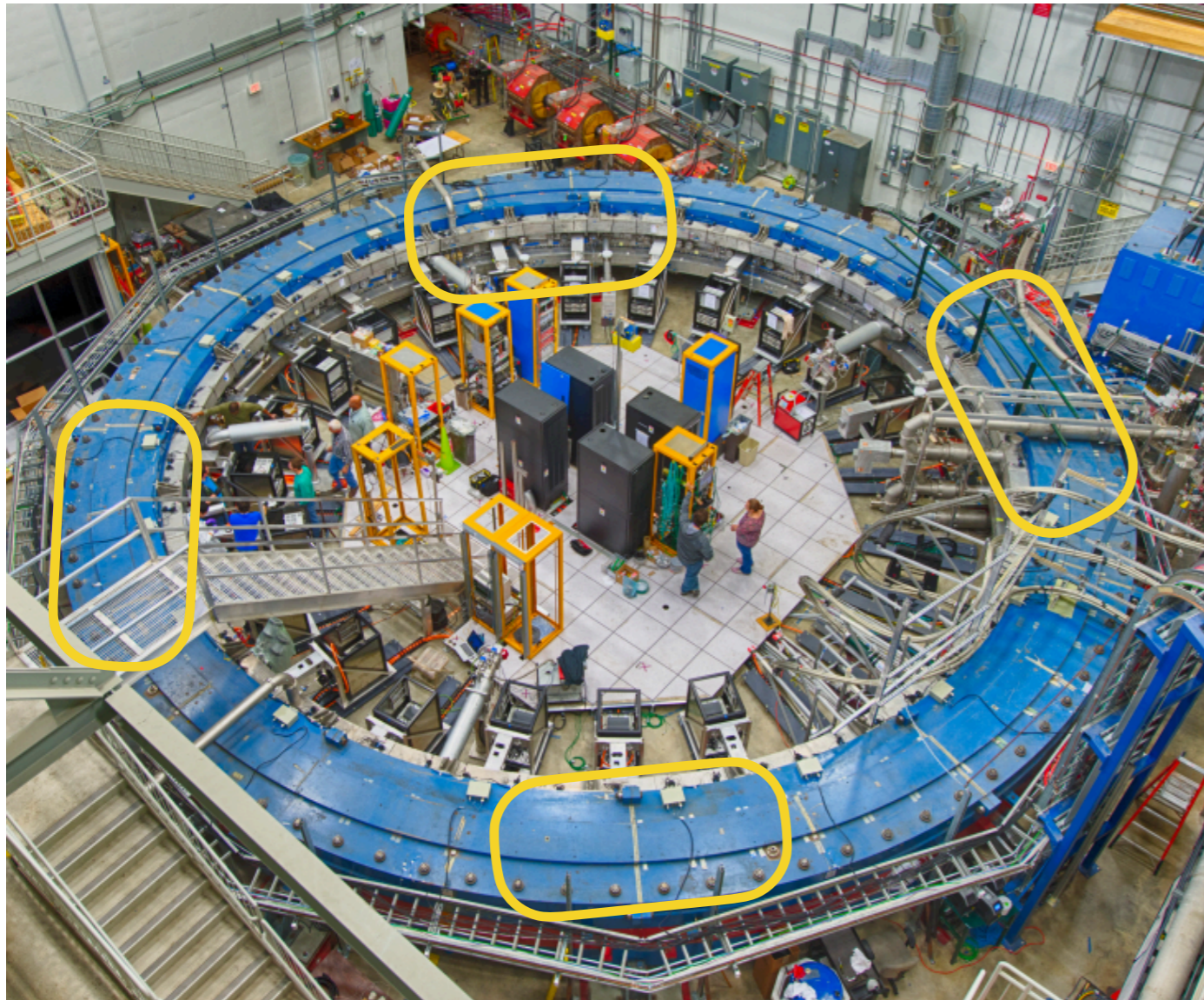
# Storing the Muons: Electrostatic Quadrupoles

- **Electrostatic Quadrupoles**

- 4 sets of quads which cover 43% of the ring
- **Electrostatic quadrupoles are used to focus the beam vertically while the storage ring field provides horizontal focusing**
- Cancels out leading order of electric field contribution running at magic momentum  $p = 3.094 \text{ GeV}/c$



# Storing the Muons: Electrostatic Quadrupoles



- **Electrostatic Quadrupoles**

- 4 sets of quads which cover 43% of the ring
- Electrostatic quadrupoles are used to focus the beam vertically while the storage ring field provides horizontal focusing
- **Cancels out leading order of electric field contribution running at magic momentum  $p = 3.094 \text{ GeV}/c$**

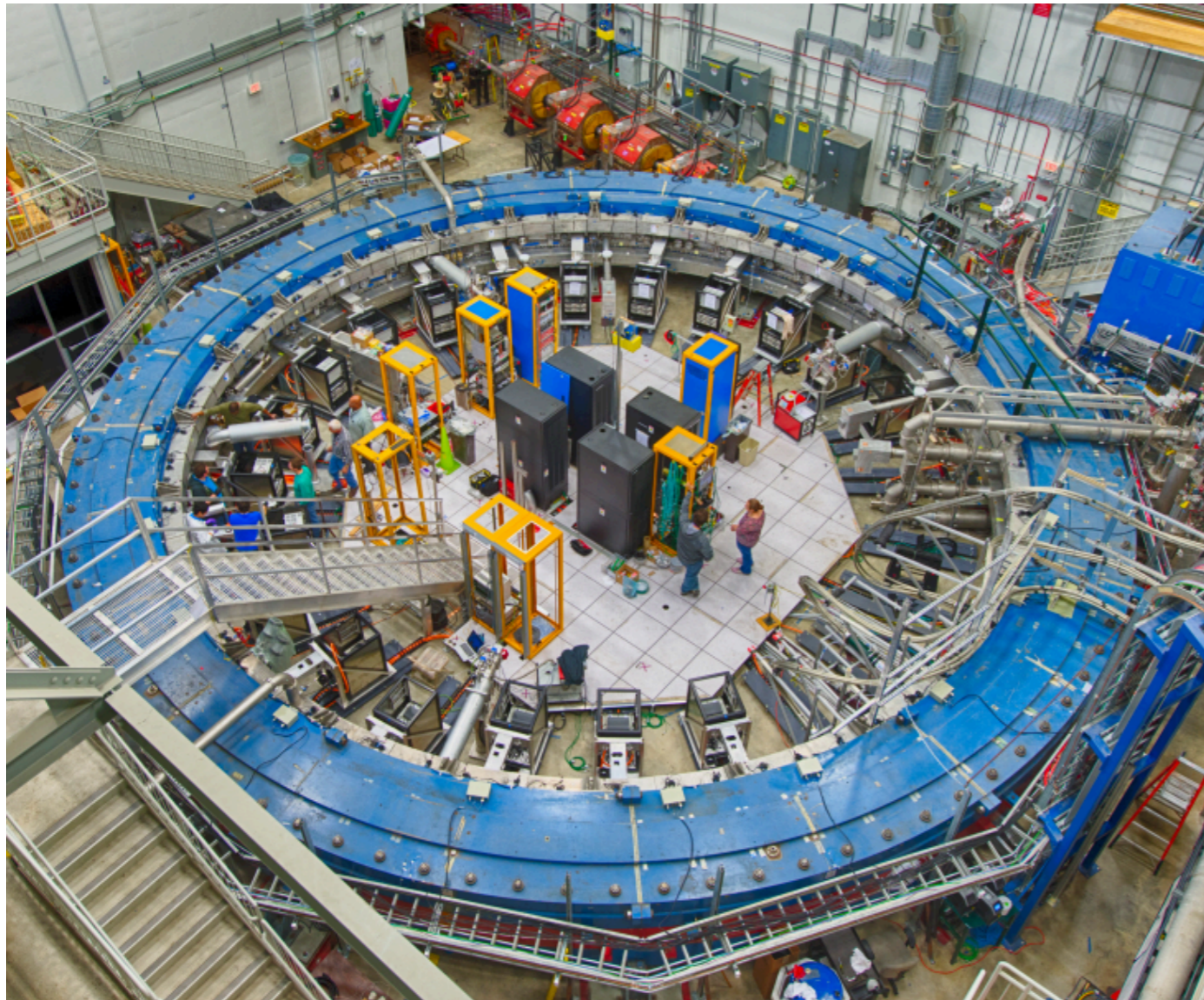
$$\vec{\omega}_a = \frac{e}{m} \left[ a_\mu \vec{B} - a_\mu \frac{\gamma}{\gamma+1} (\vec{\beta} \cdot \vec{B}) \vec{\beta} - \left( a_\mu - \frac{1}{\gamma^2-1} \right) \vec{\beta} \times \vec{E} \right]$$

0 if in plane

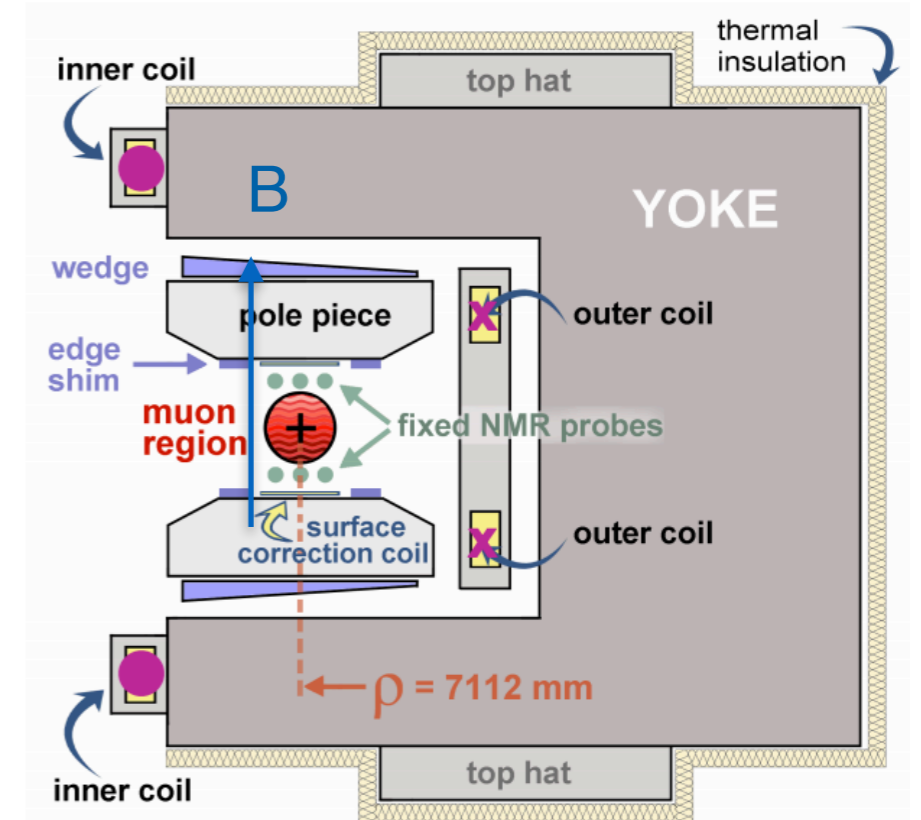
Term cancels at the magic momentum



# Storing the Muons: Magnet



Achieved 25 ppm on field uniformity

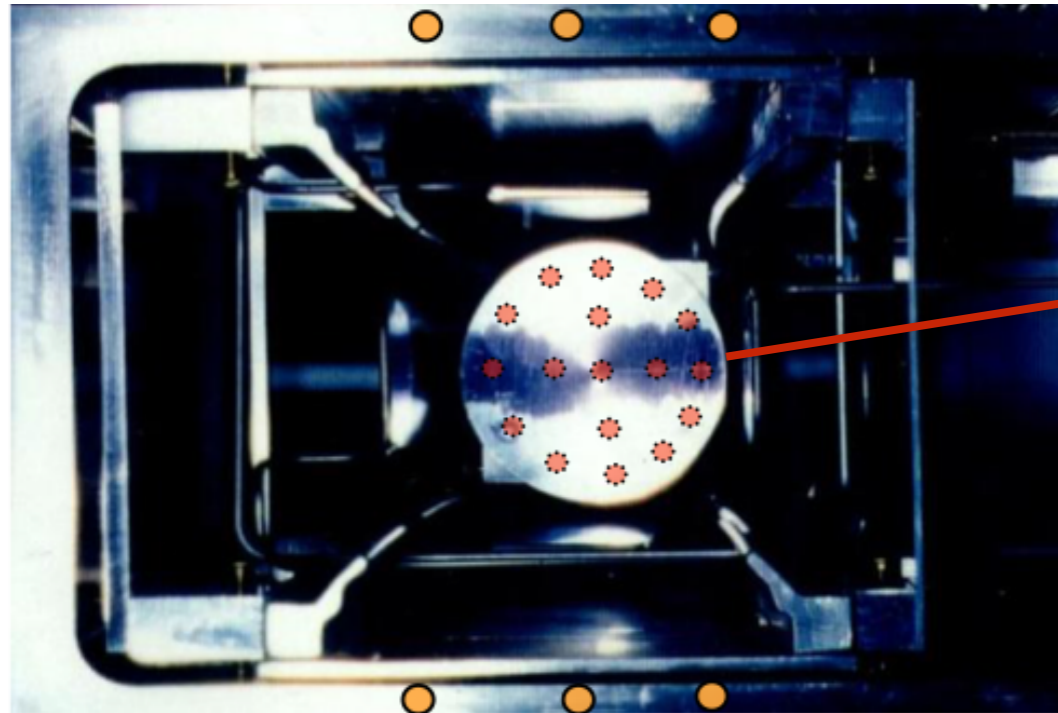


**g-2 Magnet in Cross Section**

## Superconducting C shaped magnet

- Provides 1.45T B field (vertical and uniform)
- **12 Yokes:** Open on the inside, allows the decay positrons to reach to the detectors.
- **72 poles:** Low-carbon steel to minimize the impurity
- **144 Edge shims:** Minimize the local sextupole field by changing edge shim thickness
- **864 Steel wedges:** Angle adjustment (compensate quadrupole component), radial adjustment (shim local dipole field).
- **Surface correction coil:** Reduces non-uniformities on higher moment of field.

# Measuring $\omega_p$ : Monitoring and Measuring the Magnetic Field



Electronics,  
Microcontroller,  
Communication

Position of NMR probes

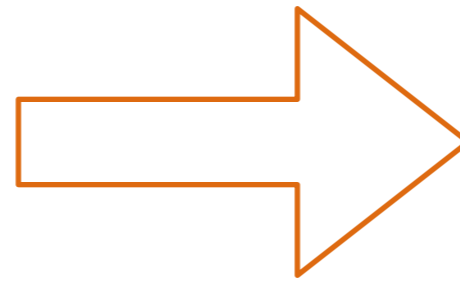
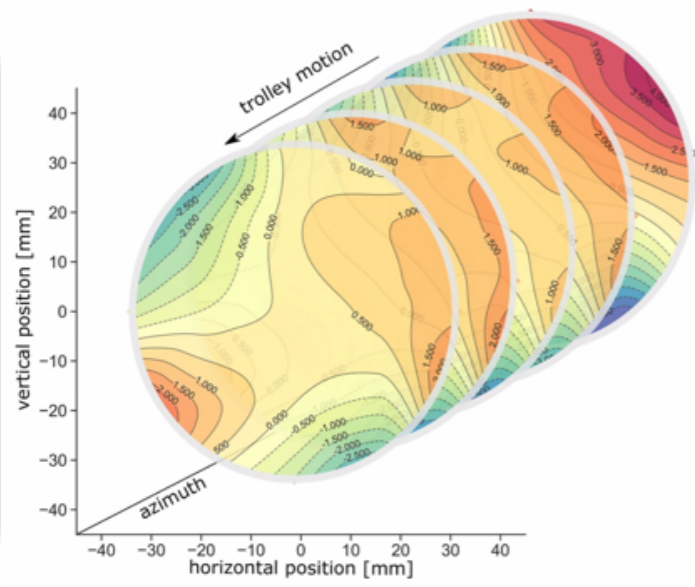
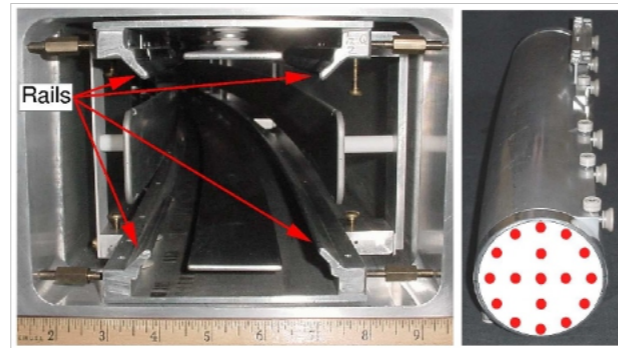
- **Fixed probes:**

- 378 probes located on vacuum chamber
- Measure the magnetic field while muons are inside the storage ring

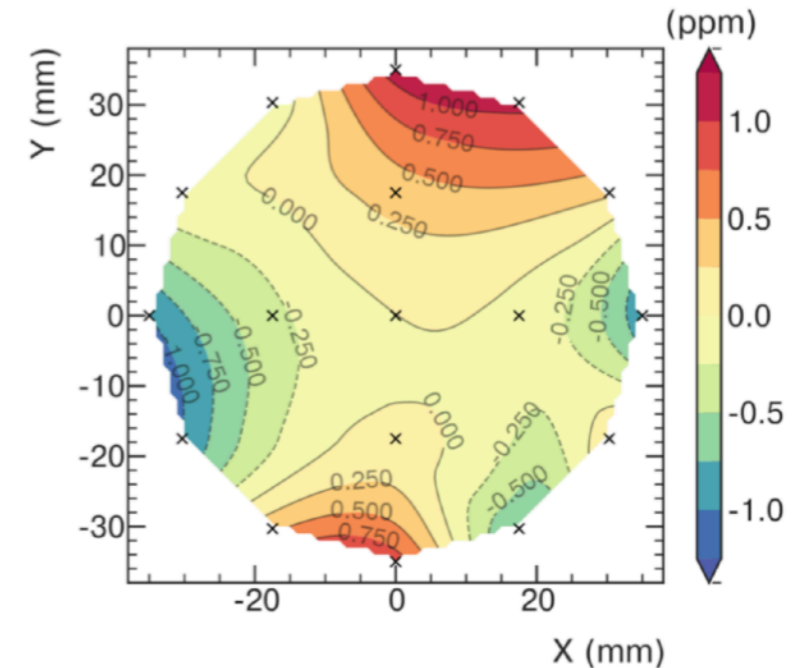
- **Trolley(Motorized cart):**

- 17 NMR probes
- Circles around the ring on periodically
- Measures the magnetic field in the storage region
- Used to calibrate FP measurements

# Measuring $\omega_p$ : Monitoring and Measuring the Magnetic Field



azimuthally averaged field



To determine  $\omega_p$  at all times:

- Map the magnetic field in the storage region with trolley runs every 3 days
- Use fixed probes to interpolate the field between trolley runs

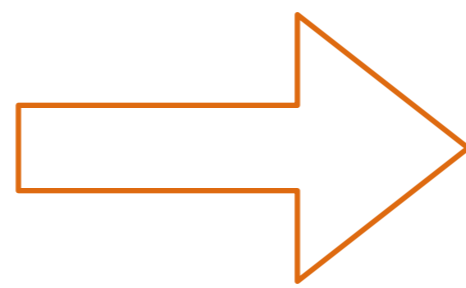
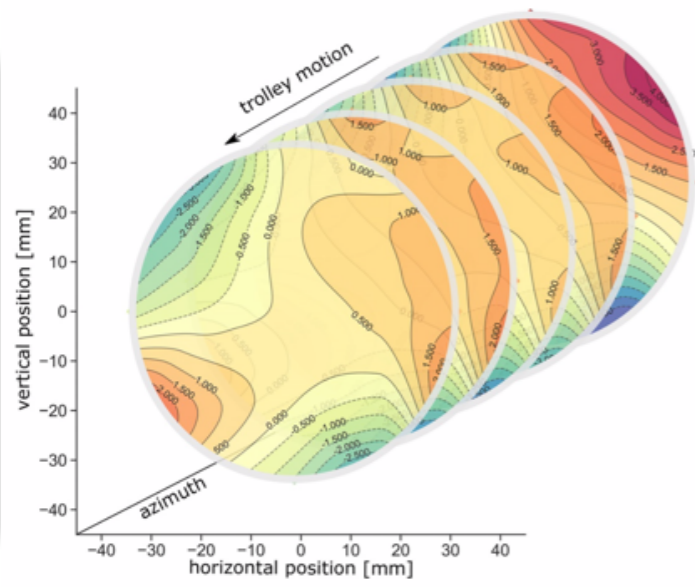
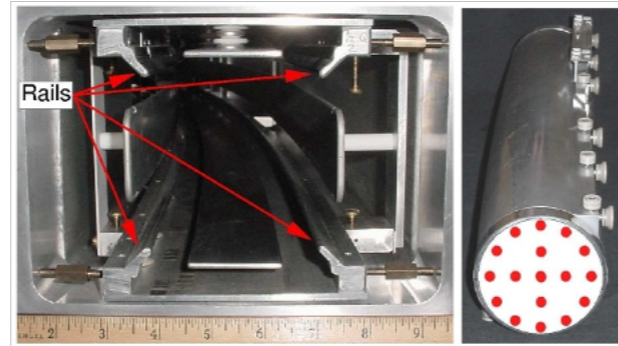
$$a_\mu = \left(\frac{g_e}{2}\right) \left(\frac{\omega_a}{\langle\omega_p\rangle}\right) \left(\frac{\mu_p}{\mu_e}\right) \left(\frac{m_\mu}{m_e}\right)$$

$$\langle\omega_p\rangle \approx \omega_p \otimes \rho(r)$$

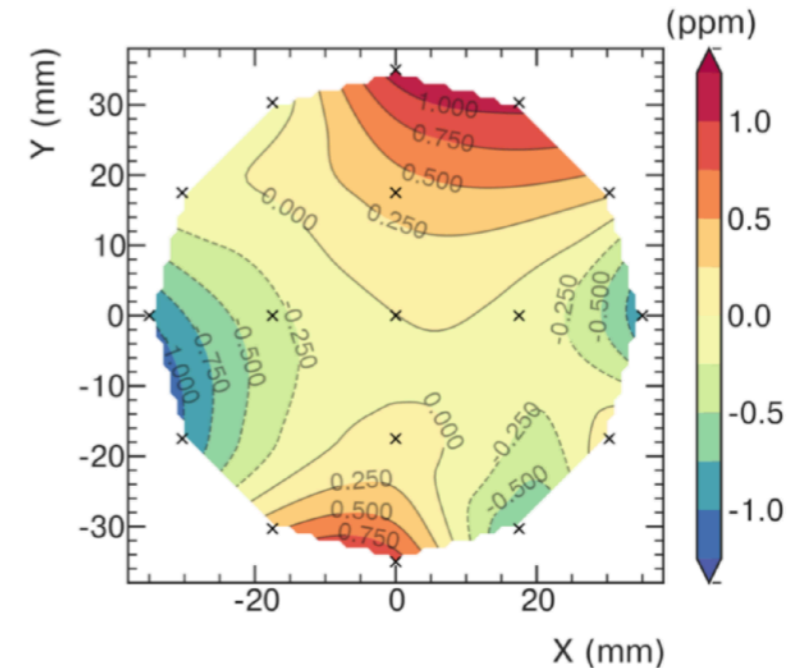
$\omega_p$ : free proton precession frequency

Using proton NMR  $\hbar\omega_p = 2\mu_p B$

# Measuring $\omega_p$ : Monitoring and Measuring the Magnetic Field



azimuthally averaged field

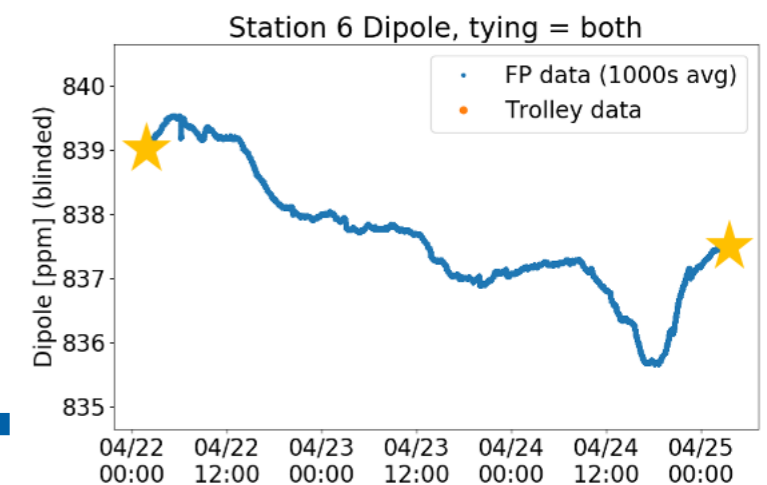


To determine  $\omega_p$  at all times:

- Map the magnetic field in the storage region with trolley runs every 3 days
- Use fixed probes to interpolate the field between trolley runs

$$a_\mu = \left(\frac{g_e}{2}\right) \left(\frac{\omega_a}{\langle\omega_p\rangle}\right) \left(\frac{\mu_p}{\mu_e}\right) \left(\frac{m_\mu}{m_e}\right)$$

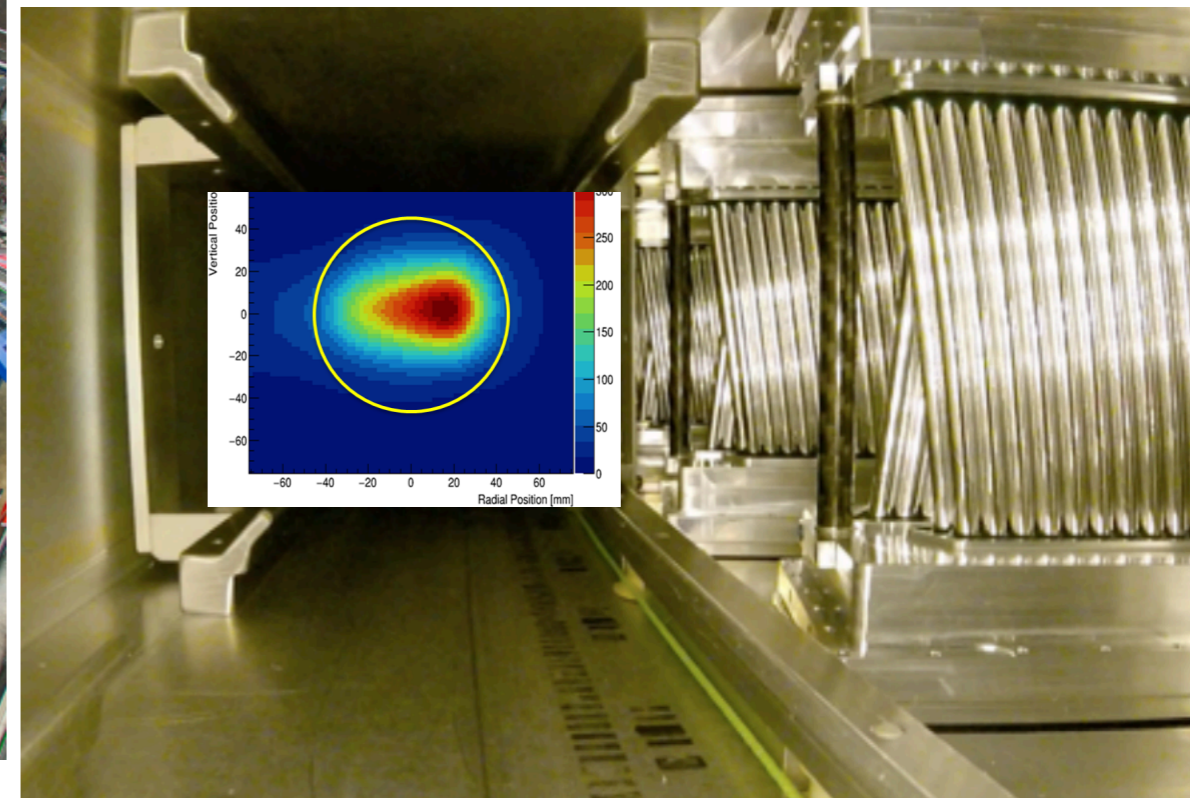
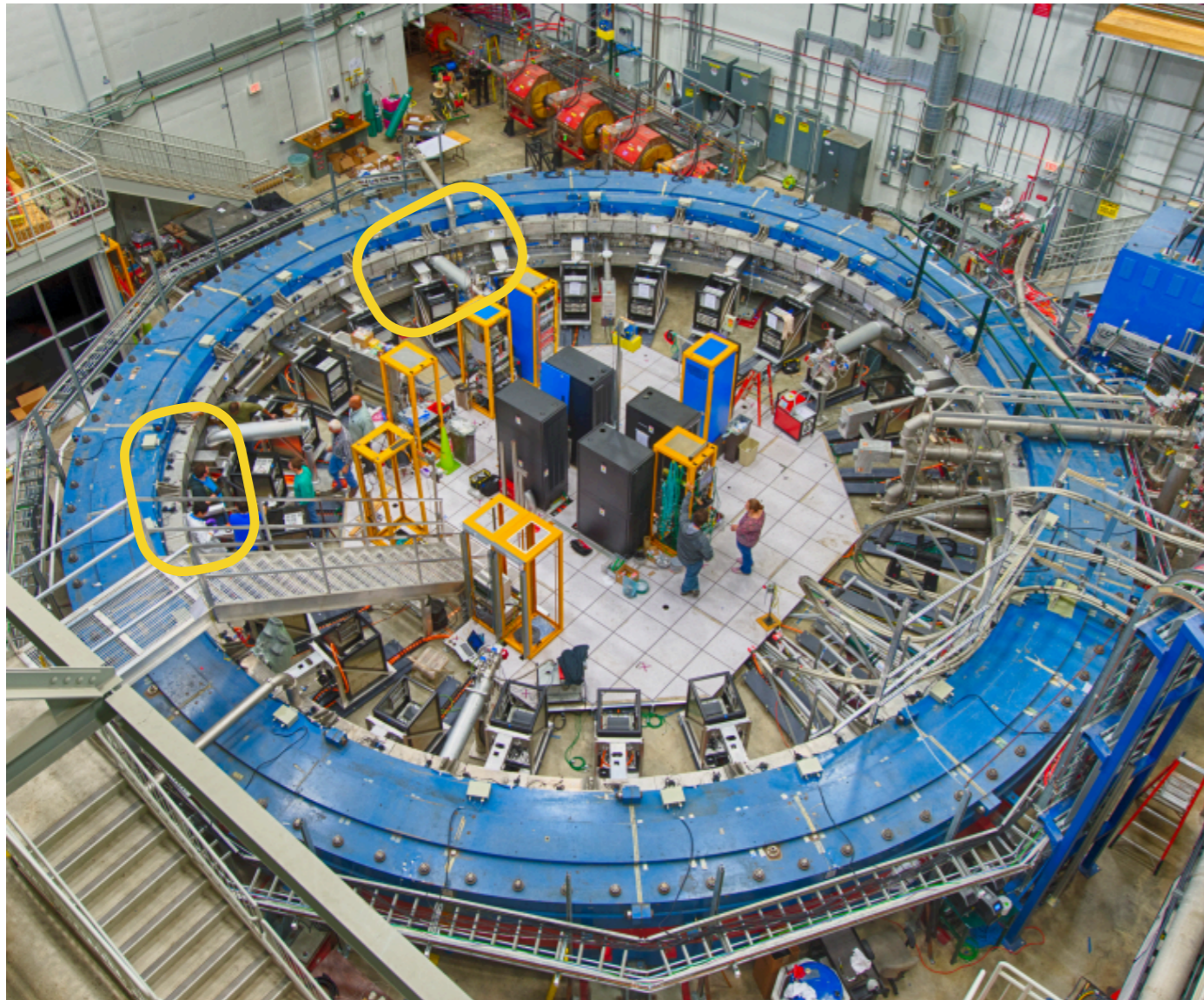
$$\langle\omega_p\rangle \approx \omega_p \otimes \rho(r)$$



# Detectors: Trackers for Reconstructing the Beam Profile



- Trackers
  - 2 straw-tracker stations
  - 8 modules per station each with 128 straws
  - Reconstruct muon beam profile from positron trajectories

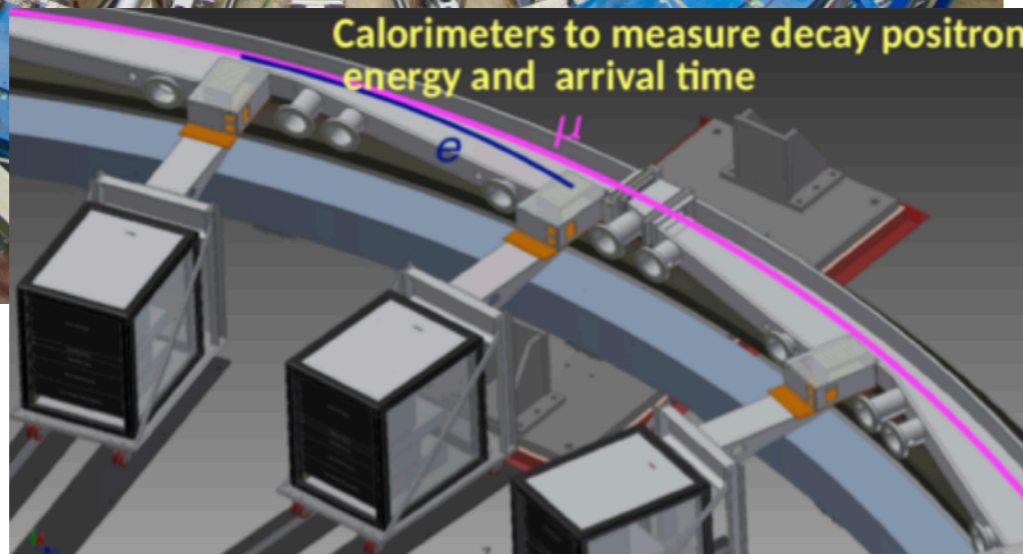
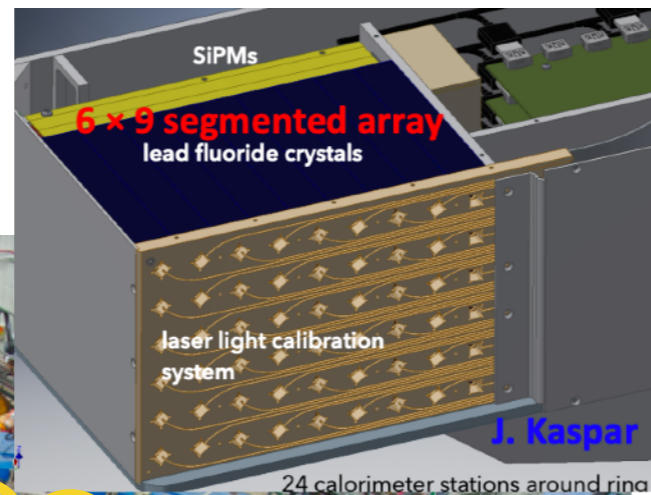


$$a_\mu = \left( \frac{g_e}{2} \right) \left( \frac{\omega_a}{\langle \omega_p \rangle} \right) \left( \frac{\mu_p}{\mu_e} \right) \left( \frac{m_\mu}{m_e} \right)$$

$$\langle \omega_p \rangle \approx \omega_p \otimes \rho(r)$$

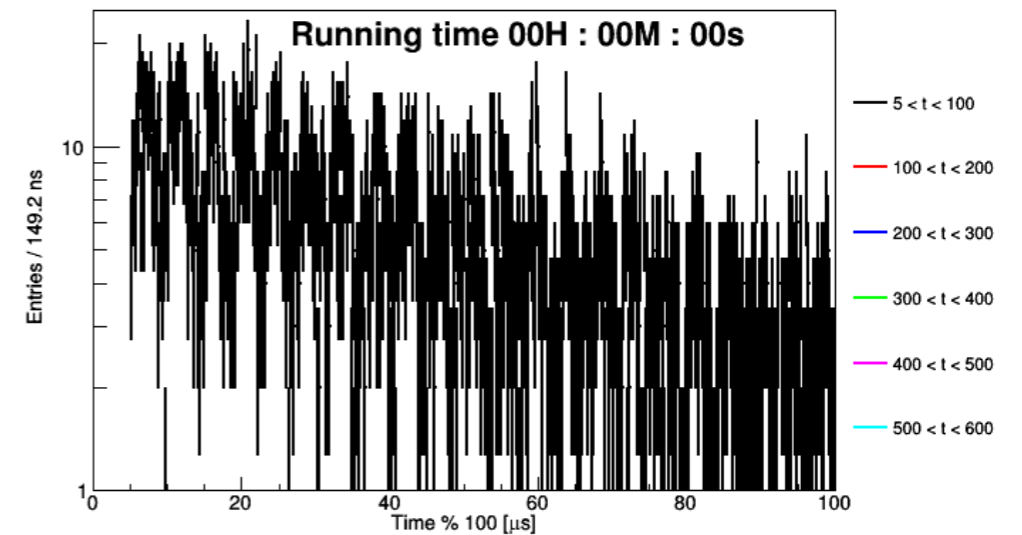


# Detectors : Calorimeters



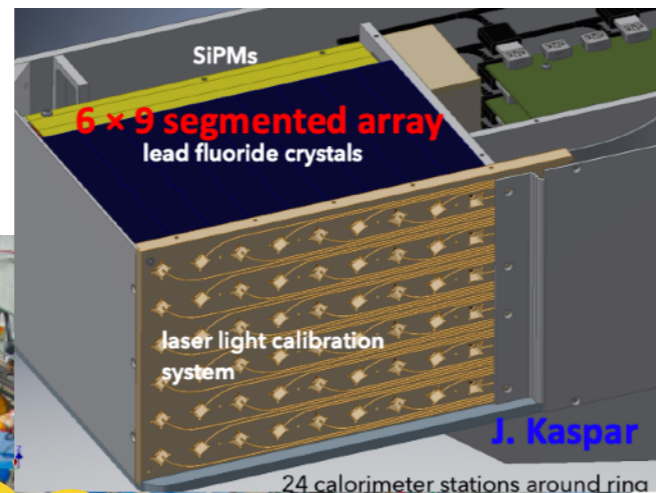
## • Calorimeters

- 24 segmented PbF<sub>2</sub> crystal calorimeters stationed around the ring
- Detects energy and arrival time of  $e^+$  decayed from muons:  $\mu^+ \rightarrow e^+ \bar{\nu}_\mu \nu_e$

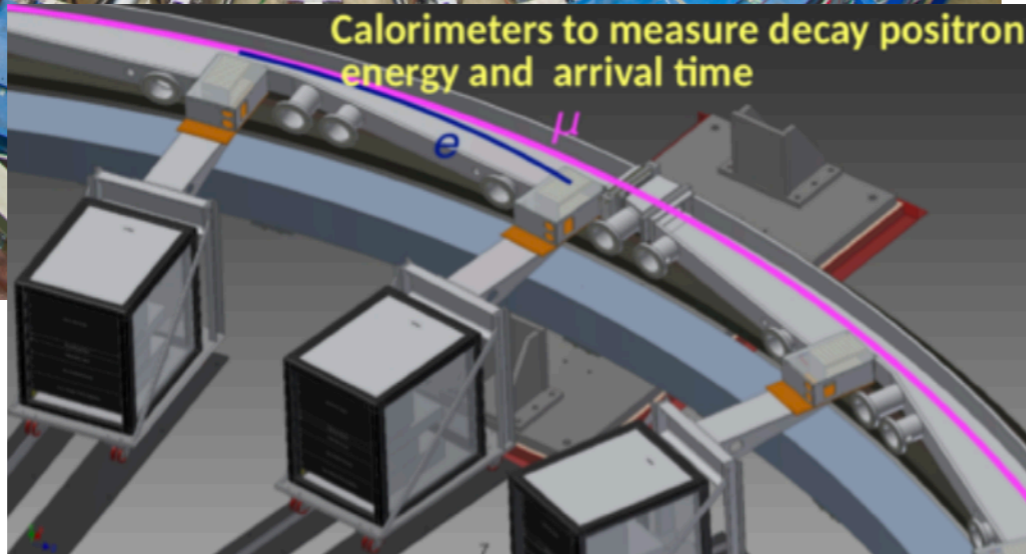




# Detectors : Calorimeters

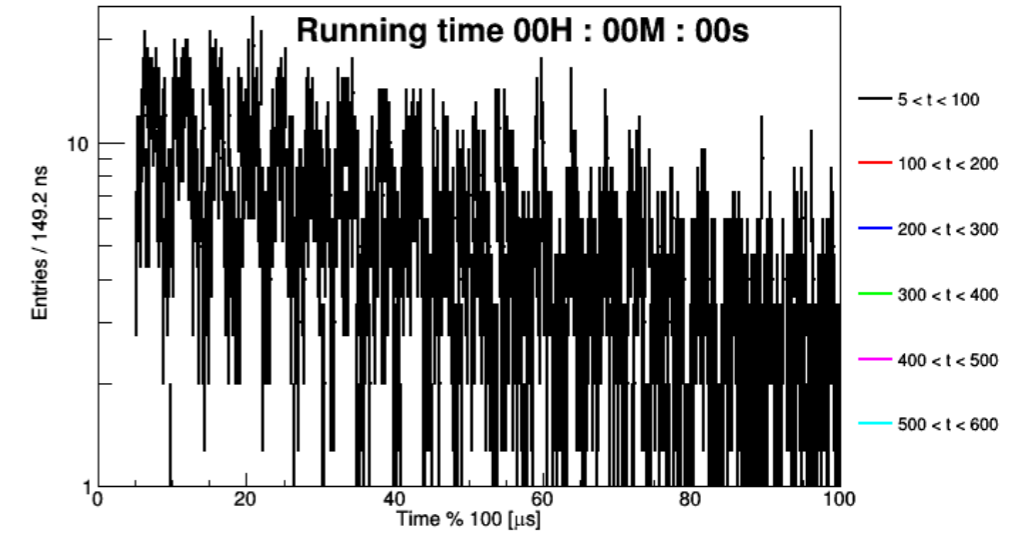


24 calorimeter stations around ring

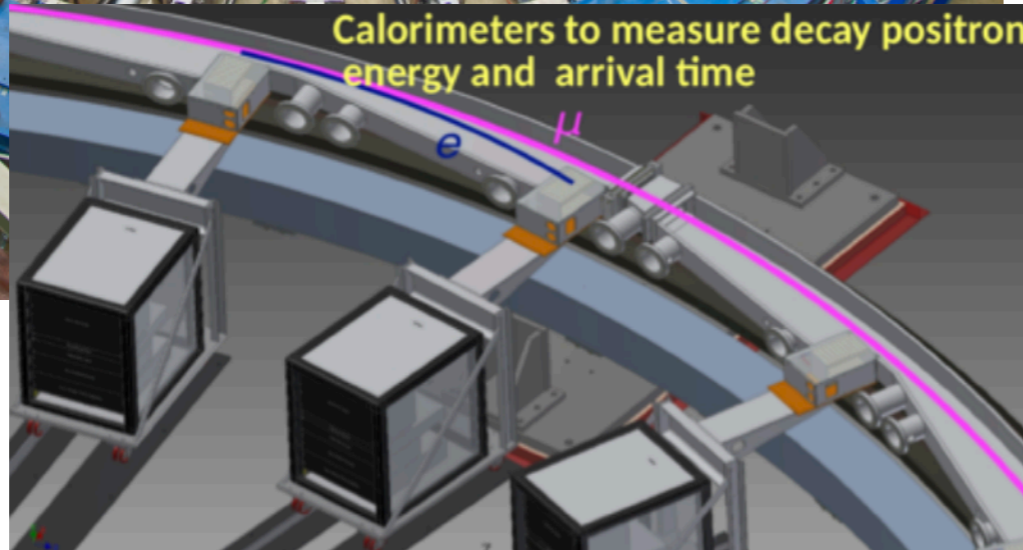
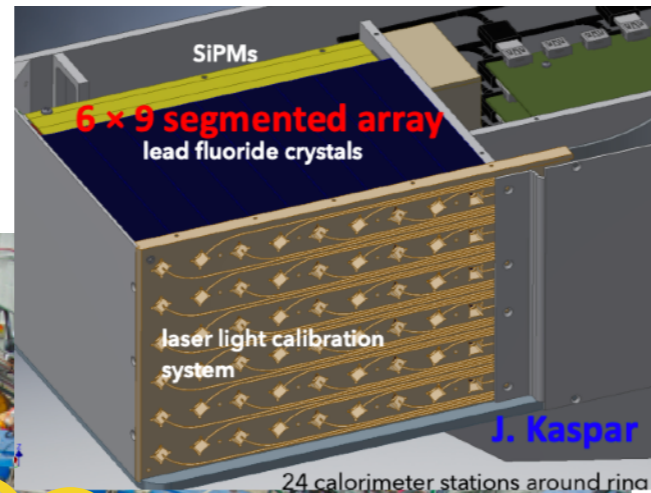


## • Calorimeters

- 24 segmented PbF<sub>2</sub> crystal calorimeters stationed around the ring
- Detects energy and arrival time of e<sup>+</sup> decayed from muons:  $\mu^+ \rightarrow e^+ \bar{\nu}_\mu \nu_e$

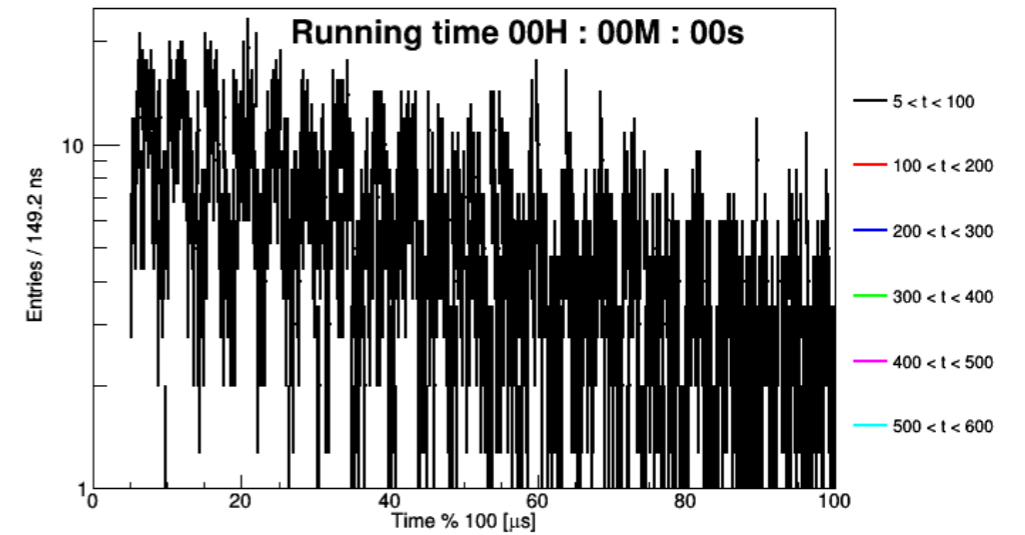


# Detectors : Calorimeters



## • Calorimeters

- 24 segmented PbF<sub>2</sub> crystal calorimeters stationed around the ring
- Detects energy and arrival time of e<sup>+</sup> decayed from muons:  $\mu^+ \rightarrow e^+ \bar{\nu}_\mu \nu_e$

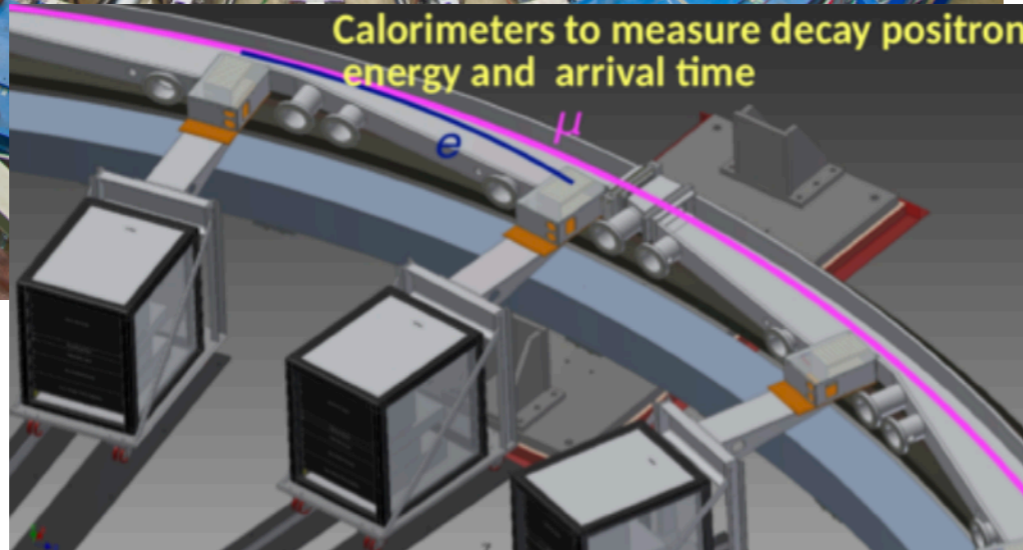
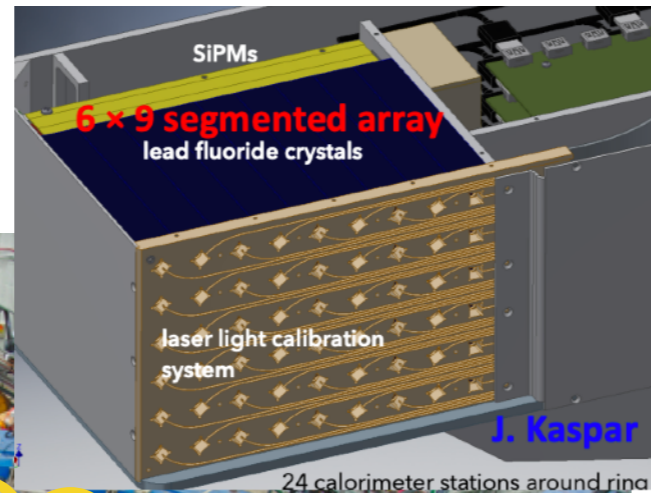


$$N(t) = N_0 e^{-t/\tau} [1 + A \cos(\omega_a t + \phi)]$$

$$a_\mu = \left( \frac{g_e}{2} \right) \left( \frac{\omega_a}{\langle \omega_p \rangle} \right) \left( \frac{\mu_p}{\mu_e} \right) \left( \frac{m_\mu}{m_e} \right)$$

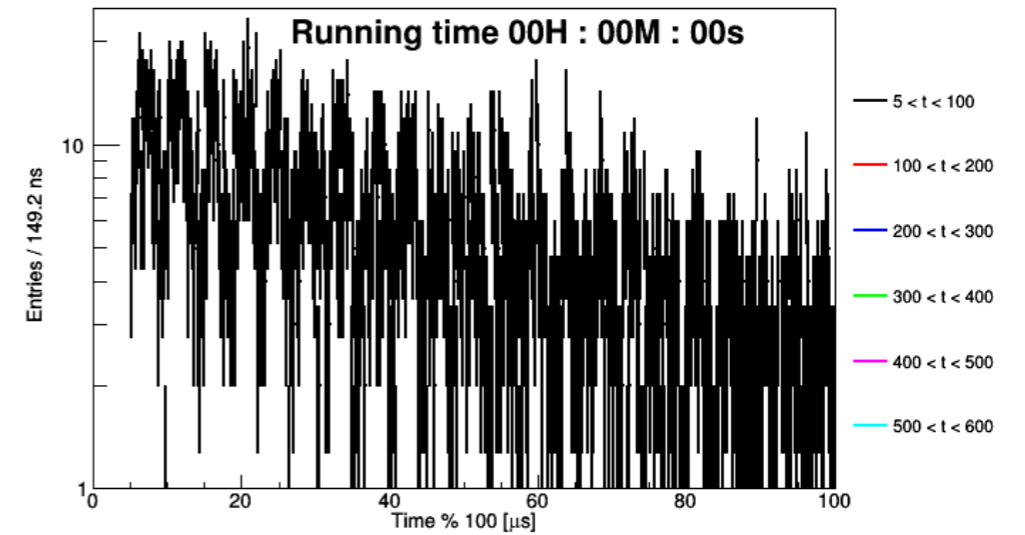


# Detectors : Calorimeters



## • Calorimeters

- 24 segmented PbF<sub>2</sub> crystal calorimeters stationed around the ring
- Detects energy and arrival time of e<sup>+</sup> decayed from muons:  $\mu^+ \rightarrow e^+ \bar{\nu}_\mu \nu_e$



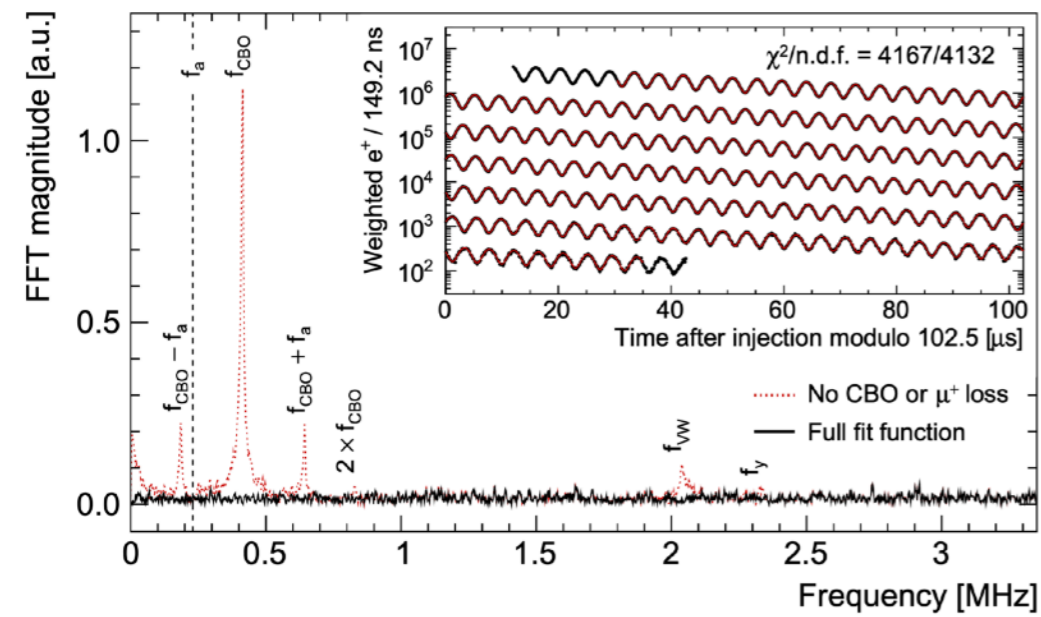
$$N(t) = N_0 e^{-t/\tau} [1 + A \cos(\omega_a t + \phi)]$$

$$a_\mu = \left( \frac{g_e}{2} \right) \left( \frac{\omega_a}{\langle \omega_p \rangle} \right) \left( \frac{\mu_p}{\mu_e} \right) \left( \frac{m_\mu}{m_e} \right)$$

# Calculating $\omega_a$ : Hidden information in the wiggle plot



## FFT analysis of fit residuals



# Calculating $\omega_a$ : Hidden information in the wiggle plot

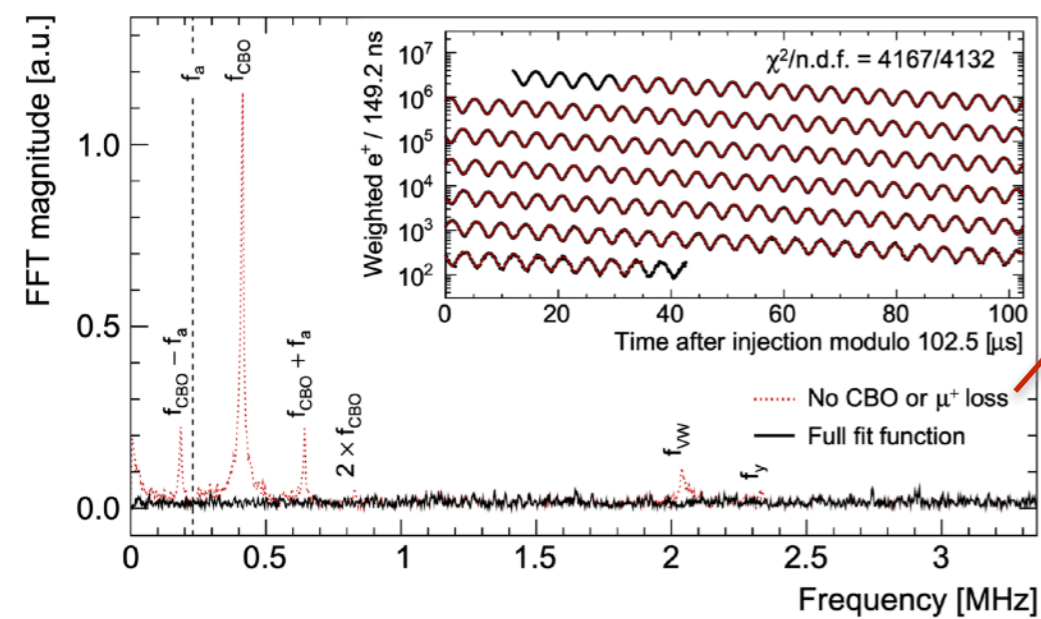


## Underling Physics

5 parameter fit function

$$N(t) = N_0 e^{-t/\tau} [1 + A \cos(\omega_a t + \phi)]$$

## FFT analysis of fit residuals



# Calculating $\omega_a$ : Hidden information in the wiggle plot



## Underling Physics

5 parameter fit function

$$N(t) = N_0 e^{-t/\tau} [1 + A \cos(\omega_a t + \phi)]$$

## Systematic Effects

Including CBO, lost muon, other beam dynamics related parameters improve the fit results

$$N_0 e^{-\frac{t}{\tau}} (1 + A \cdot A_{BO}(t) \cos(\omega_a t + \phi \cdot \phi_{BO}(t))) \cdot N_{CBO}(t) \cdot N_{VW}(t) \cdot N_y(t) \cdot N_{2CBO}(t) \cdot J(t)$$

$$A_{BO}(t) = 1 + A_A \cos(\omega_{CBO}(t) + \phi_A) e^{-\frac{t}{\tau_{CBO}}}$$

$$\phi_{BO}(t) = 1 + A_\phi \cos(\omega_{CBO}(t) + \phi_\phi) e^{-\frac{t}{\tau_{CBO}}}$$

$$N_{CBO}(t) = 1 + A_{CBO} \cos(\omega_{CBO}(t) + \phi_{CBO}) e^{-\frac{t}{\tau_{CBO}}}$$

$$N_{2CBO}(t) = 1 + A_{2CBO} \cos(2\omega_{CBO}(t) + \phi_{2CBO}) e^{-\frac{t}{2\tau_{CBO}}}$$

$$N_{VW}(t) = 1 + A_{VW} \cos(\omega_{VW}(t)t + \phi_{VW}) e^{-\frac{t}{\tau_{VW}}}$$

$$N_y(t) = 1 + A_y \cos(\omega_y(t)t + \phi_y) e^{-\frac{t}{\tau_y}}$$

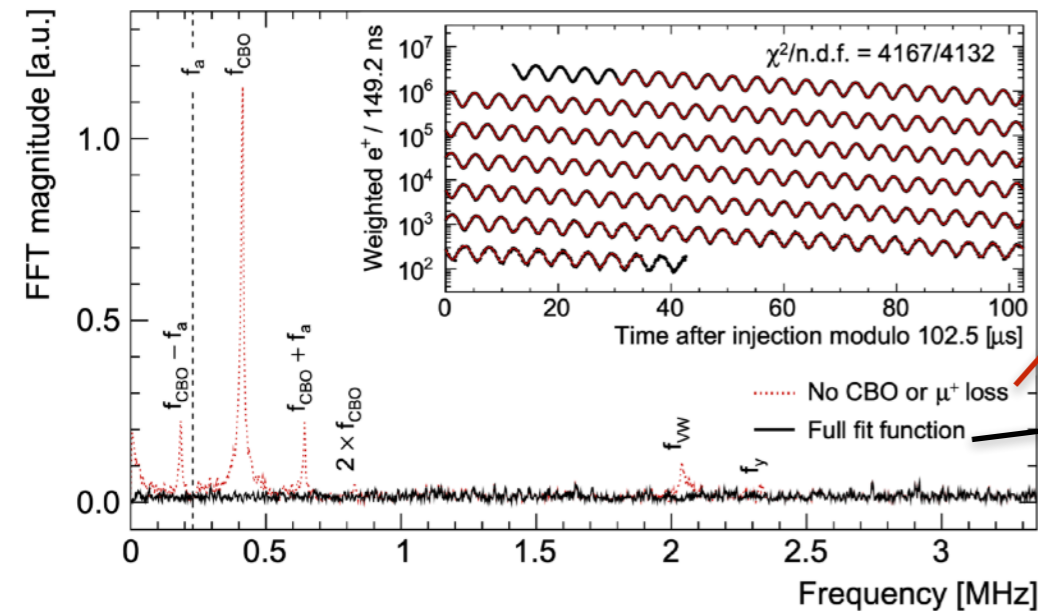
$$J(t) = 1 - k_{LM} \int_{t_0}^t \Lambda(t) dt$$

$$\omega_{CBO}(t) = \omega_0 t + A e^{-\frac{t}{\tau_A}} + B e^{-\frac{t}{\tau_B}}$$

$$\omega_y(t) = F \omega_{CBO}(t) \sqrt{2\omega_c / F \omega_{CBO}(t) - 1}$$

$$\omega_{VW}(t) = \omega_c - 2\omega_y(t)$$

## FFT analysis of fit residuals



# Calculating $\omega_a$ : Hidden information in the wiggle plot



## Underling Physics

5 parameter fit function

$$N(t) = N_0 e^{-t/\tau} [1 + A \cos(\omega_a t + \phi)]$$

## Systematic Effects

Including CBO, lost muon, other beam dynamics related parameters improve the fit results

$$N_0 e^{-\frac{t}{\tau}} (1 + A \cdot A_{BO}(t) \cos(\omega_a t + \phi \cdot \phi_{BO}(t))) \cdot N_{CBO}(t) \cdot N_{VW}(t) \cdot N_y(t) \cdot N_{2CBO}(t) \cdot J(t)$$

$$A_{BO}(t) = 1 + A_A \cos(\omega_{CBO}(t) + \phi_A) e^{-\frac{t}{\tau_{CBO}}}$$

$$\phi_{BO}(t) = 1 + A_\phi \cos(\omega_{CBO}(t) + \phi_\phi) e^{-\frac{t}{\tau_{CBO}}}$$

$$N_{CBO}(t) = 1 + A_{CBO} \cos(\omega_{CBO}(t) + \phi_{CBO}) e^{-\frac{t}{\tau_{CBO}}}$$

$$N_{2CBO}(t) = 1 + A_{2CBO} \cos(2\omega_{CBO}(t) + \phi_{2CBO}) e^{-\frac{t}{2\tau_{CBO}}}$$

$$N_{VW}(t) = 1 + A_{VW} \cos(\omega_{VW}(t)t + \phi_{VW}) e^{-\frac{t}{\tau_{VW}}}$$

$$N_y(t) = 1 + A_y \cos(\omega_y(t)t + \phi_y) e^{-\frac{t}{\tau_y}}$$

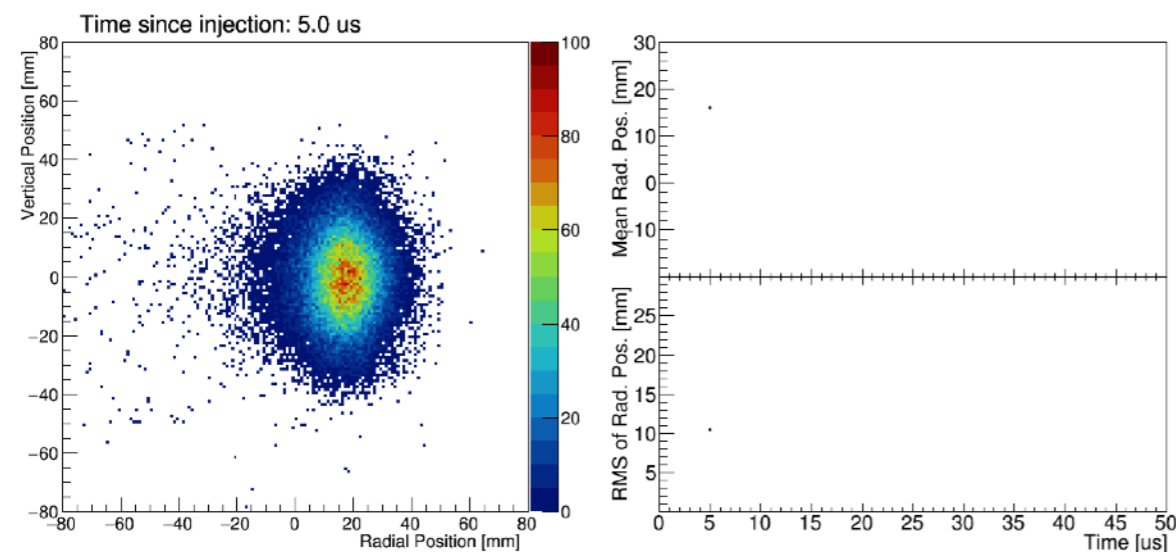
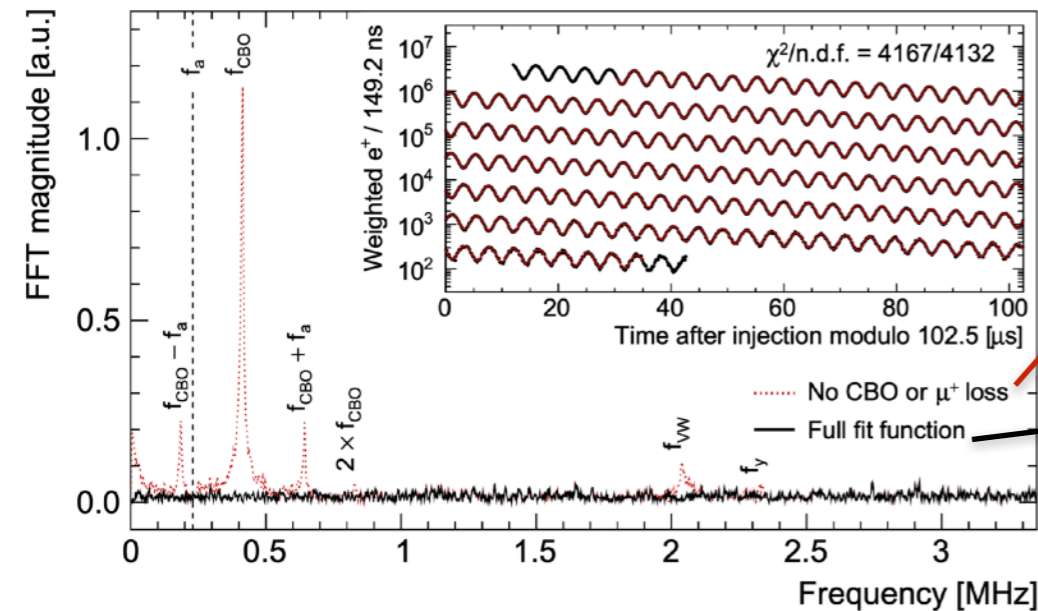
$$J(t) = 1 - k_{LM} \int_{t_0}^t \Lambda(t) dt$$

$$\omega_{CBO}(t) = \omega_0 t + A e^{-\frac{t}{\tau_A}} + B e^{-\frac{t}{\tau_B}}$$

$$\omega_y(t) = F \omega_{CBO}(t) \sqrt{2\omega_c / F \omega_{CBO}(t) - 1}$$

$$\omega_{VW}(t) = \omega_c - 2\omega_y(t)$$

## FFT analysis of fit residuals



# Calculating $\omega_a$ : Hidden information in the wiggle plot



## Underling Physics

5 parameter fit function

$$N(t) = N_0 e^{-t/\tau} [1 + A \cos(\omega_a t + \phi)]$$

## Systematic Effects

Including CBO, lost muon, other beam dynamics related parameters improve the fit results

$$N_0 e^{-\frac{t}{\tau}} (1 + A \cdot A_{BO}(t) \cos(\omega_a t + \phi \cdot \phi_{BO}(t))) \cdot N_{CBO}(t) \cdot N_{VW}(t) \cdot N_y(t) \cdot N_{2CBO}(t) \cdot J(t)$$

$$A_{BO}(t) = 1 + A_A \cos(\omega_{CBO}(t) + \phi_A) e^{-\frac{t}{\tau_{CBO}}}$$

$$\phi_{BO}(t) = 1 + A_\phi \cos(\omega_{CBO}(t) + \phi_\phi) e^{-\frac{t}{\tau_{CBO}}}$$

$$N_{CBO}(t) = 1 + A_{CBO} \cos(\omega_{CBO}(t) + \phi_{CBO}) e^{-\frac{t}{\tau_{CBO}}}$$

$$N_{2CBO}(t) = 1 + A_{2CBO} \cos(2\omega_{CBO}(t) + \phi_{2CBO}) e^{-\frac{t}{2\tau_{CBO}}}$$

$$N_{VW}(t) = 1 + A_{VW} \cos(\omega_{VW}(t)t + \phi_{VW}) e^{-\frac{t}{\tau_{VW}}}$$

$$N_y(t) = 1 + A_y \cos(\omega_y(t)t + \phi_y) e^{-\frac{t}{\tau_y}}$$

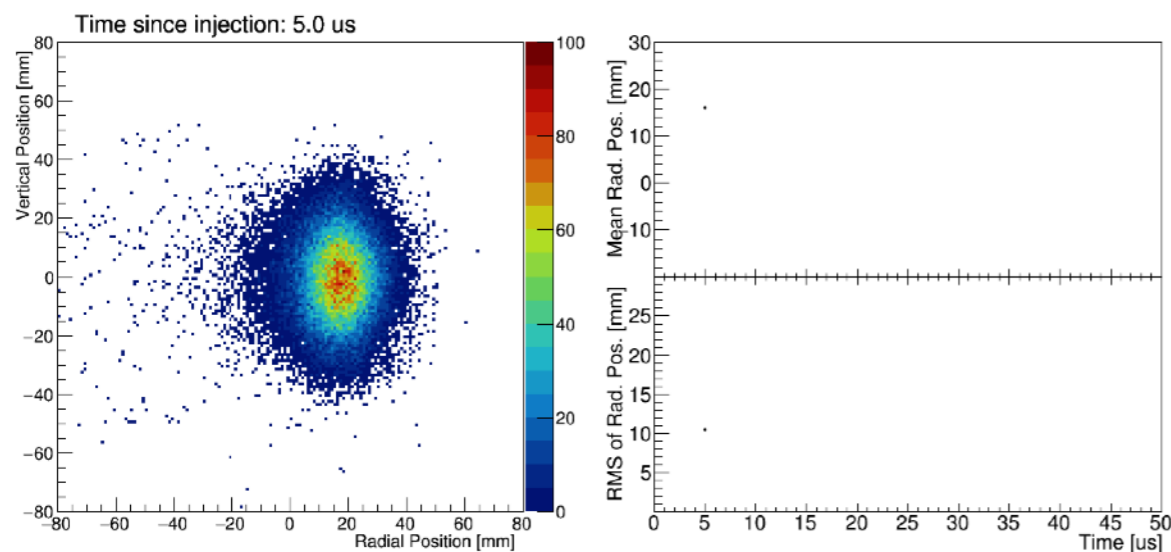
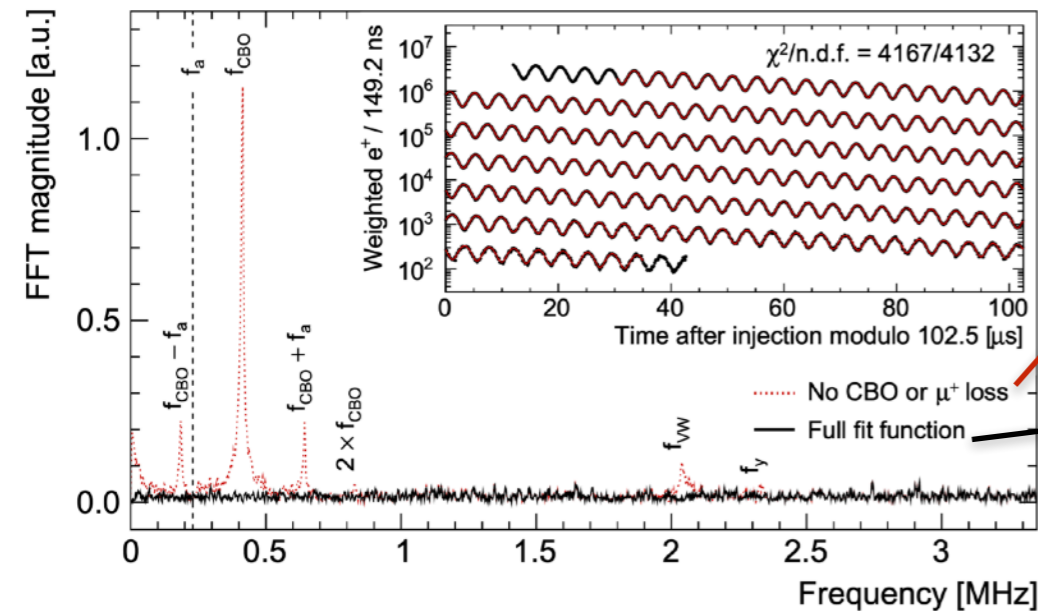
$$J(t) = 1 - k_{LM} \int_{t_0}^t \Lambda(t) dt$$

$$\omega_{CBO}(t) = \omega_0 t + A e^{-\frac{t}{\tau_A}} + B e^{-\frac{t}{\tau_B}}$$

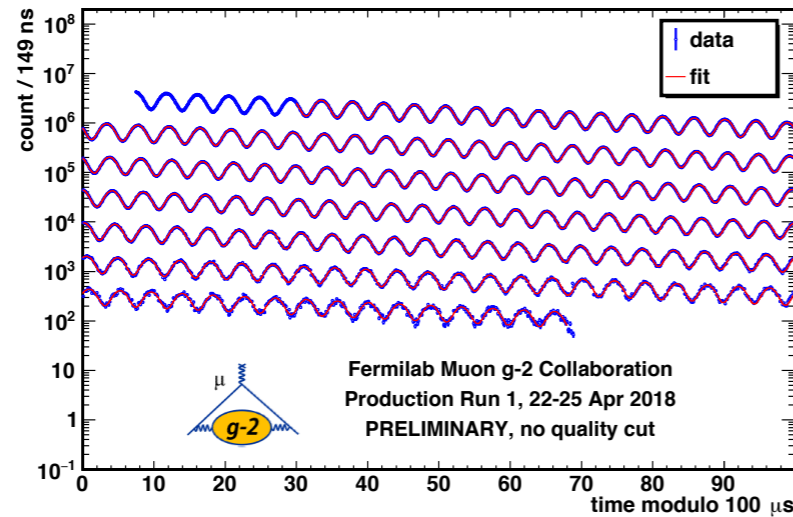
$$\omega_y(t) = F \omega_{CBO}(t) \sqrt{2\omega_c / F \omega_{CBO}(t) - 1}$$

$$\omega_{VW}(t) = \omega_c - 2\omega_y(t)$$

## FFT analysis of fit residuals



# Measuring the Muon Anomaly

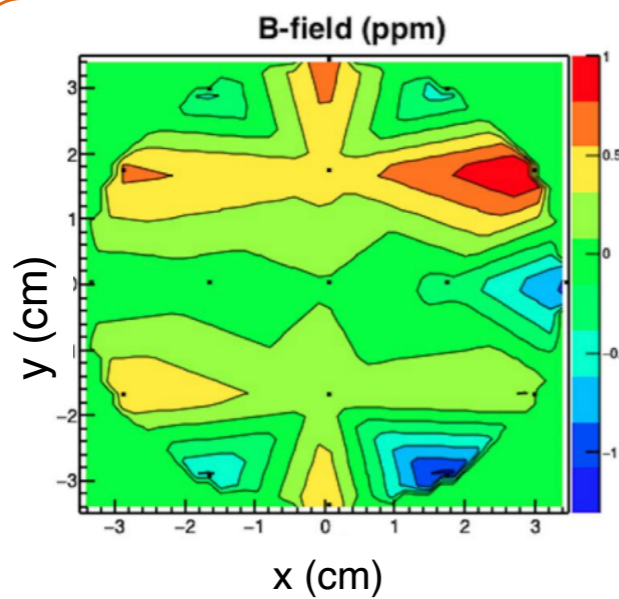


$\omega_a$

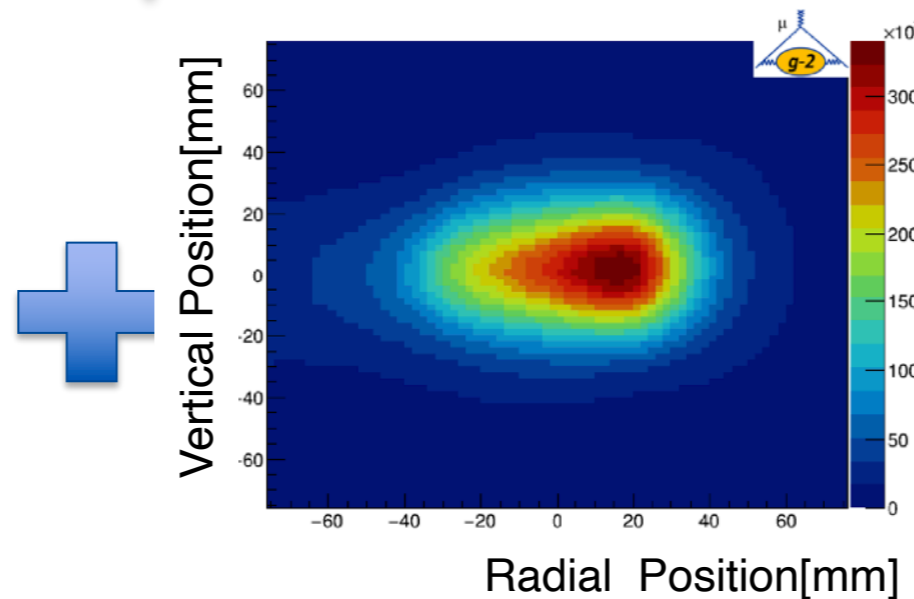
Extract from decay positron time spectra  
 $N(t) = N_0 e^{-t/\tau_\mu} [1 + A \cos(\omega_a t + \phi)]$

$$a_\mu = \left( \frac{g_e}{2} \right) \left( \frac{\omega_a}{\langle \omega_p \rangle} \right) \left( \frac{\mu_p}{\mu_e} \right) \left( \frac{m_\mu}{m_e} \right)$$

0.26 ppt
3 ppb
22 ppb
⇒ 2017 CODATA



Map the magnetic field



Obtain muon distribution In the storage ring

$$\langle \omega_p \rangle \approx \omega_p \otimes \rho(r)$$

Average magnetic field weighted by muon distribution

$\omega_p$ : free proton precession frequency  
 Using proton NMR  $\hbar\omega_p = 2\mu_p B$

# Systematics from Run-1

$$a_{\mu} \propto \frac{f_{\text{clock}} \omega_a^m (1 + C_e + C_p + C_{ml} + C_{pa})}{f_{\text{calib}} \langle \omega'_p(x, y, \phi) \times M(x, y, \phi) \rangle (1 + B_k + B_q)}$$

$f_{\text{clock}}$  •Blinded clock

$\omega_a^m$  •Measured precession frequency

$C_e$  •Electric field correction

$C_p$  •Pitch correction

$C_{ml}$  •Muon loss correction

$C_{pa}$  •Phase-acceptance correction

$f_{\text{calib}}$  •Absolute magnetic field calibration

$\omega'_p(x, y, \phi)$  •Field tracking multipole distribution

$M(x, y, \phi)$  •Muon weighted multipole distributed

$B_k$  •Transient field from the eddy current in kicker

$B_q$  •Transient field from the quad charging

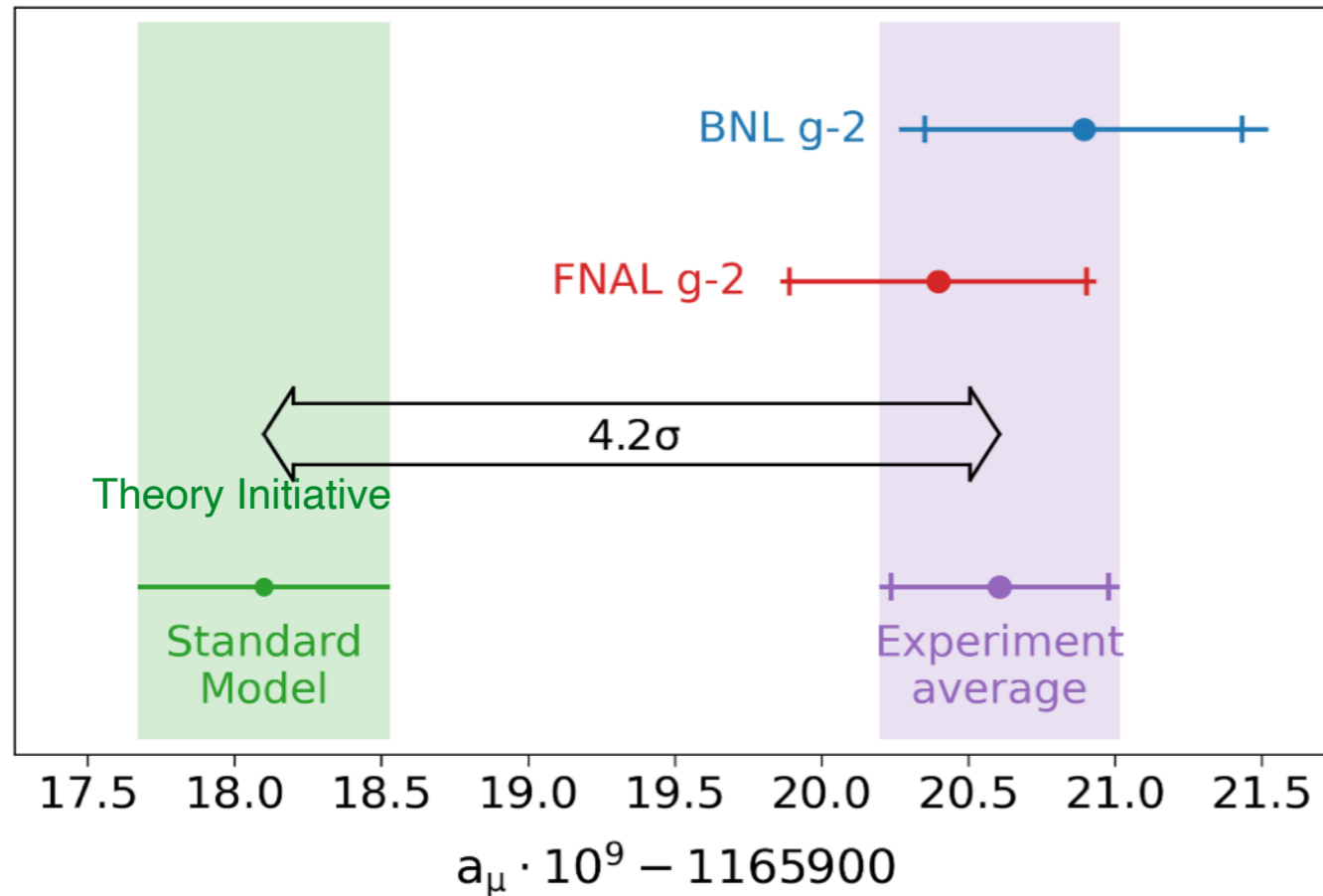
Phase acceptance and transient field corrections are the largest systematics!



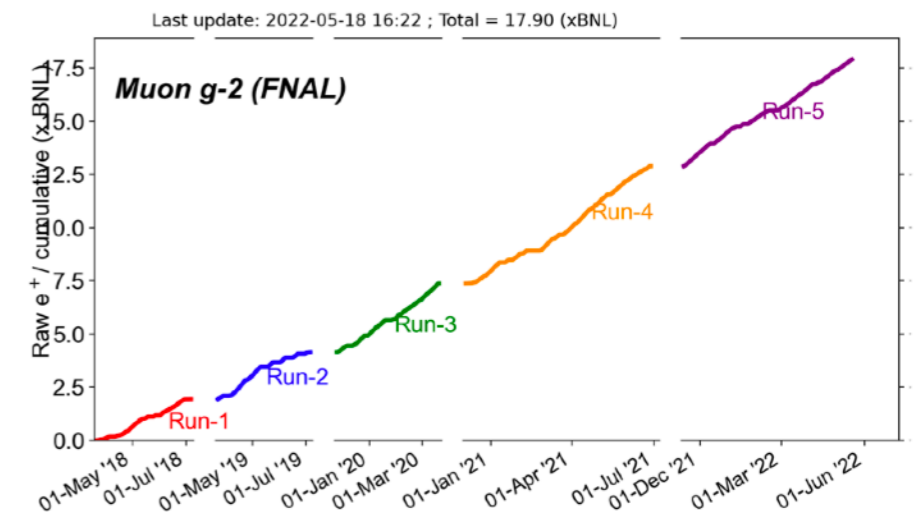
# Crunching the numbers...

Quantity	Correction Terms (ppb)	Uncertainty (ppb)	
$\omega_a$ (statistical)	–	434	Dominated by statistical uncertainty
$\omega_a$ (systematic)	–	56	
$C_e$	489	53	
$C_p$	180	13	
$C_{ml}$	-11	5	
$C_{pa}$	-158	75	← Systematics dominated by PA and Field Transients
$f_{\text{calib}} \langle \omega'_p(x, y, \phi) \times M(x, y, \phi) \rangle$	–	56	
$B_k$	-27	37	
$B_q$	-17	92	←
$\mu'_p(34.7^\circ)/\mu_e$	–	10	
$m_\mu/m_e$	–	22	
$g_e/2$	–	0	
Total systematic	–	157	← *Nearly half of BNL *Will be even better for Run-2 and beyond
Total fundamental factors	–	25	
Totals	544	462	

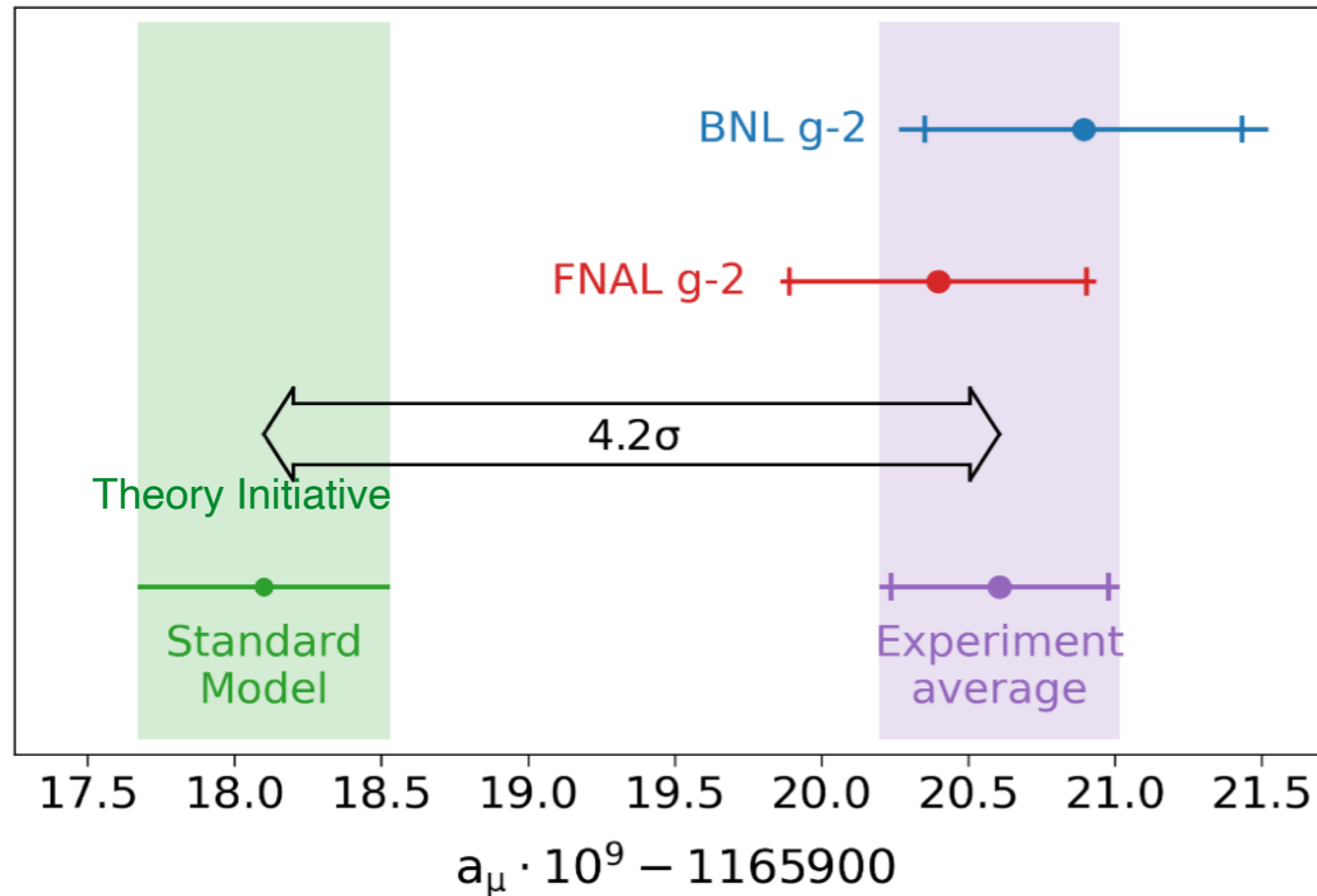
# Fermilab Muon g-2 First Result and the Comparison



- ✓ FNAL determined anomaly with 460 ppb precision
- ✓ Nothing was found that indicated contradiction with BNL results
- ✓ 15% smaller error
- ✓ Good agreement

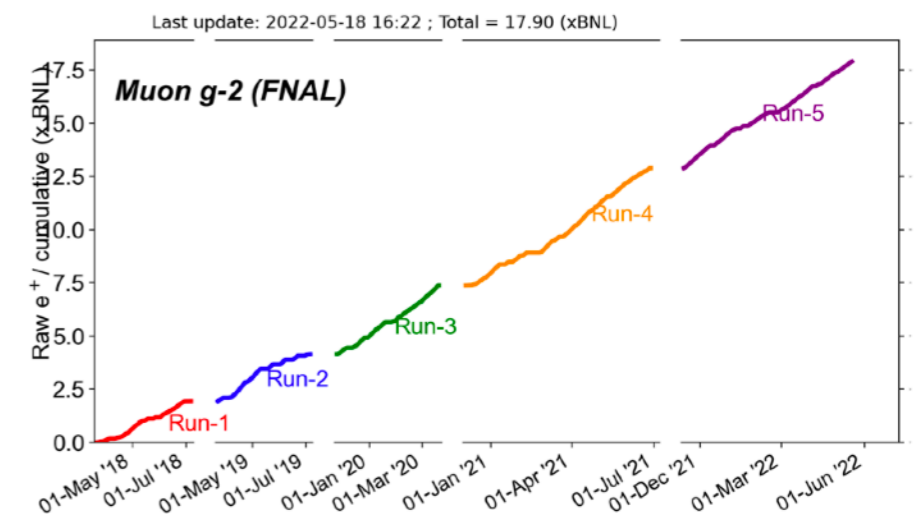


# Fermilab Muon g-2 First Result and the Comparison

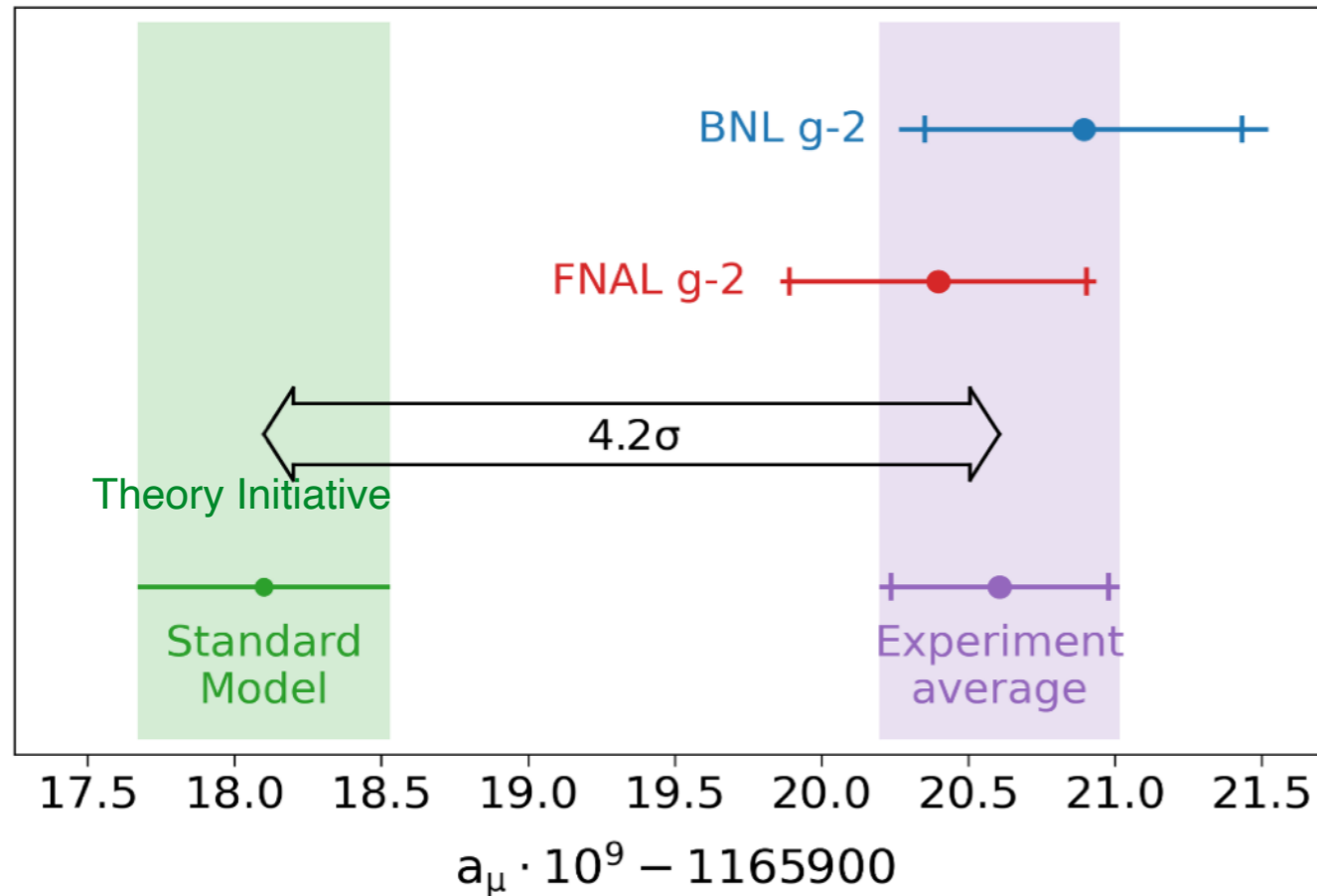


$$a_{\mu} (\text{BNL}) = 116\,592\,089(63) \times 10^{-11} \text{ (540 ppb)}$$

- ✓ FNAL determined anomaly with 460 ppb precision
- ✓ Nothing was found that indicated contradiction with BNL results
- ✓ 15% smaller error
- ✓ Good agreement



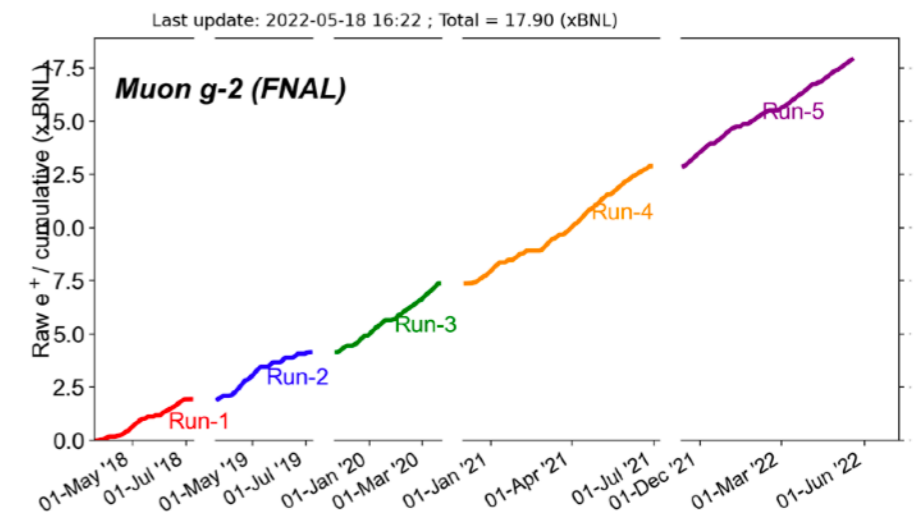
# Fermilab Muon g-2 First Result and the Comparison



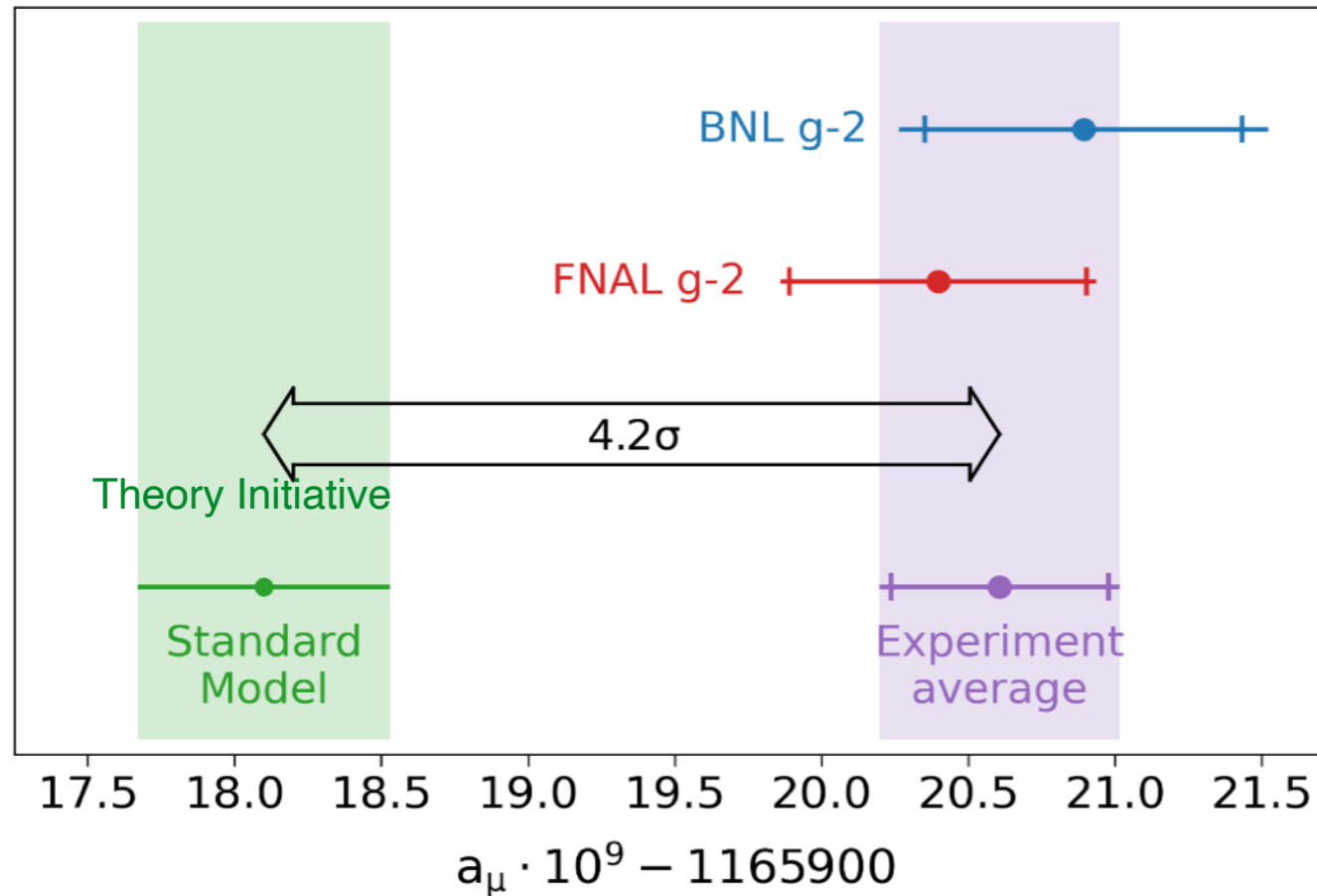
$$a_\mu (\text{BNL}) = 116\,592\,089(63) \times 10^{-11} \text{ (540 ppb)}$$

$$a_\mu (\text{FNAL}) = 116\,592\,040(54) \times 10^{-11} \text{ (460 ppb)}$$

- ✓ FNAL determined anomaly with 460 ppb precision
- ✓ Nothing was found that indicated contradiction with BNL results
- ✓ 15% smaller error
- ✓ Good agreement



# Fermilab Muon g-2 First Result and the Comparison

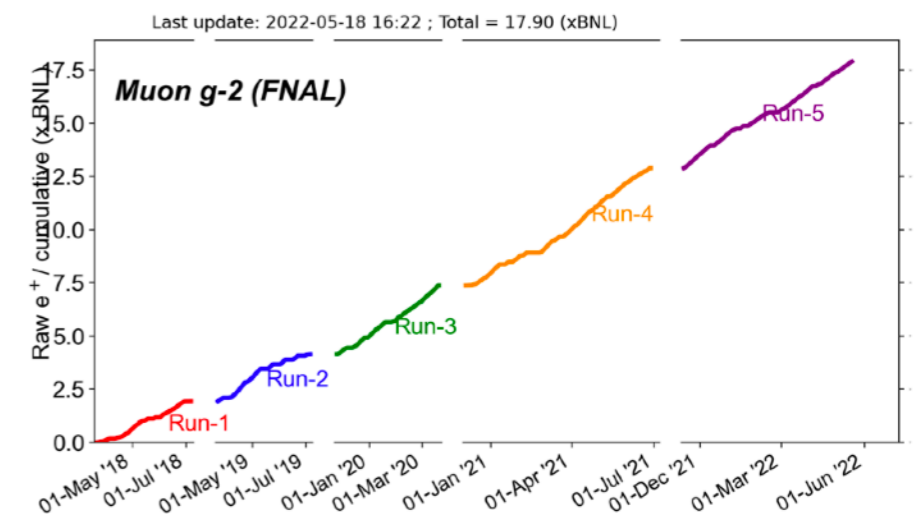


$$a_\mu (\text{BNL}) = 116\,592\,089(63) \times 10^{-11} \text{ (540 ppb)}$$

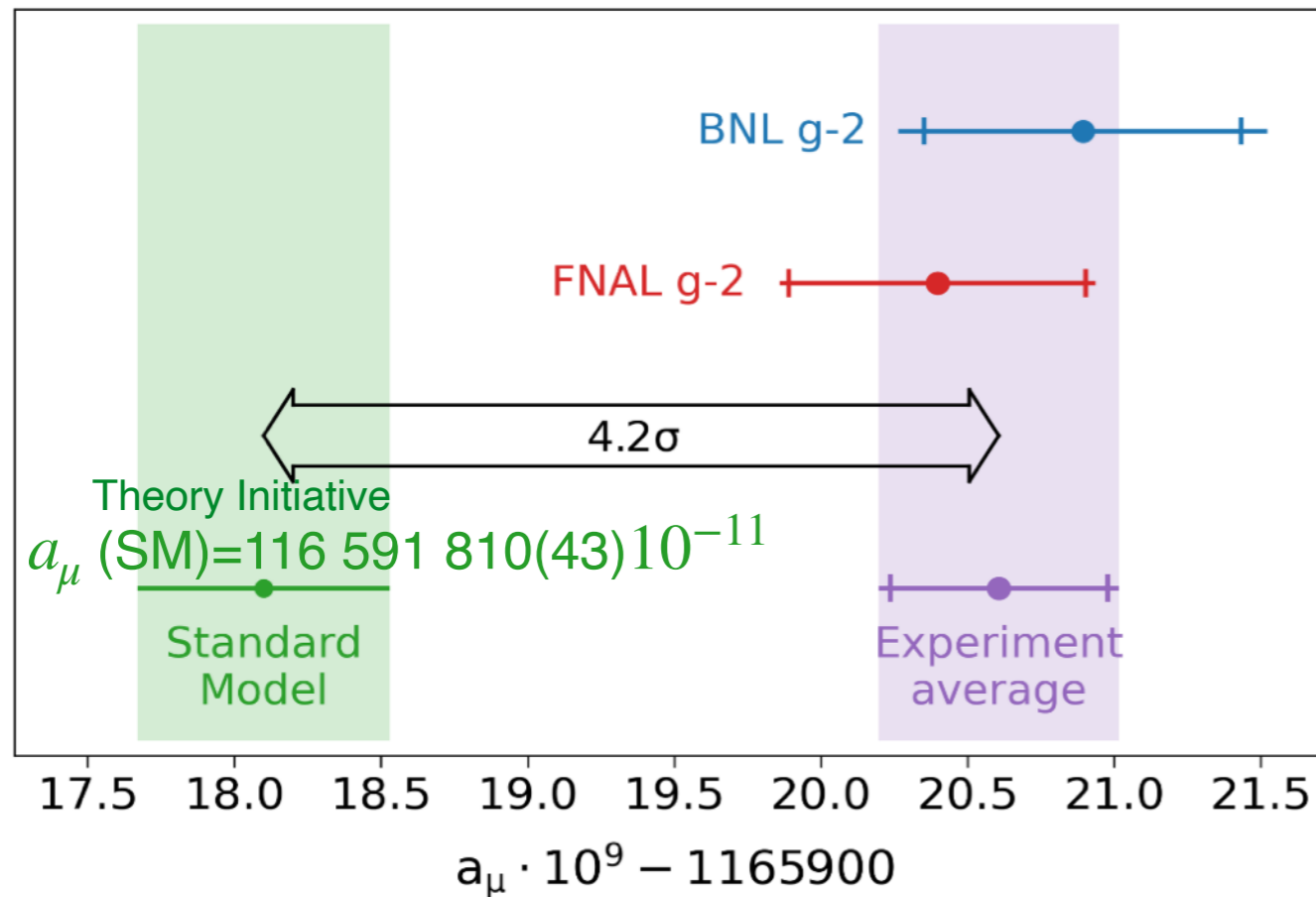
$$a_\mu (\text{FNAL}) = 116\,592\,040(54) \times 10^{-11} \text{ (460 ppb)}$$

$$a_\mu (\text{Exp}) = 116\,592\,061(41) \times 10^{-11} \text{ (350 ppb)}$$

- ✓ FNAL determined anomaly with 460 ppb precision
- ✓ Nothing was found that indicated contradiction with BNL results
- ✓ 15% smaller error
- ✓ Good agreement



# Fermilab Muon g-2 First Result and the Comparison

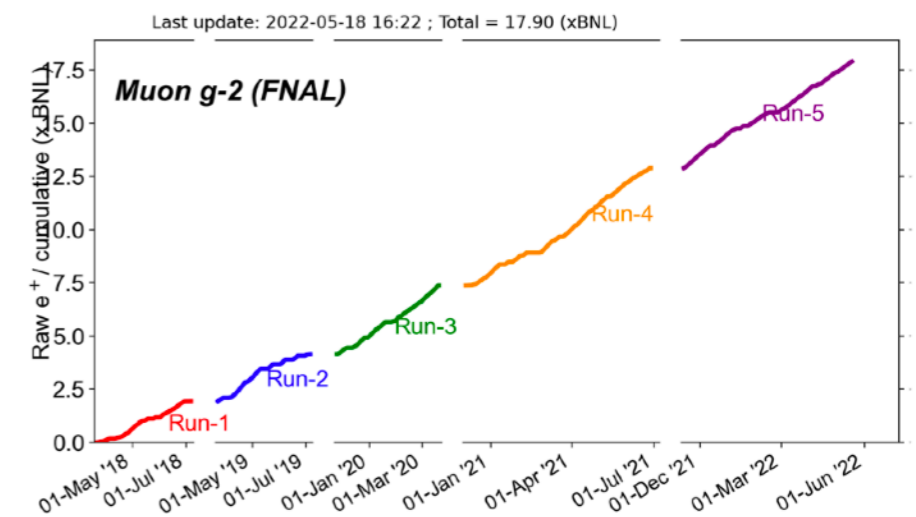


$$a_\mu \text{ (BNL)} = 116\,592\,089(63) \times 10^{-11} \text{ (540 ppb)}$$

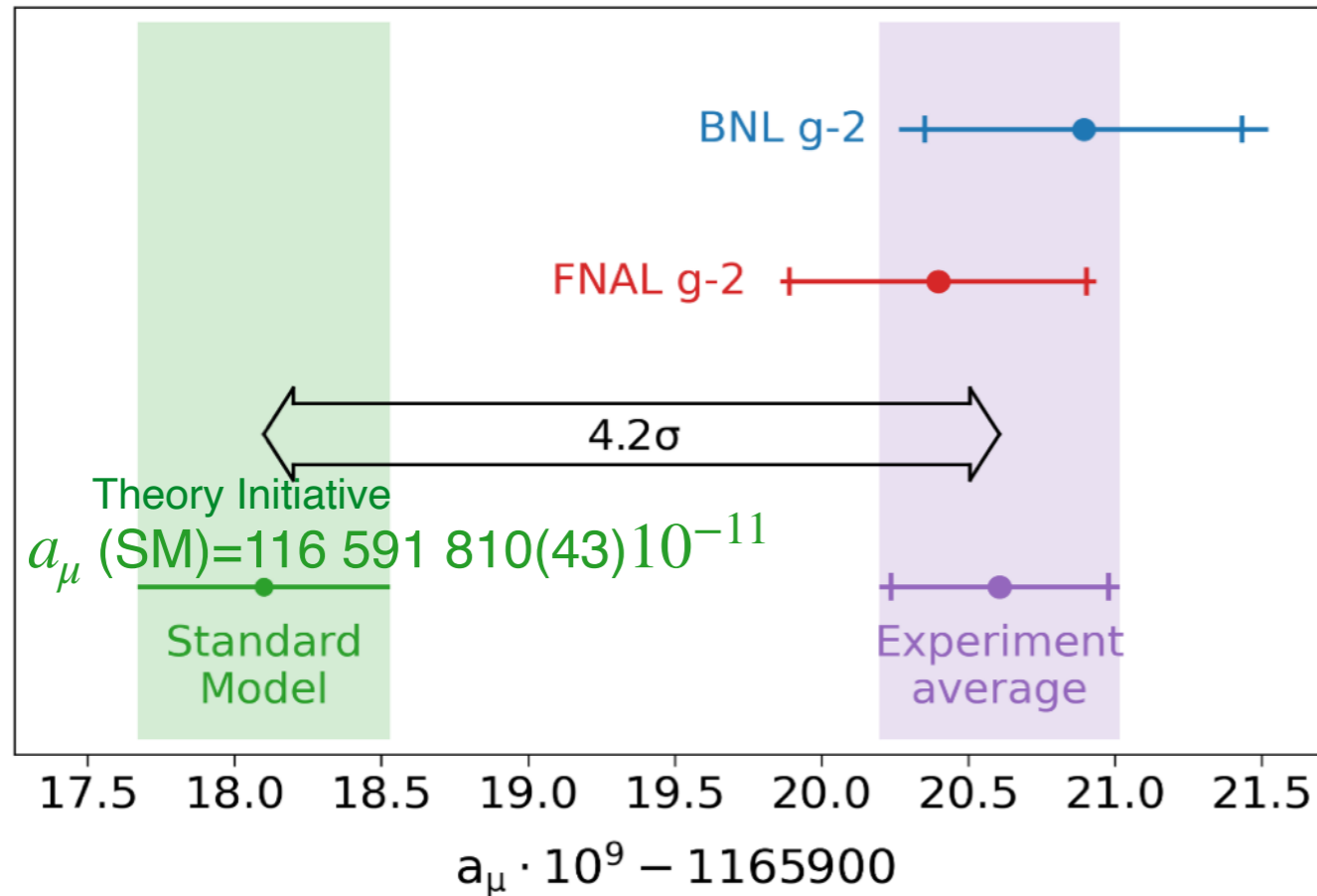
$$a_\mu \text{ (FNAL)} = 116\,592\,040(54) \times 10^{-11} \text{ (460 ppb)}$$

$$a_\mu \text{ (Exp)} = 116\,592\,061(41) \times 10^{-11} \text{ (350 ppb)}$$

- ✓ FNAL determined anomaly with 460 ppb precision
- ✓ Nothing was found that indicated contradiction with BNL results
- ✓ 15% smaller error
- ✓ Good agreement



# Fermilab Muon g-2 First Result and the Comparison



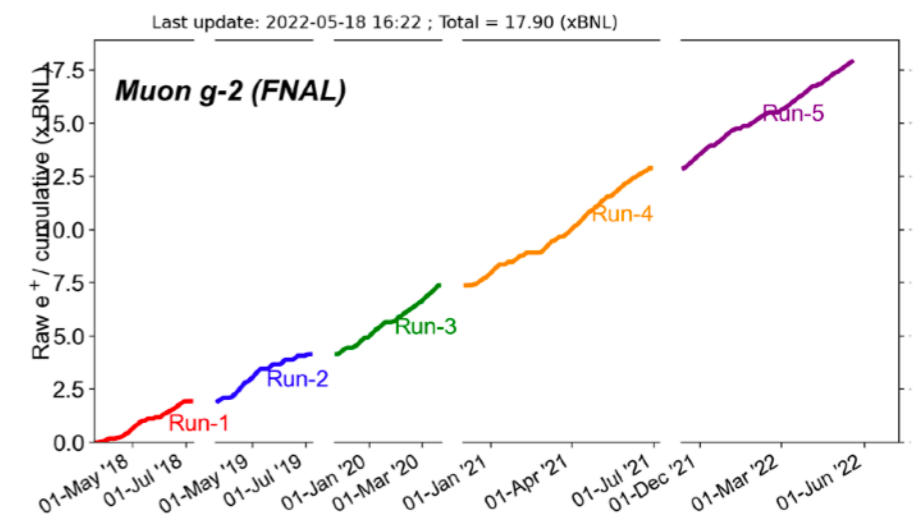
$$a_\mu \text{ (BNL)} = 116\,592\,089(63) \times 10^{-11} \text{ (540 ppb)}$$

$$a_\mu \text{ (FNAL)} = 116\,592\,040(54) \times 10^{-11} \text{ (460 ppb)}$$

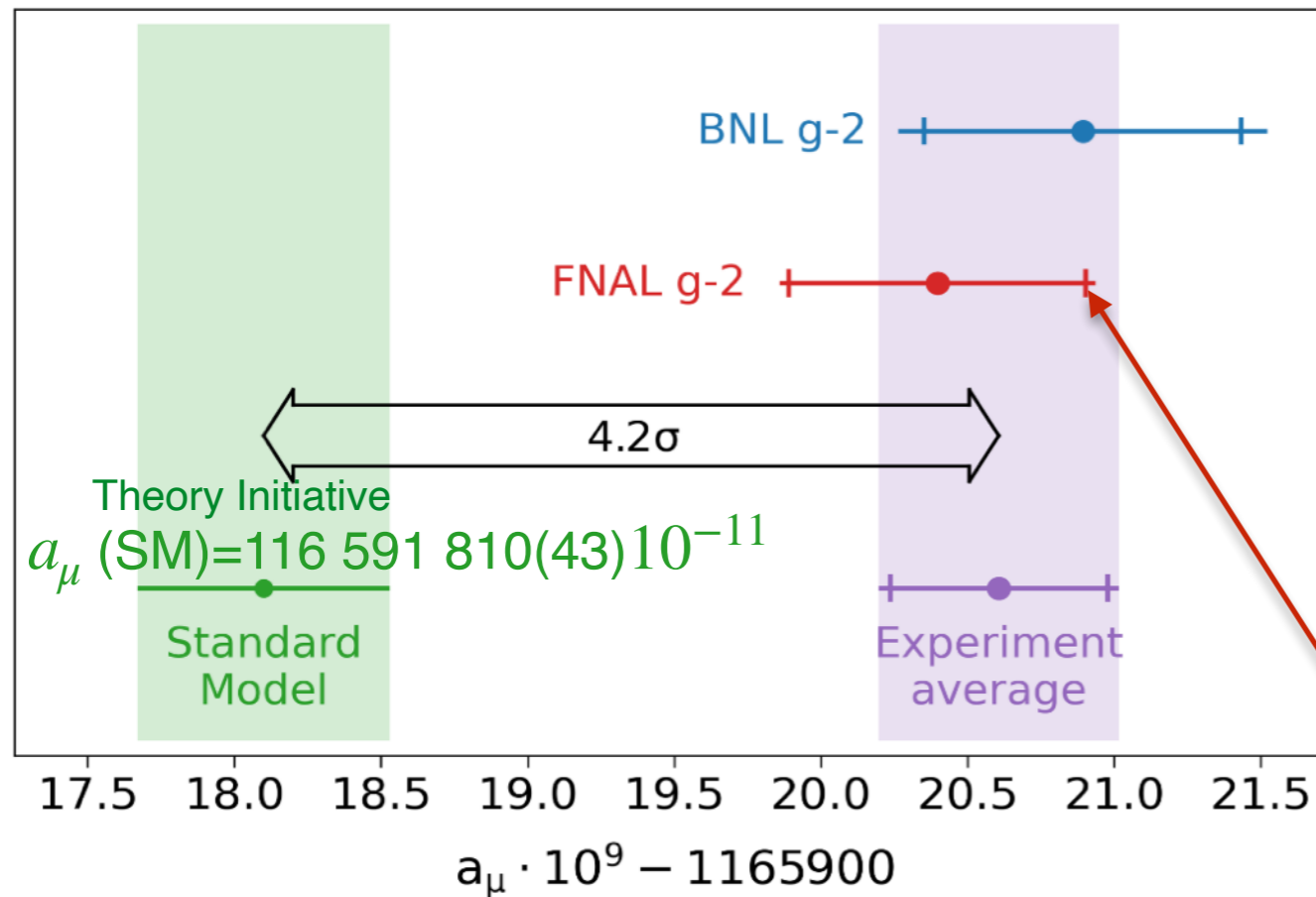
$$a_\mu \text{ (Exp-SM)} = 251(59) \times 10^{-11} \rightarrow 4.2\sigma$$

$$a_\mu \text{ (Exp)} = 116\,592\,061(41) \times 10^{-11} \text{ (350 ppb)}$$

- ✓ FNAL determined anomaly with 460 ppb precision
- ✓ Nothing was found that indicated contradiction with BNL results
- ✓ 15% smaller error
- ✓ Good agreement



# Fermilab Muon g-2 First Result and the Comparison



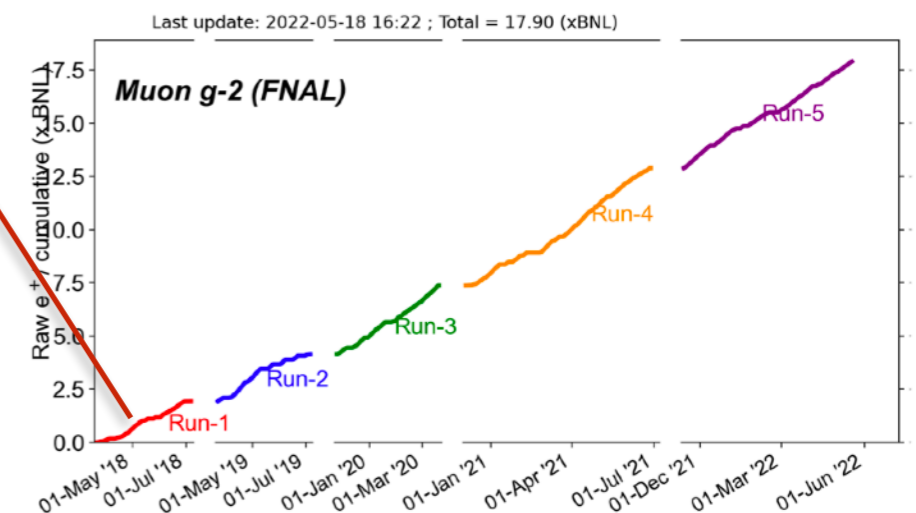
$$a_{\mu} \text{ (BNL)} = 116\,592\,089(63) \times 10^{-11} \text{ (540 ppb)}$$

$$a_{\mu} \text{ (FNAL)} = 116\,592\,040(54) \times 10^{-11} \text{ (460 ppb)}$$

$$a_{\mu} \text{ (Exp-SM)} = 251(59) \times 10^{-11} \rightarrow 4.2\sigma$$

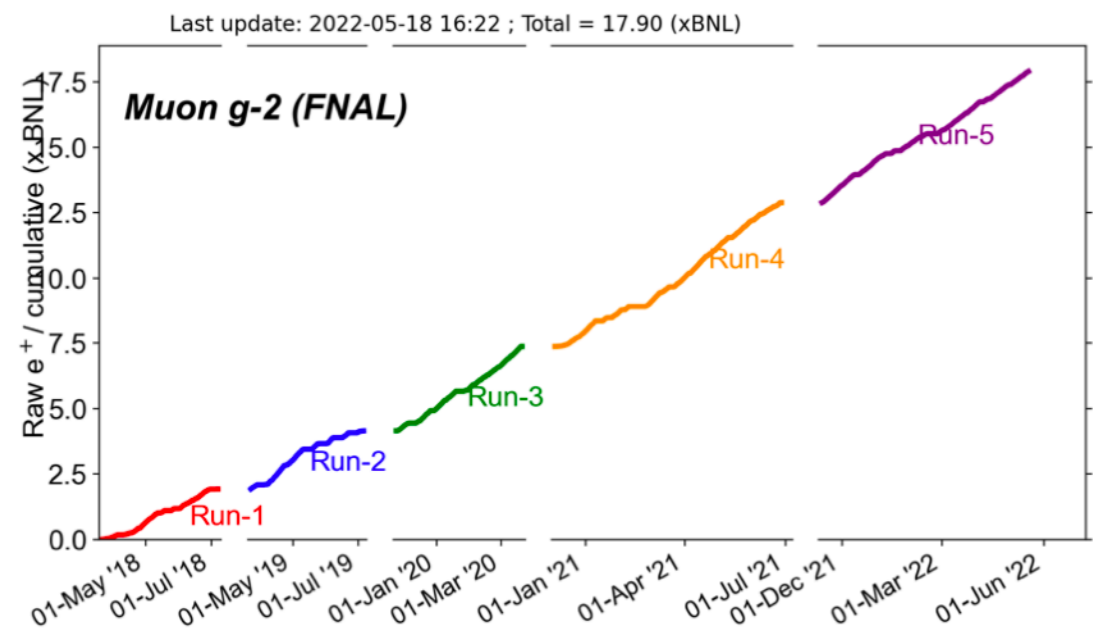
$$a_{\mu} \text{ (Exp)} = 116\,592\,061(41) \times 10^{-11} \text{ (350 ppb)}$$

- ✓ FNAL determined anomaly with 460 ppb precision
- ✓ Nothing was found that indicated contradiction with BNL results
- ✓ 15% smaller error
- ✓ Good agreement



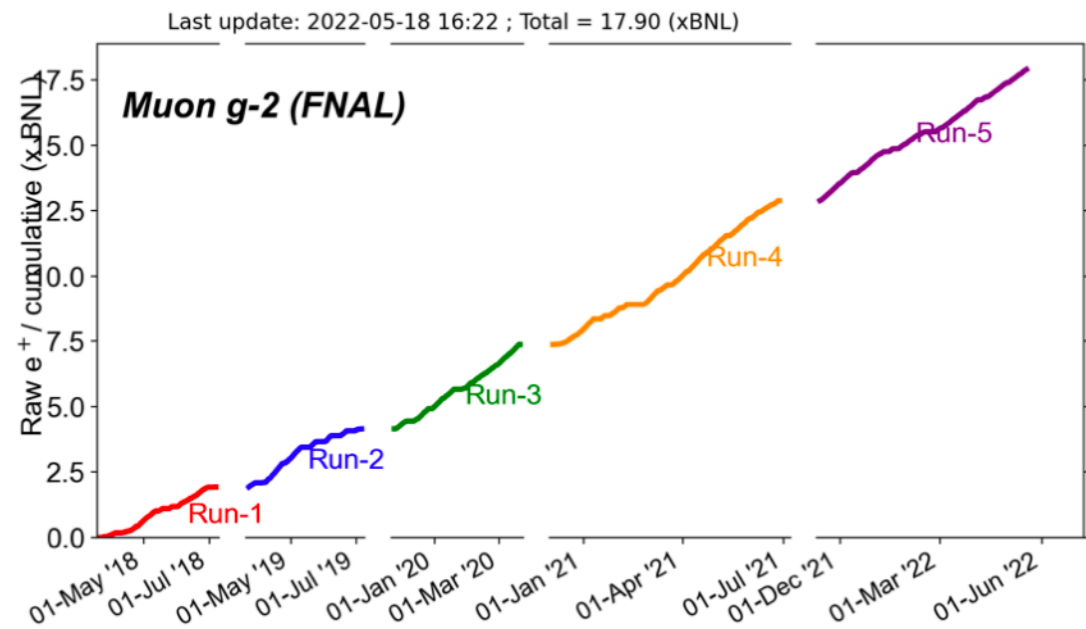


# Improvements on the g-2 uncertainty

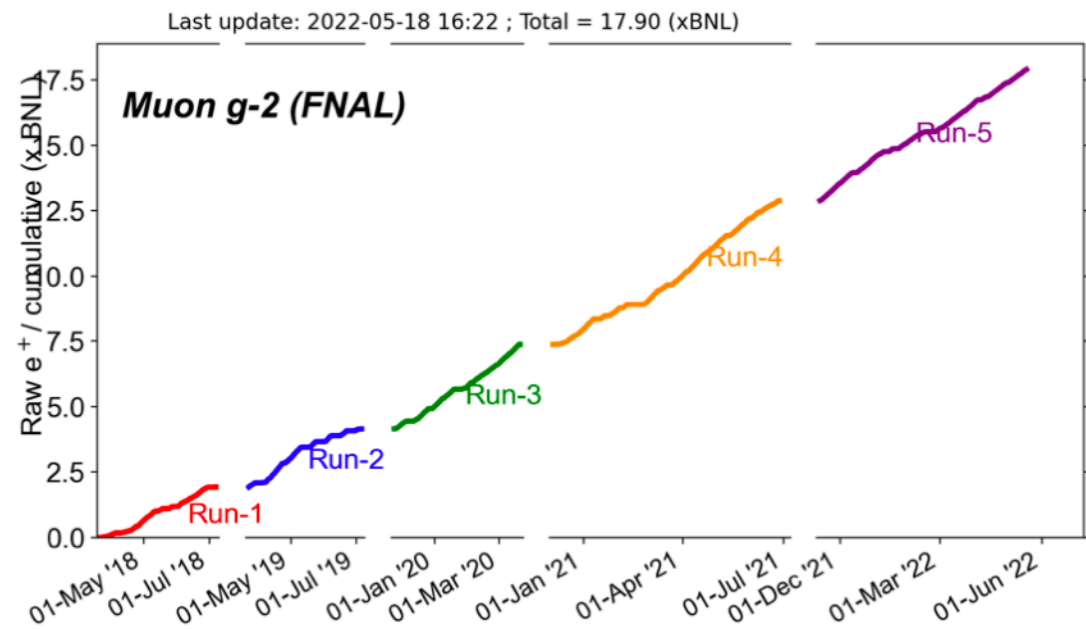


# Improvements on the g-2 uncertainty

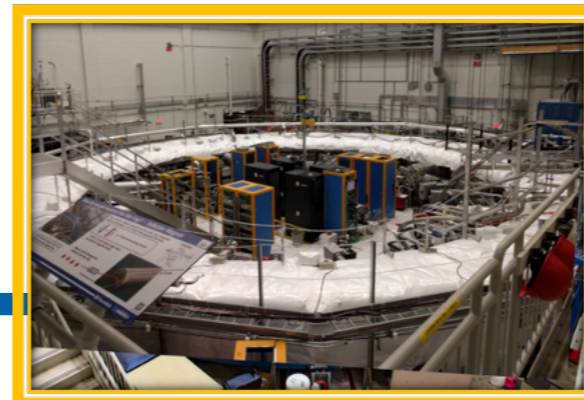
- Run-5 started in November 2021
  - Improved kick: Most recent part of Run-3 had a perfectly centered beam owing to improved kicker system.



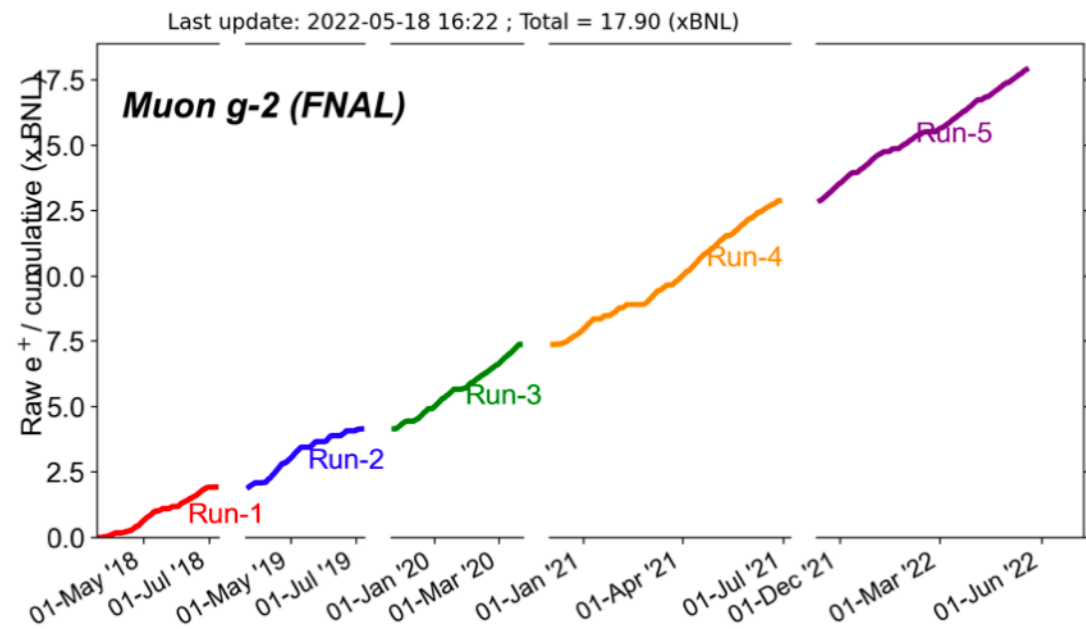
# Improvements on the g-2 uncertainty



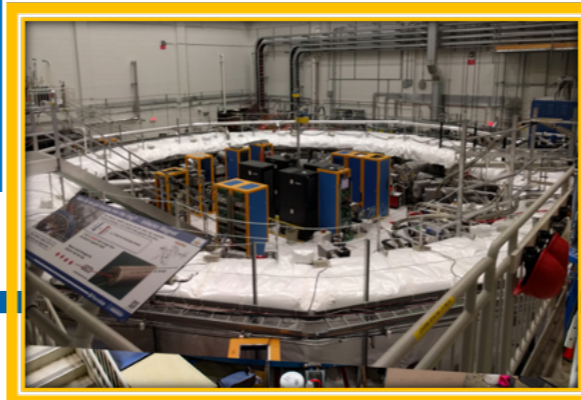
- Run-5 started in November 2021
  - Improved kick: Most recent part of Run-3 had a perfectly centered beam owing to improved kicker system.
  - Improved field stability: More stable temperature and better magnet insulation.



# Improvements on the g-2 uncertainty

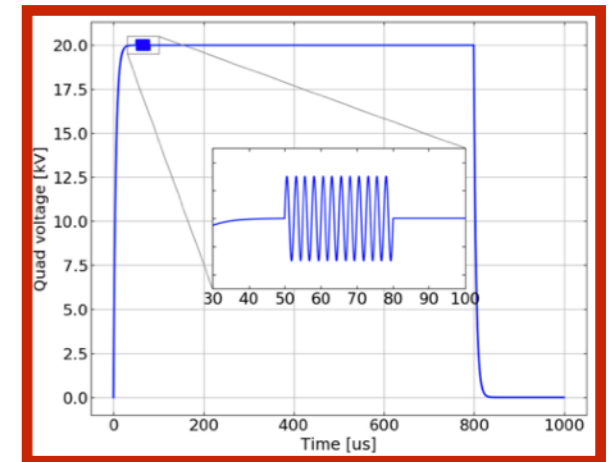
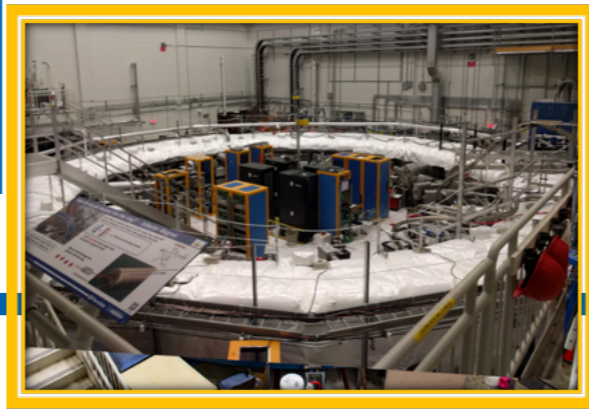
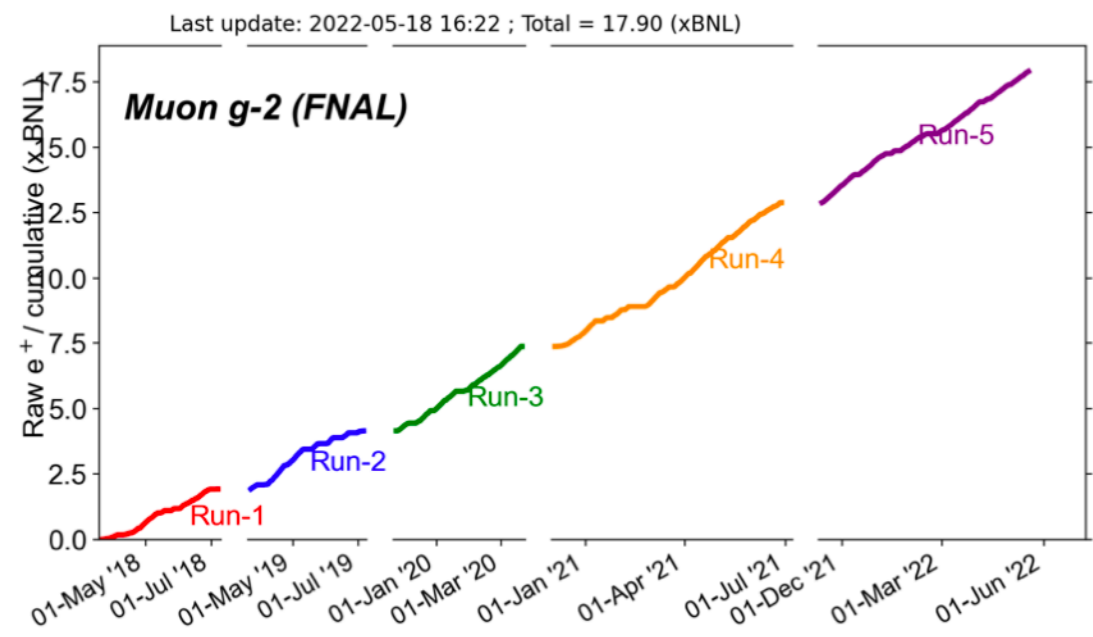


- Run-5 started in November 2021
  - Improved kick: Most recent part of Run-3 had a perfectly centered beam owing to improved kicker system.
  - Improved field stability: More stable temperature and better magnet insulation.
  - Damaged HV resistors were replaced after Run-1



# Improvements on the g-2 uncertainty

- Run-5 started in November 2021
  - Improved kick: Most recent part of Run-3 had a perfectly centered beam owing to improved kicker system.
  - Improved field stability: More stable temperature and better magnet insulation.
  - Damaged HV resistors were replaced after Run-1
  - RF System is fully integrated in Run-5

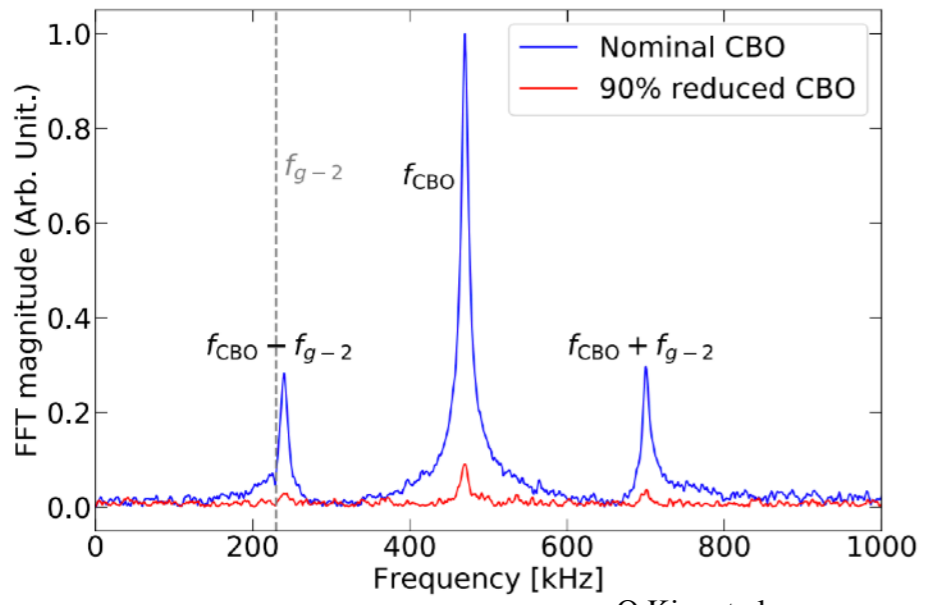


# Improvements since Run-1: Quad-RF System

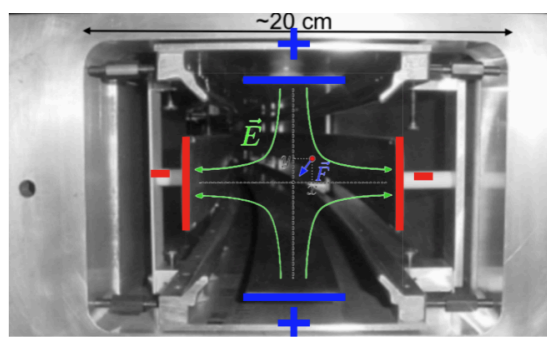
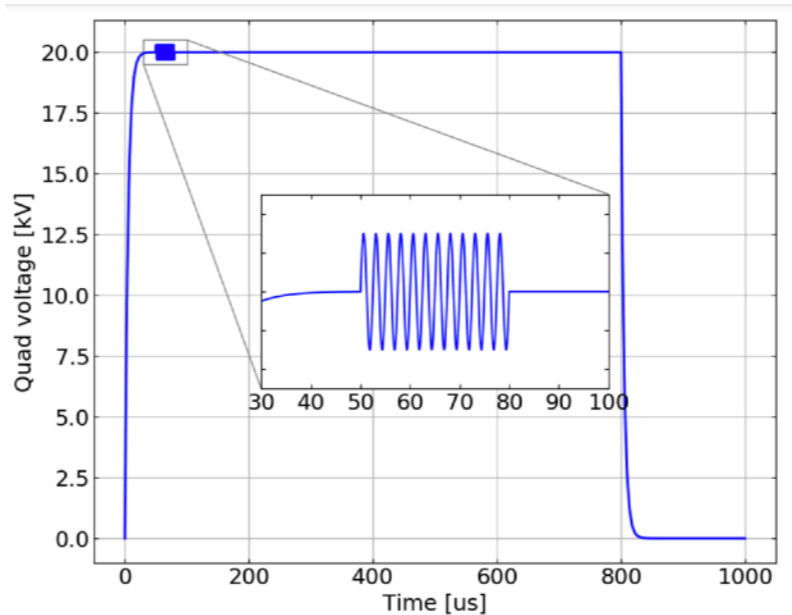
Original idea from Yuri F. Orlov and Yannis Semertzidis (Muon g-2 Note #431). By applying RF dipole or quadrupole electric field; (by kicking the beam out of phase with CBO)

- Reduce CBO Amplitude ( Due to an imperfect kicker system, the beam executes CBO oscillations with a large amplitude)
- Reduce muon loss by scraping the beam

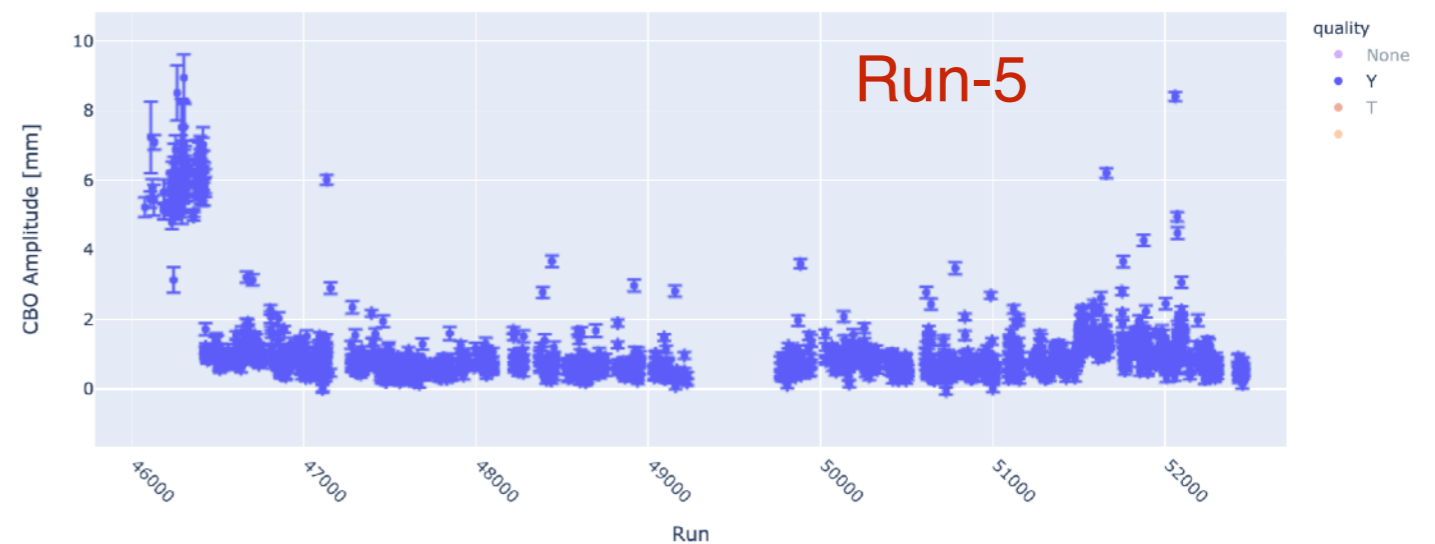
RF can be applied through the quad plates



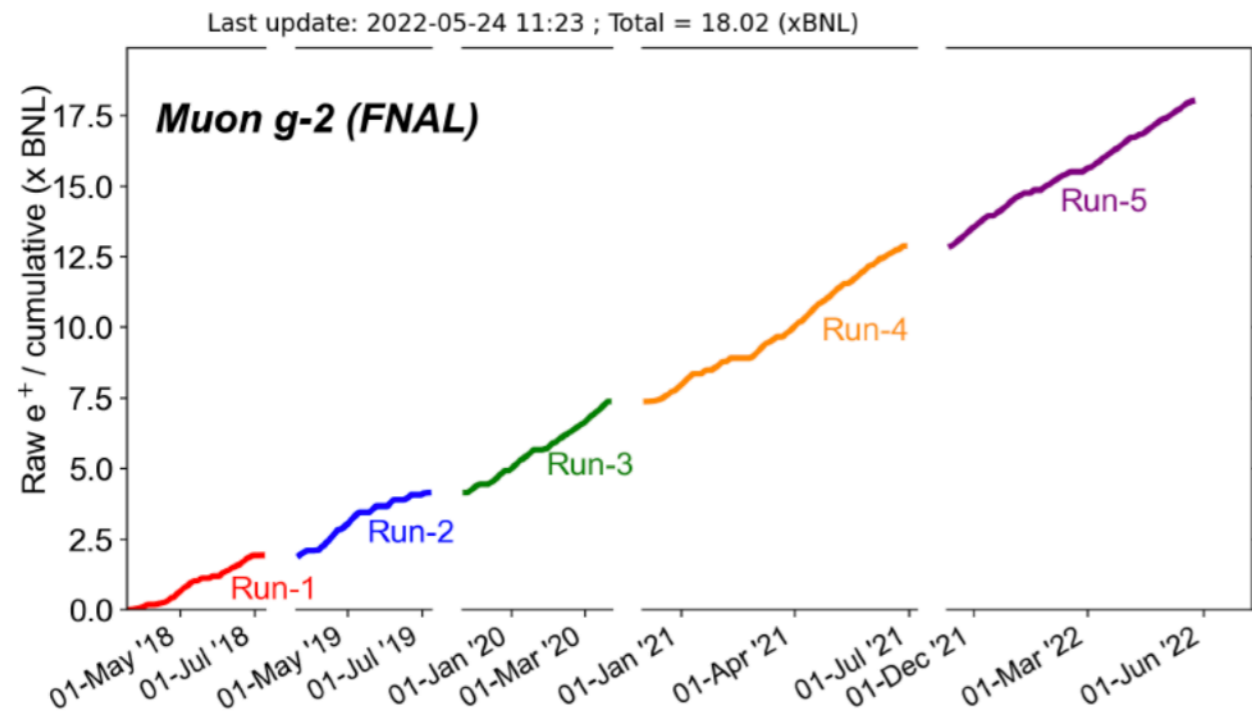
O Kim et al  
New J. Phys. 22 (2020) 063002



CBO Amplitude: 5-6mm->0.5-1mm  
 Muon Loss : factor of 4 reduction

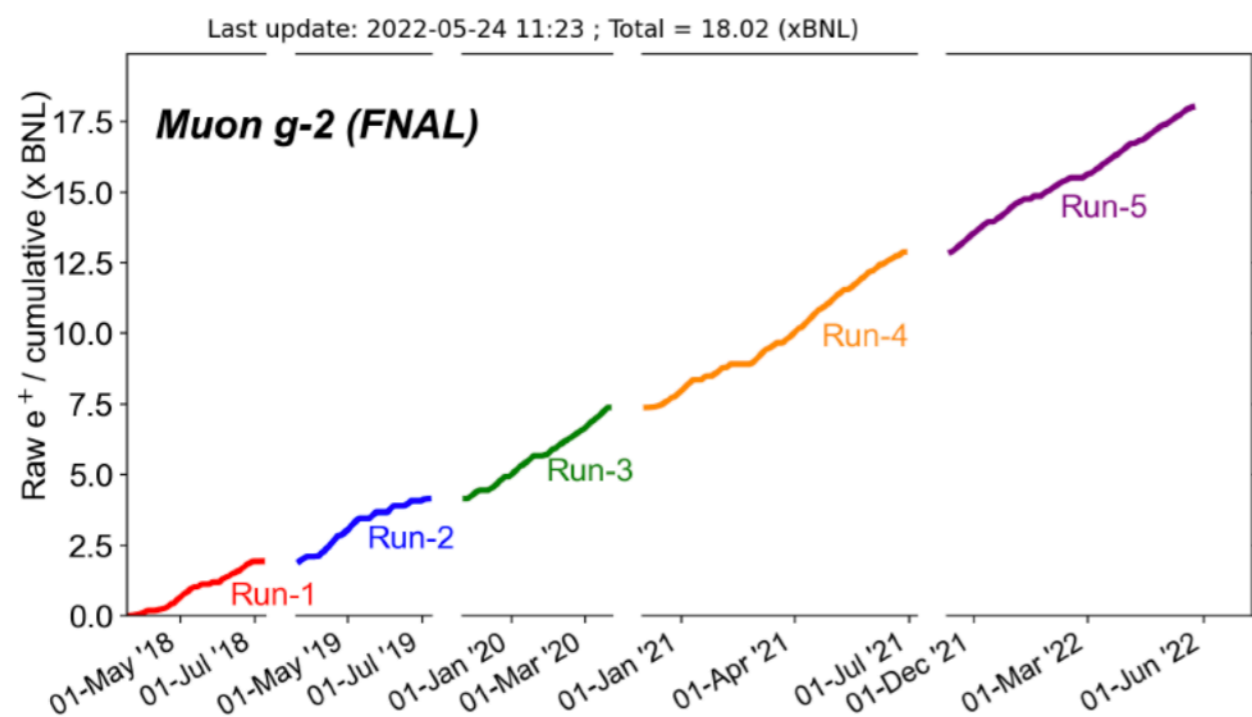


# Experiment Data Collection Status



- Run-2 and Run-3 analysis are ongoing -> reduce combined exp. error by 2 times
- Run-5 will end in July-> Run-4 and beyond will reduce the statistical uncertainties down to **100 ppb** in total.
- Run-6 will be negative muon running
  - Huge amount of polarity flip work will be done this summer during shutdown.

# Experiment Data Collection Status



- Run-2 and Run-3 analysis are ongoing -> reduce combined exp. error by 2 times
- Run-5 will end in July-> Run-4 and beyond will reduce the statistical uncertainties down to **100 ppb** in total.
- Run-6 will be negative muon running
  - Huge amount of polarity flip work will be done this summer during shutdown.

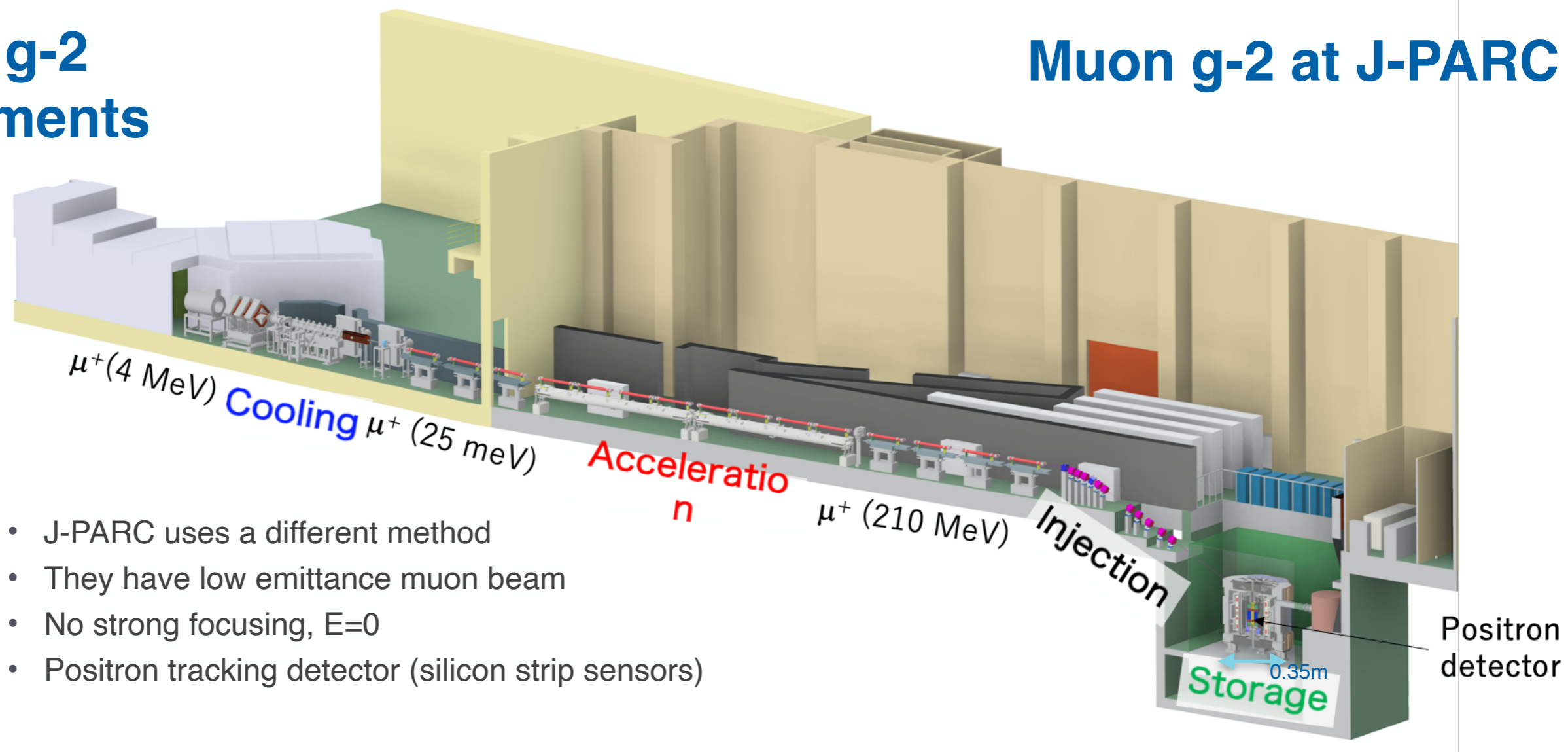
## Run-6 Negative Muon Run at Fermilab

- J-PARC can only use positive muons, so probably last chance to try it in near future
- Allow us to probe CPT and Lorentz Violation at the highest sensitivity in the muon sector
  - FNAL  $\mu^+$  & BNL  $\mu^-$
  - FNAL  $\mu^-$  & BNL  $\mu^+$
  - FNAL  $\mu^-$  & J-PARC  $\mu^+$
- Reduce the uncertainty achieved by Brookhaven in the measurement of  $g-2$  of the negative muon by **a factor of two**
- Tentative plan: 7-9 months—>4xBNL



# Future g-2 Experiments

## Muon g-2 at J-PARC



- J-PARC uses a different method
- They have low emittance muon beam
- No strong focusing,  $E=0$
- Positron tracking detector (silicon strip sensors)

- Electric field will be eliminated by using reaccelerated thermal muon beam
- Lower momentum muon beam + compact storage region with highly uniform magnetic field
- Tracking detector for decay positrons → reduced pile-up + able to measure the momentum direction of positrons.
- Final Goal is to reach **0.46ppm** → **0.1ppm** on  $a_\mu$
- Beam line construction has started and commissioning is expected to start in 2027

## Other new ideas on measuring more precise $g-2$

- No future experiments other than Muon  $g-2$  at J-PARC
- New ideas on improving the precision of magic momentum approaches -> Intense muon beam + better systematics
  - **The Heavy Ion Accelerator Facility (HIAF):** Intense muon source—> expected muon intensity is 30 times more than Fermilab Muon  $g-2$  beam line—> x2 improvement on total uncertainty.
  - **High-intensity muon beamline (HiMB) project at PSI:** Aims to upgrade production targets and beam lines -> Proposed be used for muon EDM search to measure  $g-2$ —> Possible to reach to 0.1 ppm in 1 y
  - **Non-continuous and nonuniform magnets ideas:** Different B field measurement + 15GeV muon beam—> Increased measurement time —> Increased precision

# Summary

- FNAL determined  $a_\mu$  with 460 ppb precision and confirmed BNL experimental result.
  - Run-2 and Run-3 results are expected to be published soon
  - Aiming for 100 ppb syst and 100 ppb stat. with the new improvements.
  - Getting prepared to run with  $\mu^-$  for Run-6
    - Will reduce the uncertainty achieved by Brookhaven in the measurement of  $g-2$  of the negative muon by a factor of two
    - Improve the opportunity of probing CPT and Lorentz Violation
- J-PARC preparation is ongoing, expect to start data taking in 2027
  - Goal to reduce the uncertainty on  $a_\mu$  to 0.1 ppm



**Thanks!**


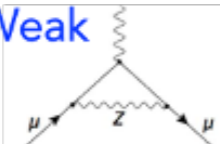
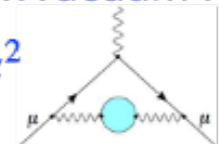
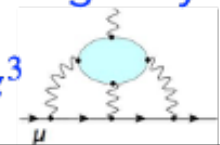
# Back-up

# Muon Magnetic Moment and Standard Model

- Dirac predicted g-factor as 2 for spin 1/2 particles
- But then Kusch & Foley measured electron spin factor as 2.00238
- Julian Schwinger calculated this deviation in QED (1948)

$$a = (g - 2)/2 = \alpha/2\pi = 0.0011636, \text{ where } \alpha = 1/137$$

More loops of calculations are added today

 <p>QED + ...</p>	$116\,584\,718.9(1) \times 10^{-11}$	0.001 ppm	Well-known
 <p>Weak + ...</p>	$153.6(1.0) \times 10^{-11}$	0.01 ppm	
<p>Hadronic...</p> <p>...Vacuum Polarization (HVP)</p>  <p><math>\alpha^2</math> + ...</p>	$6845(40) \times 10^{-11}$	0.37 ppm	Non-perturbative (Data-driven & lattice QCD)
<p>...Light-by-Light (HLbL)</p>  <p><math>\alpha^3</math> + ...</p> <p>Lattice HLbL results with 10 % total uncertainty feasible by ~2025</p>	$92(18) \times 10^{-11}$	0.15 ppm	

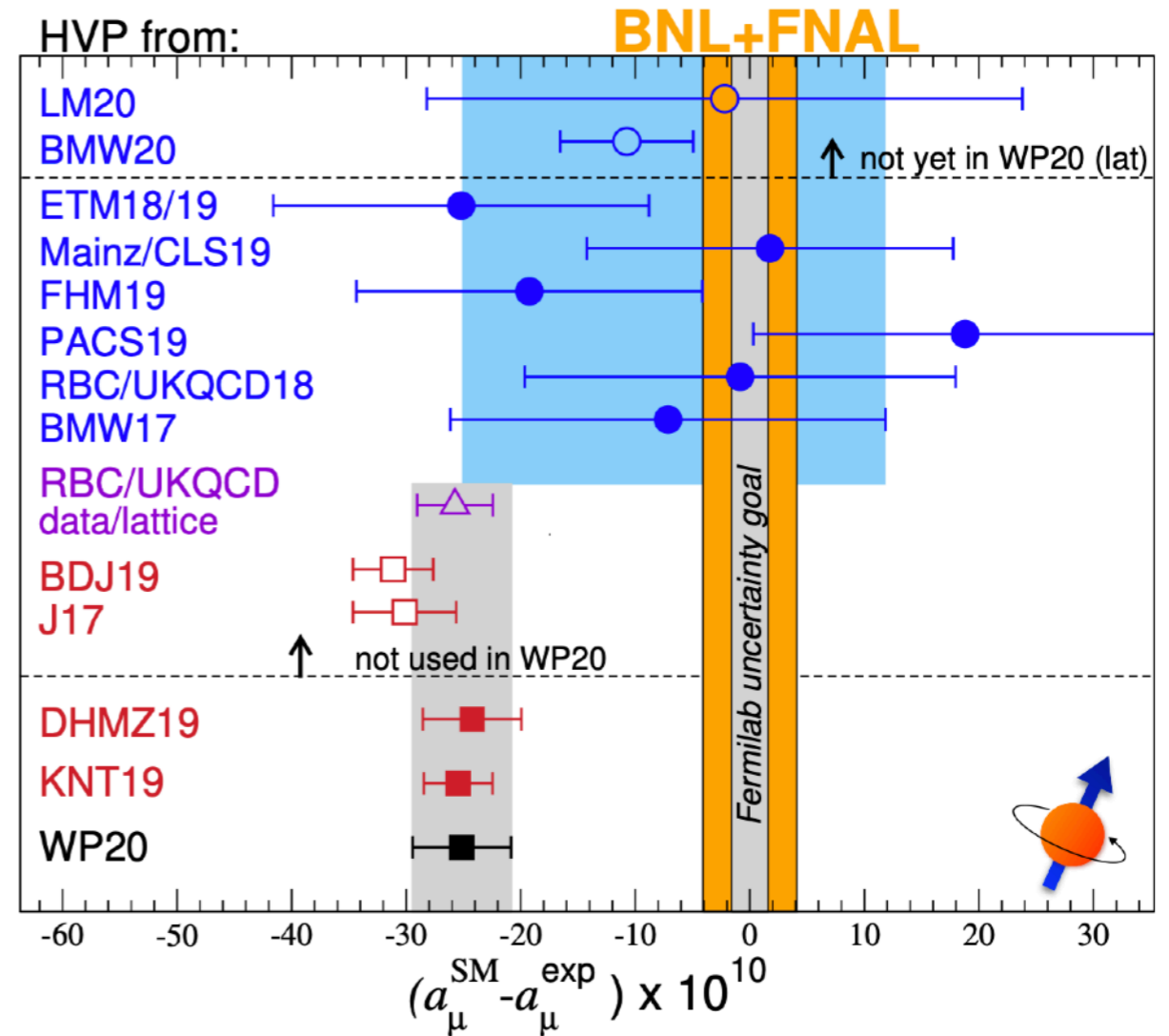
# Lattice QCD Calculations

## Lattice Data-based Dispersive Lattice and Data Official WP20

The anomalous magnetic moment of the muon in the Standard Model

T. Aoyama<sup>1,2,3</sup>, N. Asmussen<sup>4</sup>, M. Benayoun<sup>5</sup>, J. Bijnens<sup>6</sup>, T. Blum<sup>7,8</sup>, M. Bruno<sup>9</sup>, I. Caprini<sup>10</sup>,  
C. M. Carloni Calame<sup>11</sup>, M. Cè<sup>9,12,13</sup>, G. Colangelo<sup>7,14</sup>, F. Curciarello<sup>15,16</sup>, H. Czyz<sup>17</sup>, I. Danilkin<sup>12</sup>, M. Davier<sup>18</sup>,  
C. T. H. Davies<sup>19</sup>, M. Della Morte<sup>20</sup>, S. I. Eidelman<sup>21,22</sup>, A. X. El-Khadra<sup>7,23,24</sup>, A. Gérardin<sup>25</sup>, D. Giusti<sup>26,27</sup>,  
M. Golterman<sup>28</sup>, Steven Gottlieb<sup>29</sup>, V. Gülpers<sup>30</sup>, F. Hagelstein<sup>14</sup>, M. Hayakawa<sup>31,2</sup>, G. Herdoíza<sup>32</sup>, D. W. Hertzog<sup>33</sup>,  
A. Hoecker<sup>34</sup>, M. Hoferichter<sup>14,35</sup>, B.-L. Hoid<sup>36</sup>, R. J. Hudspith<sup>12,13</sup>, F. Ignatov<sup>21</sup>, T. Izubuchi<sup>37,8</sup>, F. Jegerlehner<sup>38</sup>,  
L. Jin<sup>7,8</sup>, A. Keshavarzi<sup>39</sup>, T. Kinoshita<sup>40,41</sup>, B. Kubis<sup>36</sup>, A. Kupich<sup>21</sup>, A. Kupś<sup>42,43</sup>, L. Laub<sup>14</sup>, C. Lehner<sup>126,37</sup>,  
L. Lellouch<sup>25</sup>, I. Logashenko<sup>21</sup>, B. Malaescu<sup>5</sup>, K. Maltman<sup>44,45</sup>, M. K. Marinković<sup>46,47</sup>, P. Masjuan<sup>48,49</sup>,  
A. S. Meyer<sup>37</sup>, H. B. Meyer<sup>12,13</sup>, T. Mibe<sup>11</sup>, K. Miura<sup>12,13,3</sup>, S. E. Müller<sup>50</sup>, M. Nio<sup>2,51</sup>, D. Nomura<sup>52,53</sup>,  
A. Nyffeler<sup>7,12</sup>, V. Pascalutsa<sup>12</sup>, M. Passera<sup>54</sup>, E. Perez del Rio<sup>55</sup>, S. Peris<sup>48,49</sup>, A. Portelli<sup>30</sup>, M. Procura<sup>56</sup>,  
C. F. Redmer<sup>12</sup>, B. L. Roberts<sup>57</sup>, P. Sánchez-Puertas<sup>49</sup>, S. Serednyakov<sup>21</sup>, B. Shwartz<sup>21</sup>, S. Simula<sup>27</sup>,  
D. Stöckinger<sup>58</sup>, H. Stöckinger-Kim<sup>58</sup>, P. Stoffer<sup>59</sup>, T. Teubner<sup>60</sup>, R. Van de Water<sup>24</sup>, M. Vanderhaeghen<sup>12,13</sup>,  
G. Venanzoni<sup>61</sup>, G. von Hippel<sup>12</sup>, H. Wittig<sup>12,13</sup>, Z. Zhang<sup>18</sup>,  
M. N. Achasov<sup>21</sup>, A. Bashir<sup>62</sup>, N. Cardoso<sup>47</sup>, B. Chakraborty<sup>63</sup>, E.-H. Chao<sup>12</sup>, J. Charles<sup>25</sup>, A. Crivellin<sup>64,65</sup>,  
O. Deineka<sup>12</sup>, A. Denig<sup>12,13</sup>, C. DeTar<sup>66</sup>, C. A. Dominguez<sup>67</sup>, A. E. Dorokhov<sup>68</sup>, V. P. Druzhinin<sup>21</sup>, G. Eichmann<sup>69,47</sup>,  
M. Fael<sup>70</sup>, C. S. Fischer<sup>71</sup>, E. Gámiz<sup>72</sup>, Z. Gelzer<sup>23</sup>, J. R. Green<sup>9</sup>, S. Guellati-Khelifa<sup>73</sup>, D. Hatton<sup>19</sup>,  
N. Hermansson-Truedsson<sup>14</sup>, S. Holz<sup>36</sup>, B. Hörz<sup>74</sup>, M. Knecht<sup>25</sup>, J. Koponen<sup>1</sup>, A. S. Kronfeld<sup>24</sup>, J. Laiho<sup>75</sup>,  
S. Leupold<sup>42</sup>, P. B. Mackenzie<sup>24</sup>, W. J. Marciano<sup>37</sup>, C. McNeile<sup>76</sup>, D. Mohler<sup>12,13</sup>, J. Monnard<sup>14</sup>, E. T. Neil<sup>77</sup>,  
A. V. Nesterenko<sup>68</sup>, K. Ottnad<sup>12</sup>, V. Pauk<sup>12</sup>, A. E. Radzhabov<sup>78</sup>, E. de Rafael<sup>25</sup>, K. Raya<sup>79</sup>, A. Risch<sup>12</sup>,  
A. Rodríguez-Sánchez<sup>6</sup>, P. Roig<sup>80</sup>, T. San José<sup>12,13</sup>, E. P. Solodov<sup>21</sup>, R. Sugar<sup>81</sup>, K. Yu. Todyshev<sup>21</sup>, A. Vainshtein<sup>82</sup>,  
A. Vaquero Avilés-Casco<sup>66</sup>, E. Weil<sup>71</sup>, J. Wilhelm<sup>12</sup>, R. Williams<sup>71</sup>, A. S. Zhevlakov<sup>78</sup>

04822v2 [hep-ph] 13 Nov 2020



- BMW20 is also in tension with data-based dispersive result( $2.1\sigma$ )
- Expecting results from RBC/UKQCD and FNAL/MILC in the coming months
- Will be interested to see how it evolves in future but lattice QCD calculations requires a huge amount of computing resource. But all groups are working on defining intermediate results (simpler way to compare things)
- Lattice HVP (average) with  $\approx 0.5\%$  errors feasible by 2025

RPF Spring meeting by A. El-Khadra

# Most promising models to explain the discrepancy

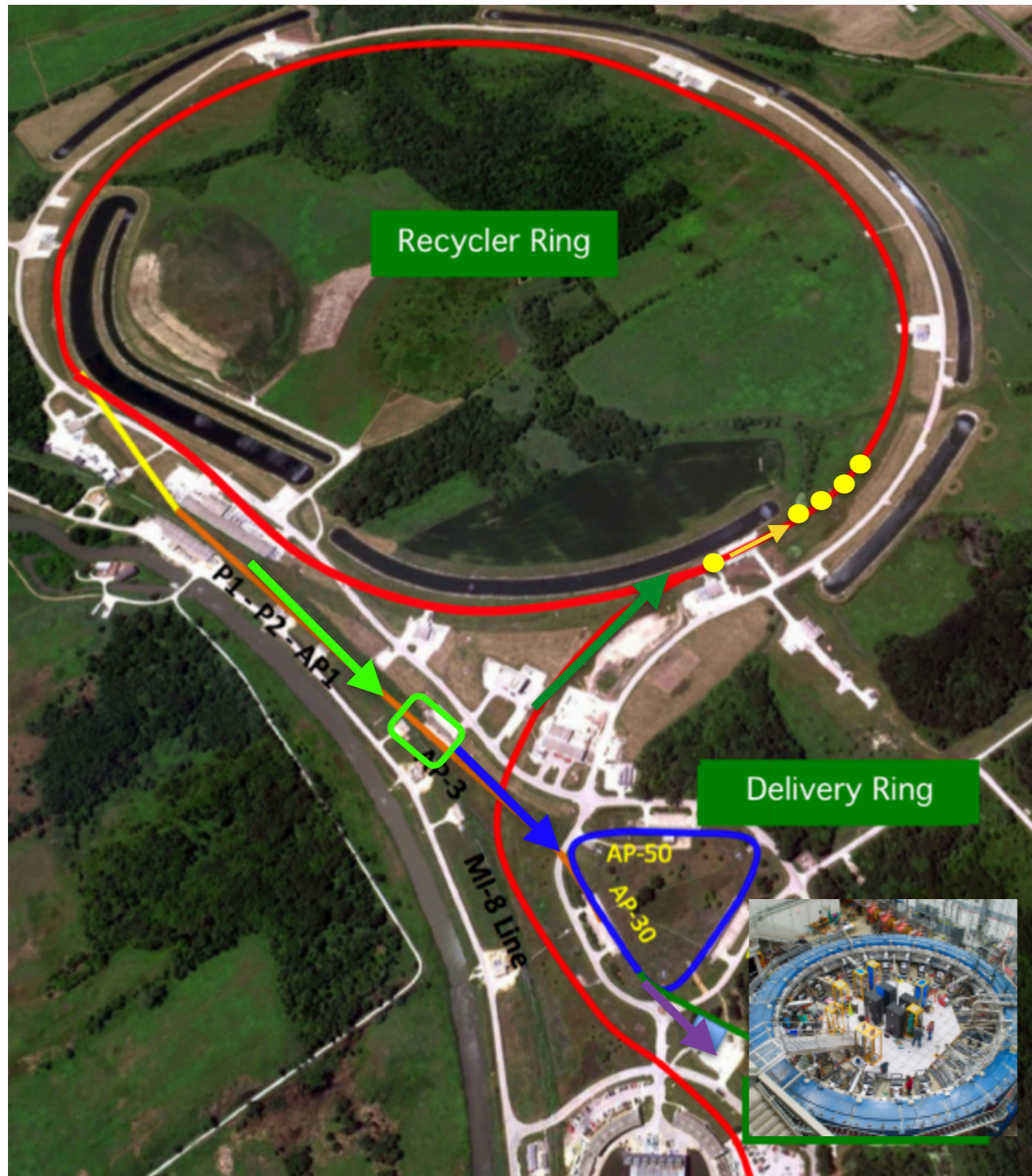
- Muon  $g-2$  can indicate if there is a CP-conserving, lepton-flavor conserving or BSM chirality-flipping interaction but can't tell which one is the most promising.
- Possible explanations:
  - SUSY models (while evading LHC limits)
  - Leptoquark models (if leptoquark masses are above all LHC limits)
  - 2-Higgs doublet models



Establishing a  $g-2$  discrepancy from SM would place a strict limit on BSM scenarios

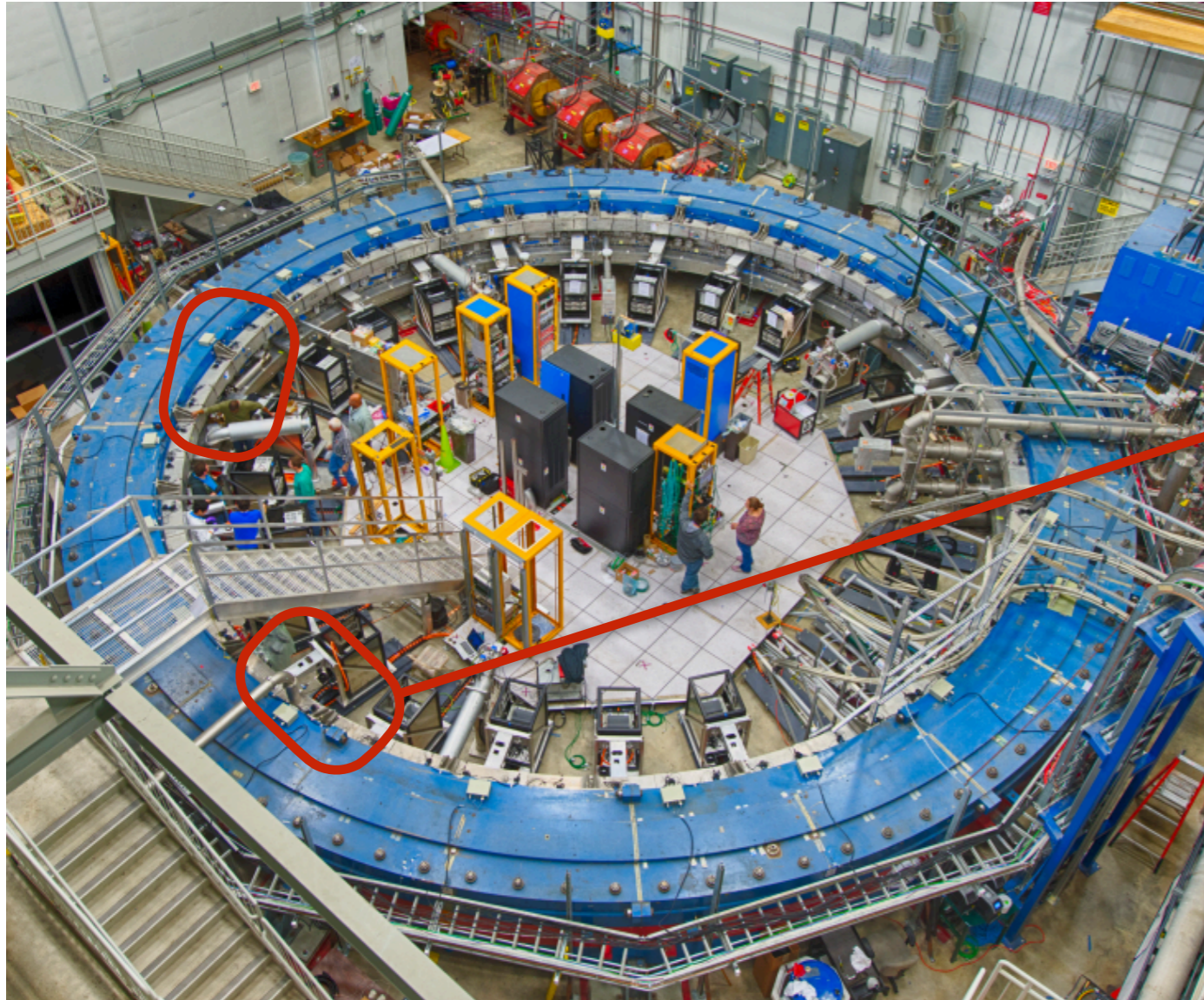


# Muon Campus at Fermilab

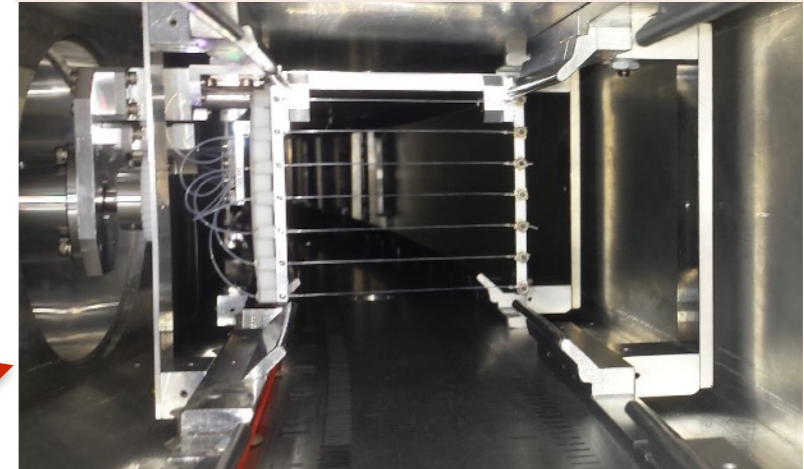


- 8 GeV protons are delivered to Recycler Ring from Booster
- Split the proton bunch into four bunches with RF system.
- Direct the proton punches to pion production target and obtain pions.
- Muons produced by pion decays circulate in the delivery ring until proton contamination is removed.
- Deliver muons to g-2 storage ring.

# Monitoring the Injected Beam

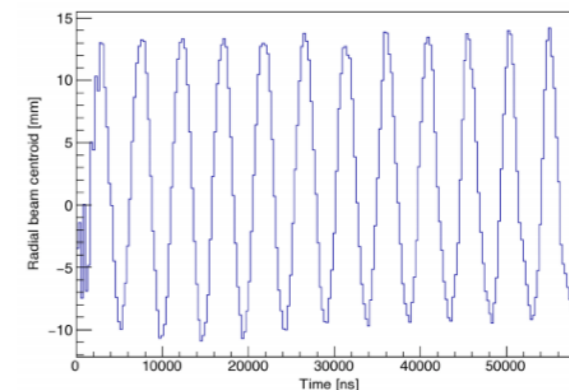


Y Profile Monitor at 180 degree position

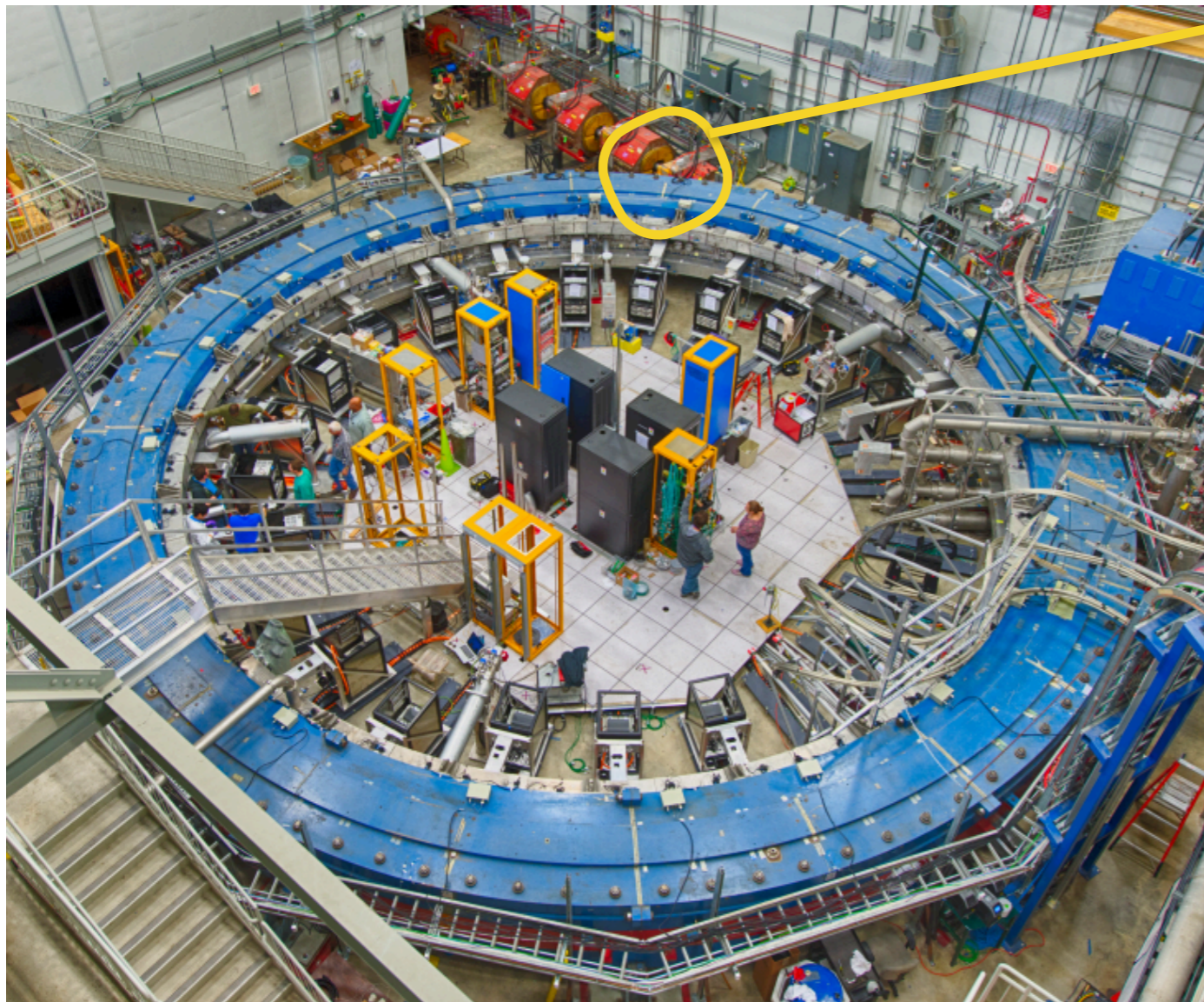


- **Fiber Harps**

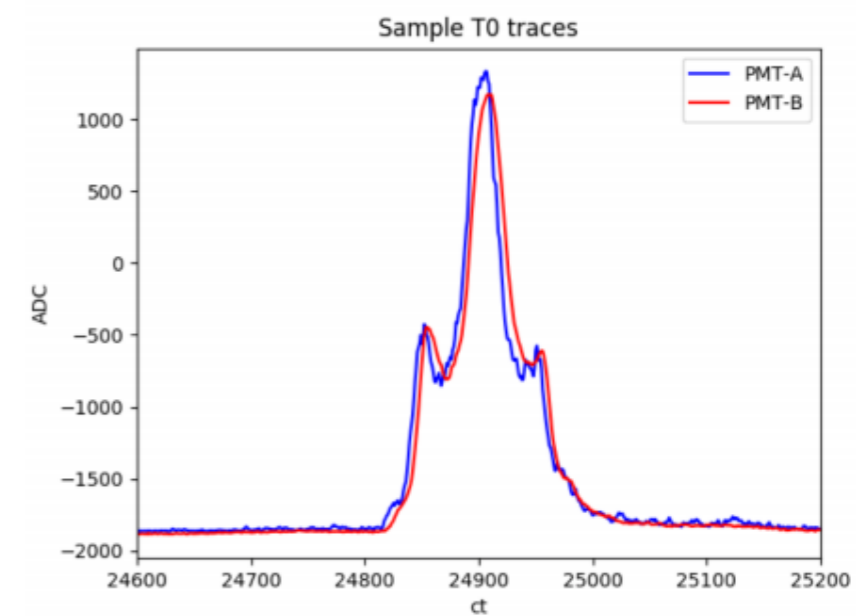
- Scintillating Fibers
- x and y profile monitoring
- Tool for beam commissioning



# Monitoring the Injected Beam: T0 counter

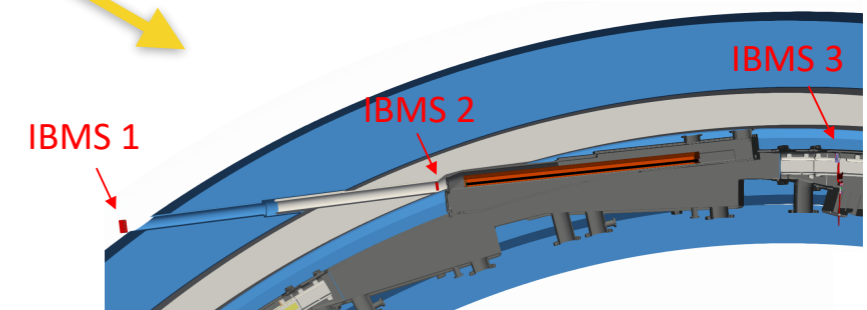
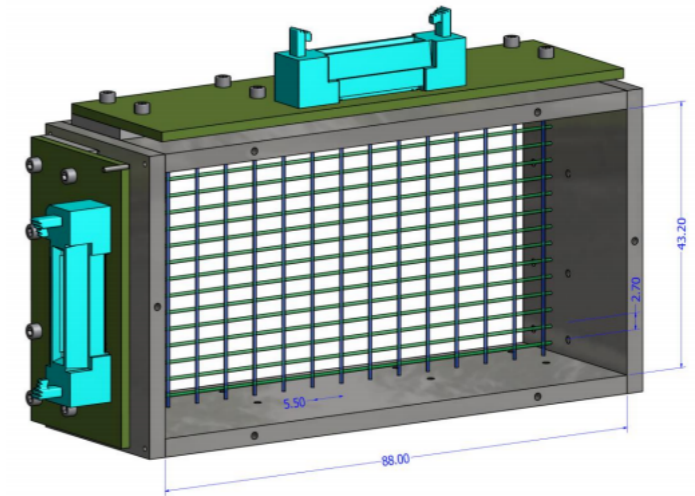
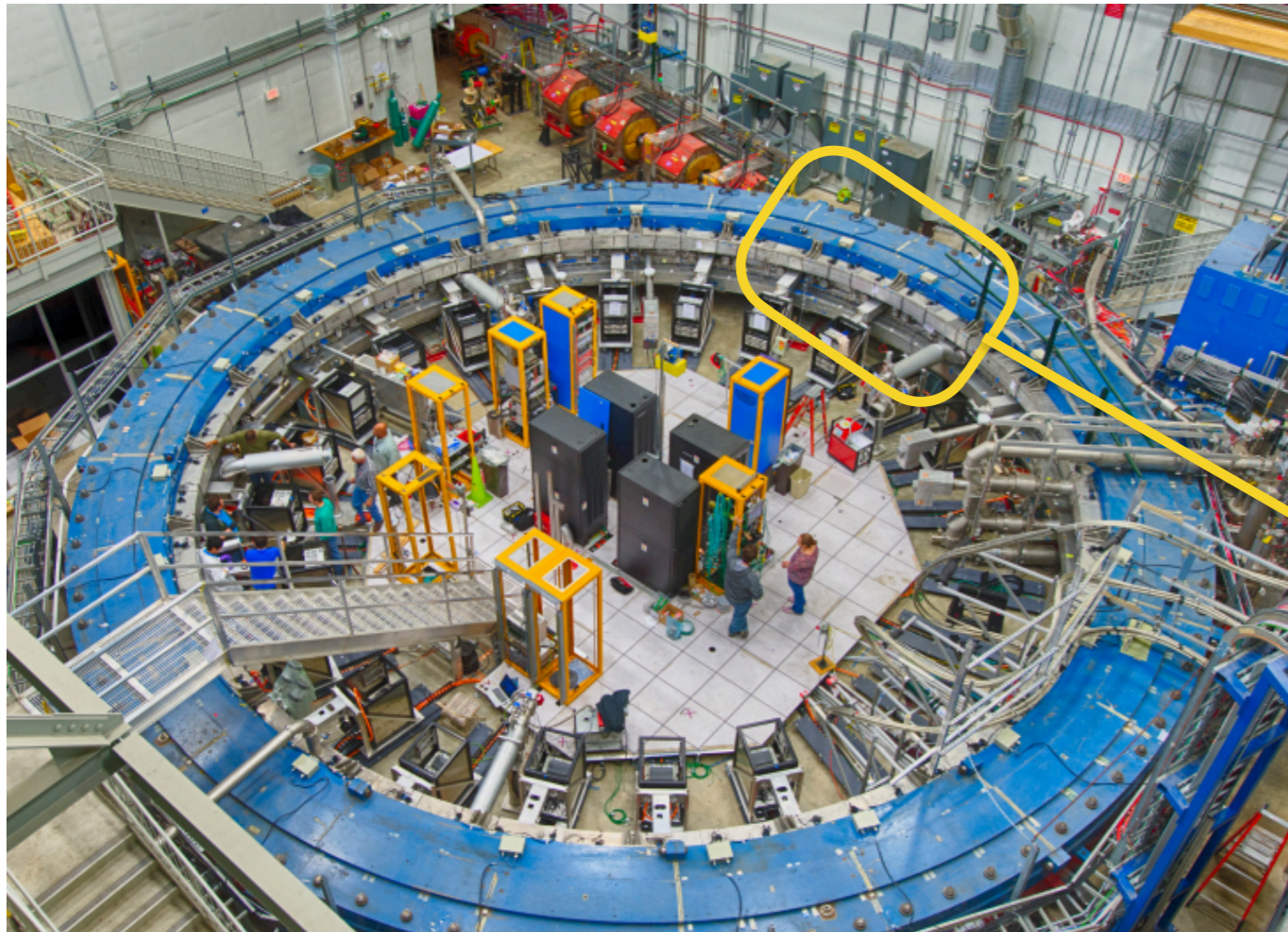


- **T0 Counter**
  - Thin scintillator with 2 PMT readouts
  - Provides beam time profile before beam enters the storage ring



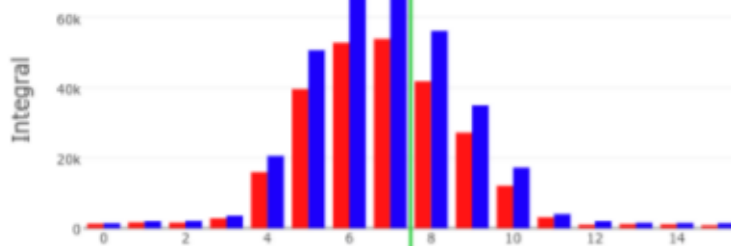
# Monitoring the Injected Beam: IBMS detectors

- IBMS (Inflector beam monitoring systems)
  - Check beam injection characteristics
  - 2 planes of scintillation fibers

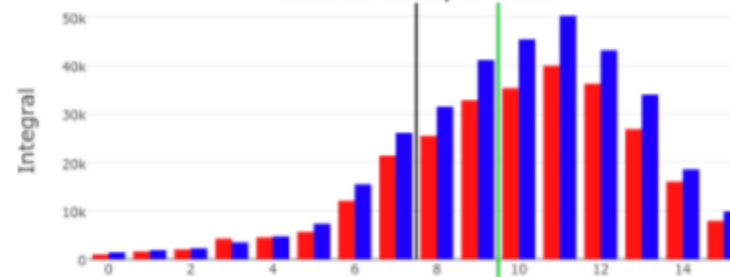


IBMS spatial beam profiles

IBMS 1 Y  
mean: 6.8 fibers, -1.8 mm  
RMS: 2.0 fibers, 5.4 mm



IBMS 1 X  
mean: 9.9 fibers, 13.3 mm  
RMS: 2.9 fibers, 15.8 mm



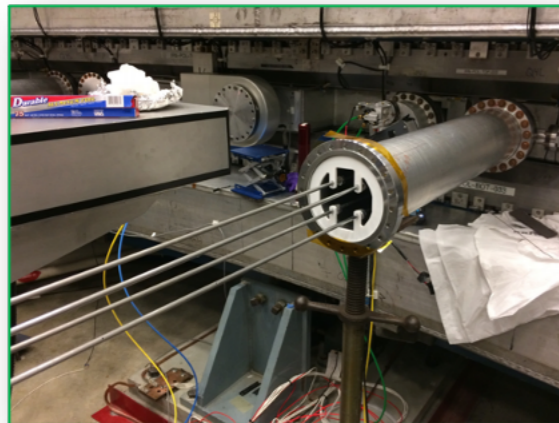
# Quad System Upgrades

## Refurbished and upgraded the BNL EQS



Adding HV Feedthrough extension to avoid spark in the HV components → Avoid damaging the system components

New HV Pulsers were designed to pulse the EQS → Reduce the spark rate and gain more reliability on operating

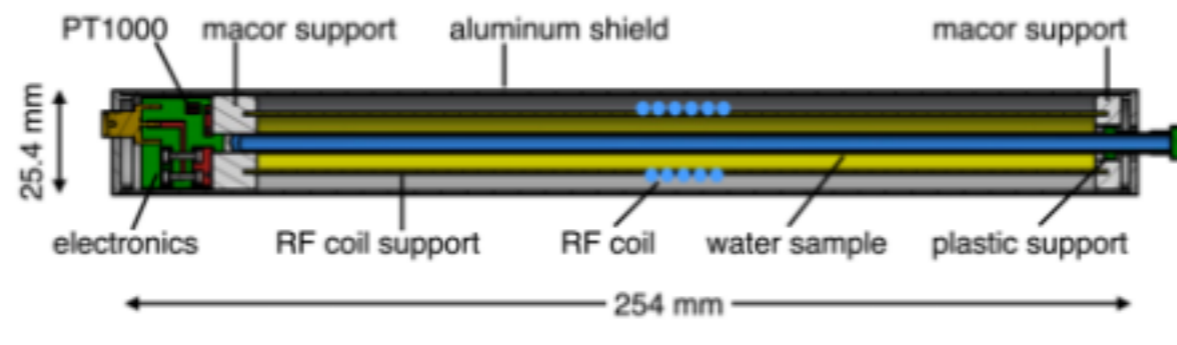
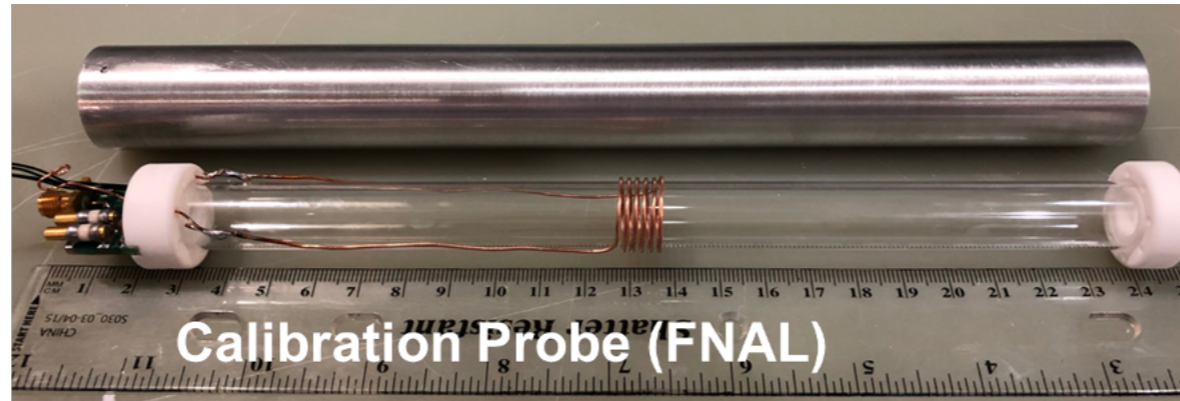


Installing additional (Macor) support to fix the HV extension lead → Prevent mechanical vibration and provide electrical isolation

# NMR Probes

## Calibration Uncertainty

$$a_{\mu} \propto \frac{f_{\text{clock}} \omega_a^m (1 + C_e + C_p + C_{ml} + C_{pa})}{f_{\text{calib}} \langle \omega'_p(x, y, \phi) \times M(x, y, \phi) \rangle (1 + B_k + B_q)}$$



### Absolute field calibration:

- Absolute probes were used to calibrate NMR probes
- Proton NMR, calibrated in terms of  $\omega_p(T_r)$  of a proton shielded in a spherical sample of water at an exact temperature.

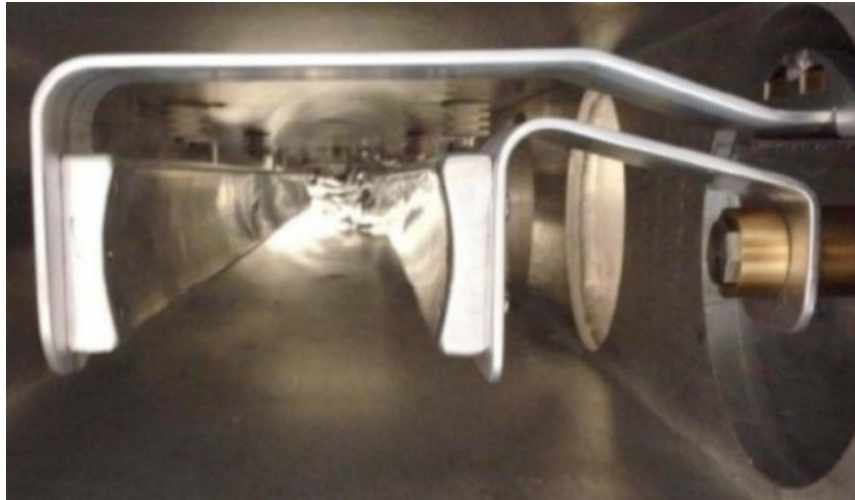
# Kicker Transients

$$a_{\mu} \propto \frac{f_{\text{clock}} \omega_a^m (1 + C_e + C_p + C_{ml} + C_{pa})}{f_{\text{calib}} \langle \omega'_p(x, y, \phi) \times M(x, y, \phi) \rangle (1 + B_k + B_q)}$$

# Kicker Transients

$$a_{\mu} \propto \frac{f_{\text{clock}} \omega_a^m (1 + C_e + C_p + C_{ml} + C_{pa})}{f_{\text{calib}} \langle \omega'_p(x, y, \phi) \times M(x, y, \phi) \rangle (1 + B_k + B_q)}$$

Kickers pulsing created influence on the average field seen by beam

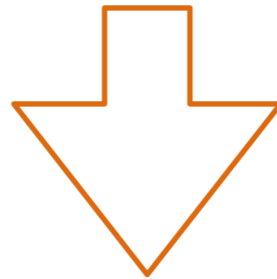




# Kicker Transients

$$a_{\mu} \propto \frac{f_{\text{clock}} \omega_a^m (1 + C_e + C_p + C_{ml} + C_{pa})}{f_{\text{calib}} \langle \omega'_p(x, y, \phi) \times M(x, y, \phi) \rangle (1 + B_k + B_q)}$$

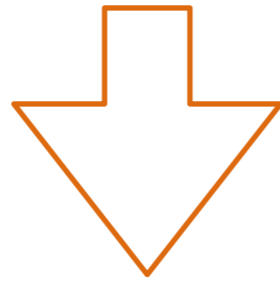
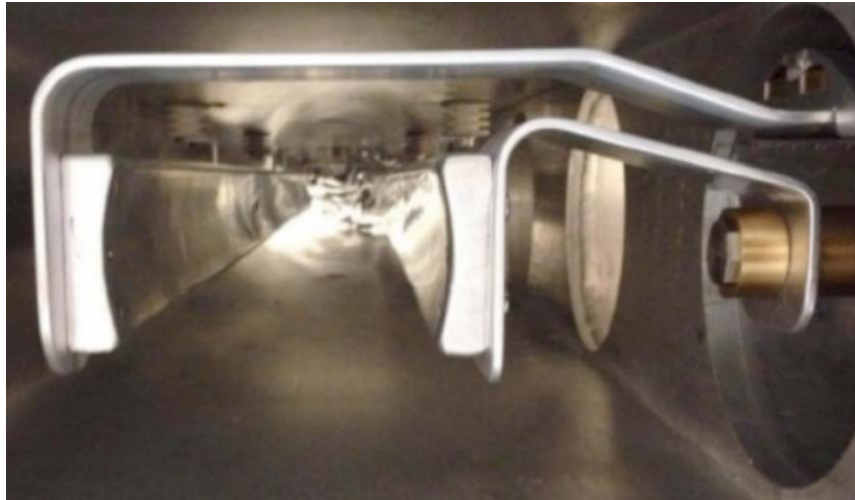
Kickers pulsing created influence on the average field seen by beam



# Kicker Transients

$$a_{\mu} \propto \frac{f_{\text{clock}} \omega_a^m (1 + C_e + C_p + C_{ml} + C_{pa})}{f_{\text{calib}} \langle \omega'_p(x, y, \phi) \times M(x, y, \phi) \rangle (1 + B_k + B_q)}$$

Kickers pulsing created influence on the average field seen by beam

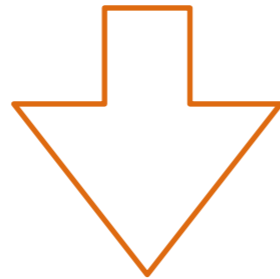


Field Perturbation

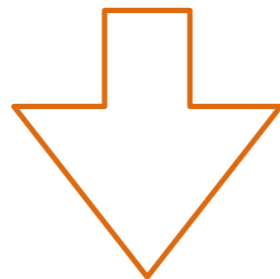
# Kicker Transients

$$a_{\mu} \propto \frac{f_{\text{clock}} \omega_a^m (1 + C_e + C_p + C_{ml} + C_{pa})}{f_{\text{calib}} \langle \omega'_p(x, y, \phi) \times M(x, y, \phi) \rangle (1 + B_k + B_q)}$$

Kickers pulsing created influence on the average field seen by beam



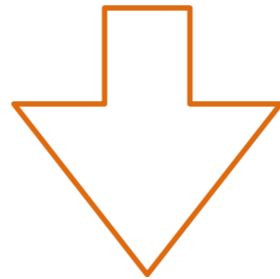
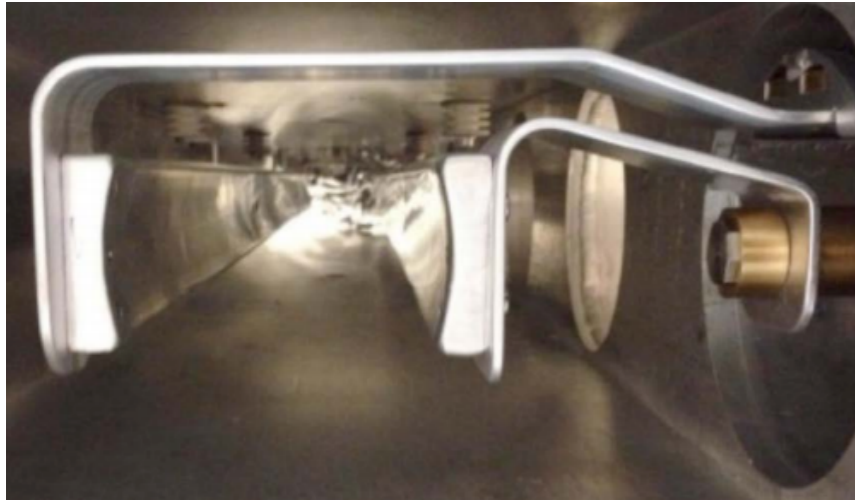
Field Perturbation



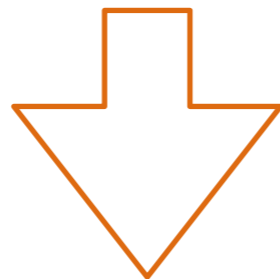
# Kicker Transients

$$a_{\mu} \propto \frac{f_{\text{clock}} \omega_a^m (1 + C_e + C_p + C_{ml} + C_{pa})}{f_{\text{calib}} \langle \omega'_p(x, y, \phi) \times M(x, y, \phi) \rangle (1 + B_k + B_q)}$$

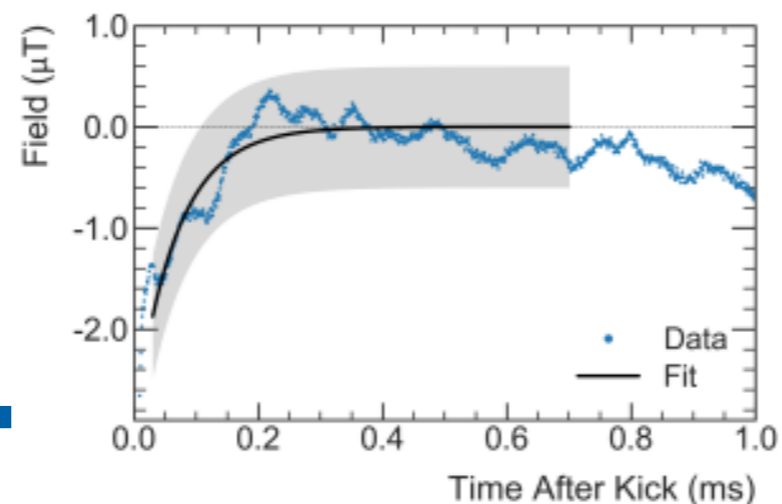
Kickers pulsing created influence on the average field seen by beam



Field Perturbation

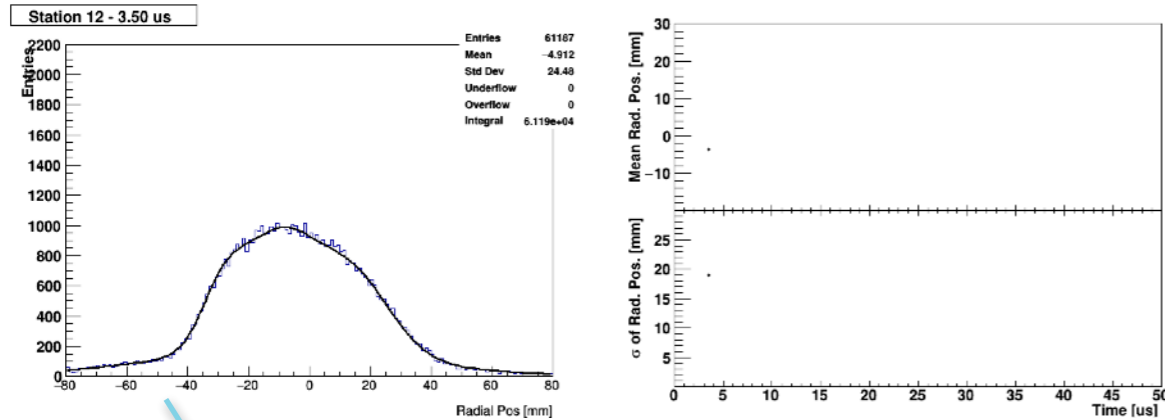


Used a magnetometer to measure the transient

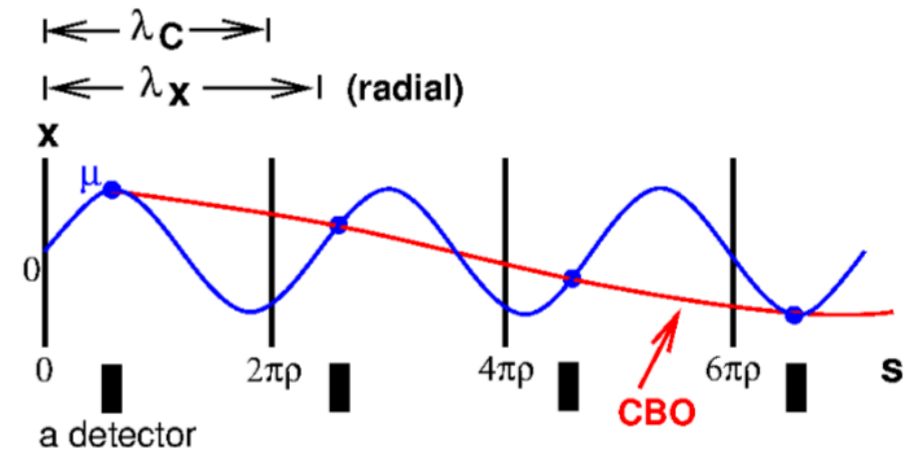
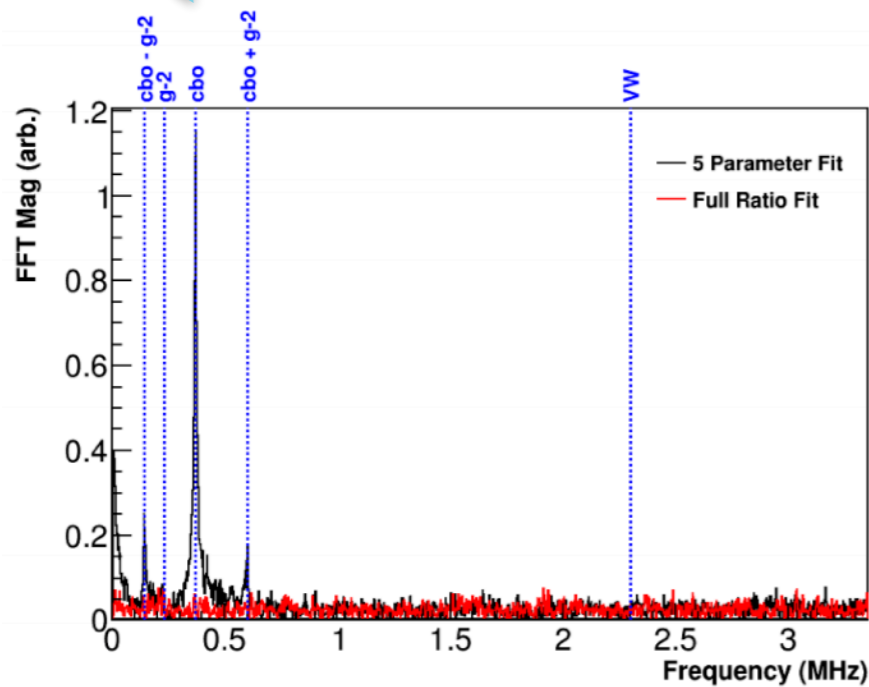


# Beam Dynamics

- CBO - Coherent Beam Oscillation



Radial CBO movement



$\lambda_x$  - radial wavelength

$\lambda_c$  - cyclotron wavelength

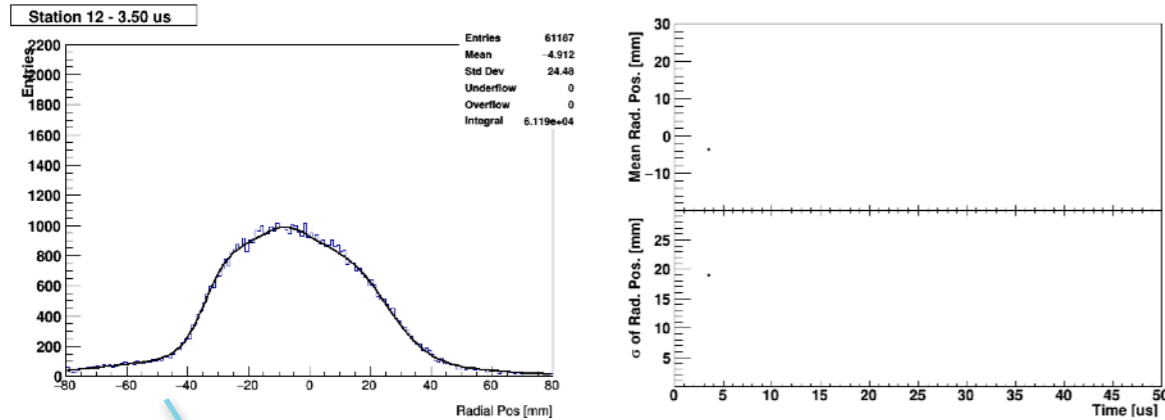
Frequency from detector point of view =  $f_c - f_x$

$$x = x_e + A_x \cos(f_x t + \delta_x) \quad y = A_y \cos(f_y t + \delta_y)$$

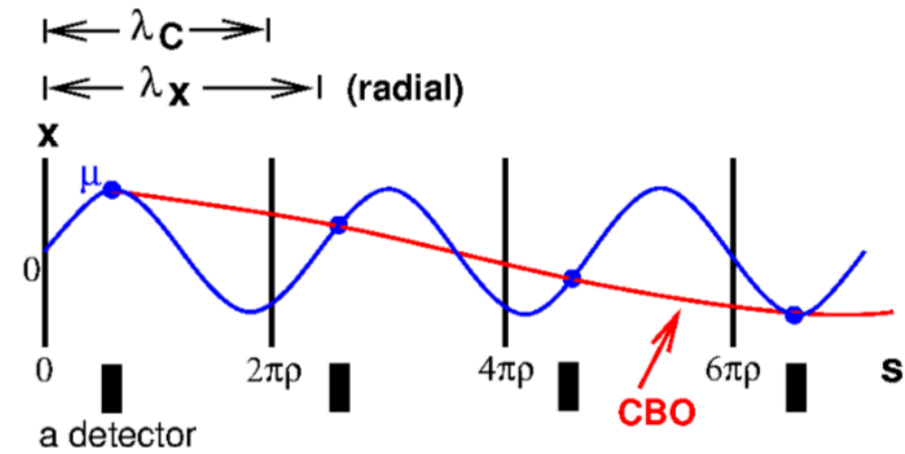
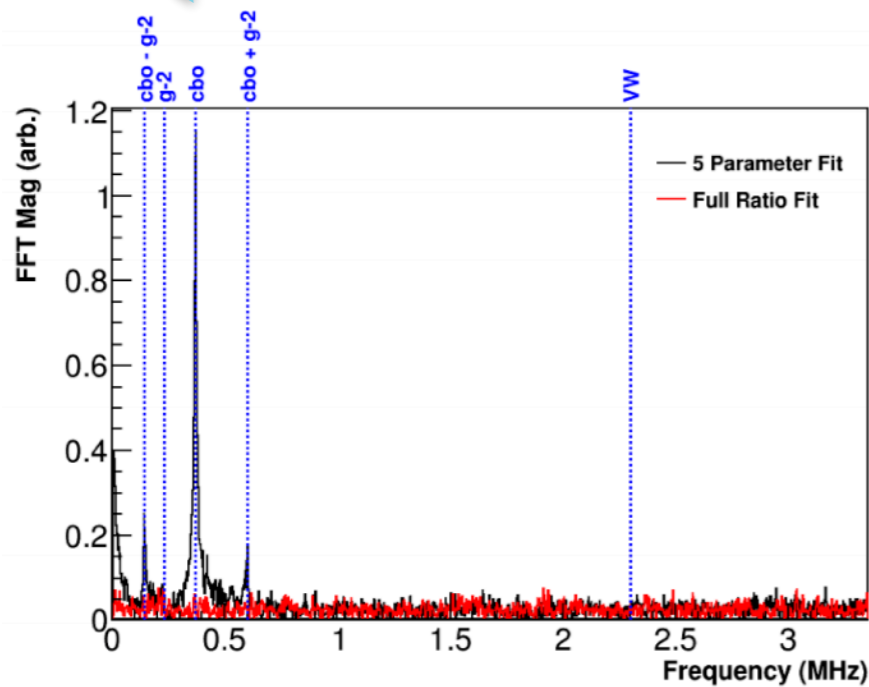
Simple Harmonic Motion

# Beam Dynamics

- CBO - Coherent Beam Oscillation



Radial CBO movement



$\lambda_x$  - radial wavelength

$\lambda_c$  - cyclotron wavelength

Frequency from detector point of view =  $f_c - f_x$

$$x = x_e + A_x \cos(f_x t + \delta_x) \quad y = A_y \cos(f_y t + \delta_y)$$

Simple Harmonic Motion

## Phase Acceptance

$$a_{\mu} \propto \frac{f_{\text{clock}} \omega_a^m (1 + C_e + C_p + C_{ml} + C_{pa})}{f_{\text{calib}} \langle \omega'_p(x, y, \phi) \times M(x, y, \phi) \rangle (1 + B_k + B_q)}$$

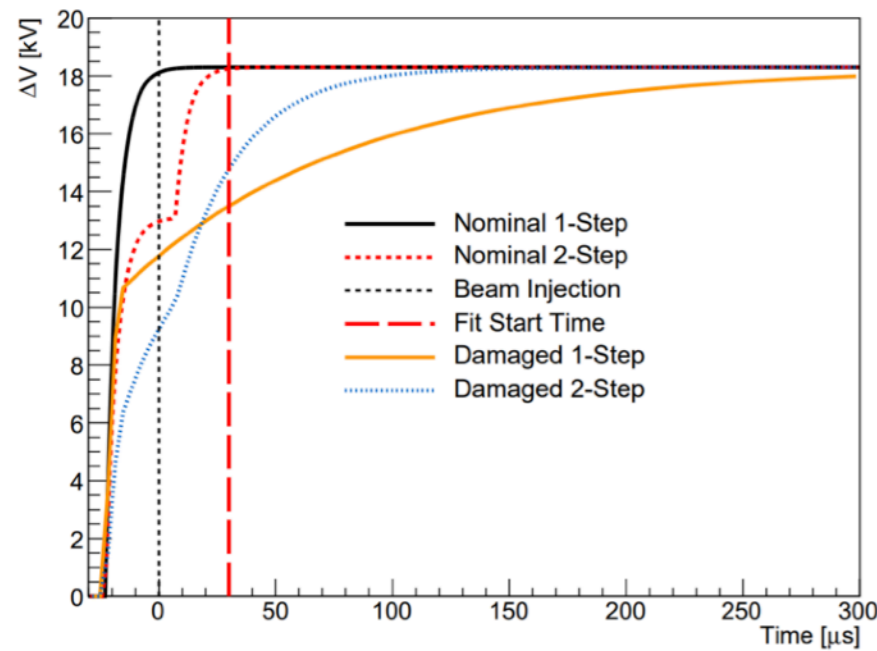
When there is a time dependent phase,

It shifts the  $\omega_a$  !

# Phase Acceptance

$$a_{\mu} \propto \frac{f_{\text{clock}} \omega_a^m (1 + C_e + C_p + C_{ml} + C_{pa})}{f_{\text{calib}} \langle \omega'_p(x, y, \phi) \times M(x, y, \phi) \rangle (1 + B_k + B_q)}$$

When there is a time dependent phase,  
It shifts the  $\omega_a$  !



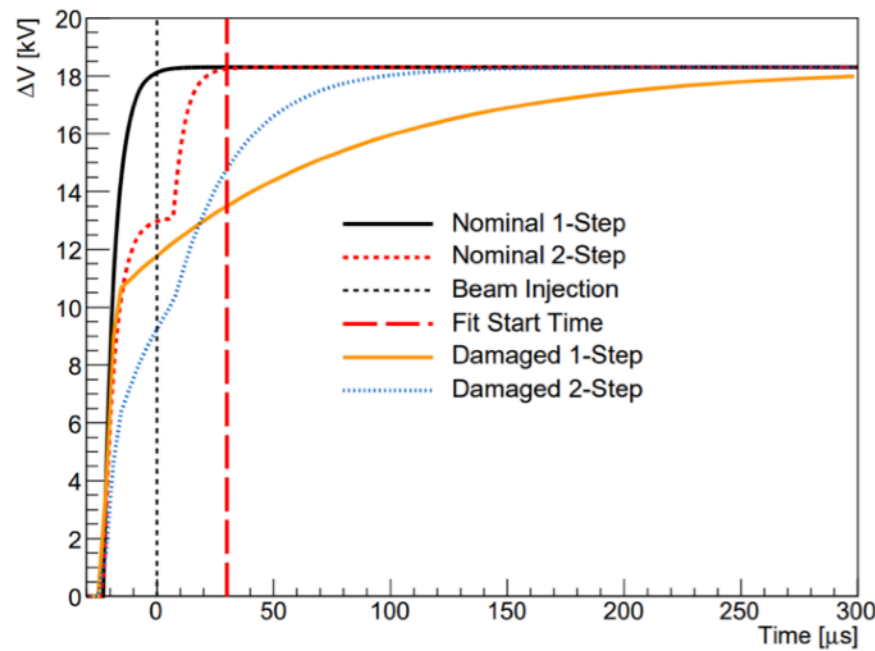
Due to damaged HV resistors; stored beam distribution was unstable.



# Phase Acceptance

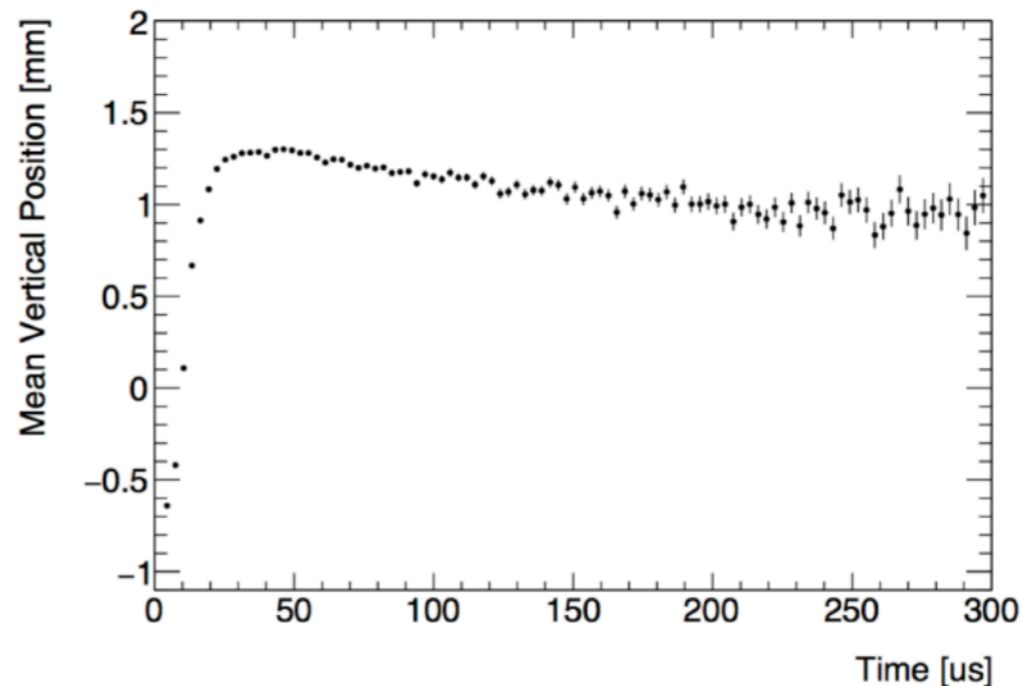
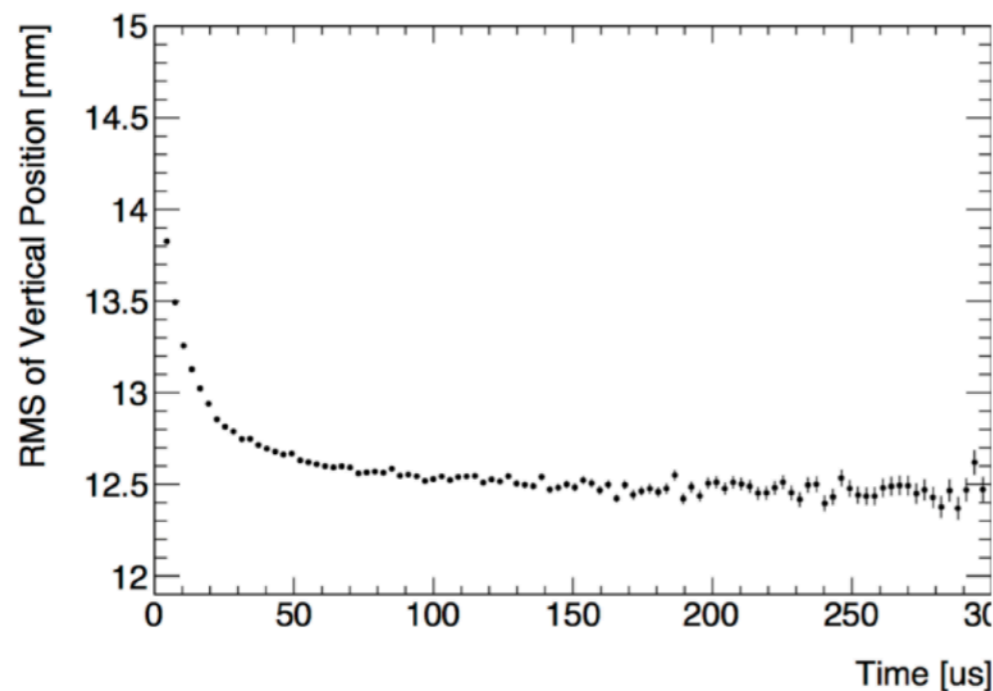
$$a_{\mu} \propto \frac{f_{\text{clock}} \omega_a^m (1 + C_e + C_p + C_{ml} + C_{pa})}{f_{\text{calib}} \langle \omega'_p(x, y, \phi) \times M(x, y, \phi) \rangle (1 + B_k + B_q)}$$

When there is a time dependent phase,  
It shifts the  $\omega_a$  !



Due to damaged HV resistors; stored beam distribution was unstable.

It caused a time dependent phase  
Beam vertical mean and width changed



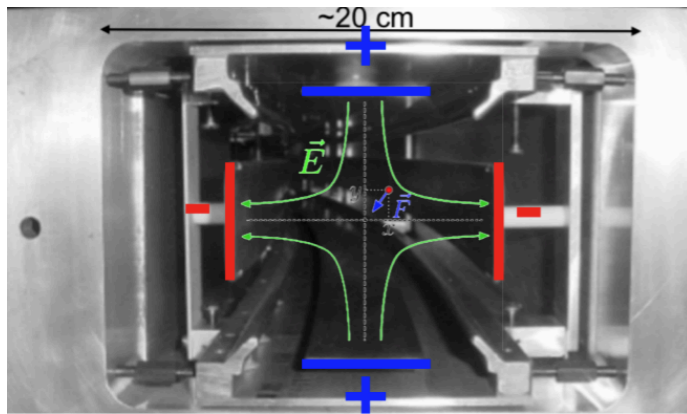
# ESQ Transients

$$a_{\mu} \propto \frac{f_{\text{clock}} \omega_a^m (1 + C_e + C_p + C_{ml} + C_{pa})}{f_{\text{calib}} \langle \omega'_p(x, y, \phi) \times M(x, y, \phi) \rangle (1 + B_k + B_q)}$$

# ESQ Transients

$$a_{\mu} \propto \frac{f_{\text{clock}} \omega_a^m (1 + C_e + C_p + C_{ml} + C_{pa})}{f_{\text{calib}} \langle \omega'_p(x, y, \phi) \times M(x, y, \phi) \rangle (1 + B_k + B_q)}$$

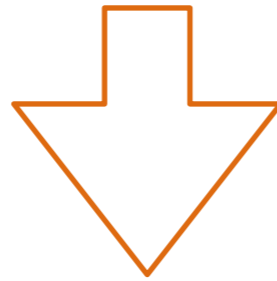
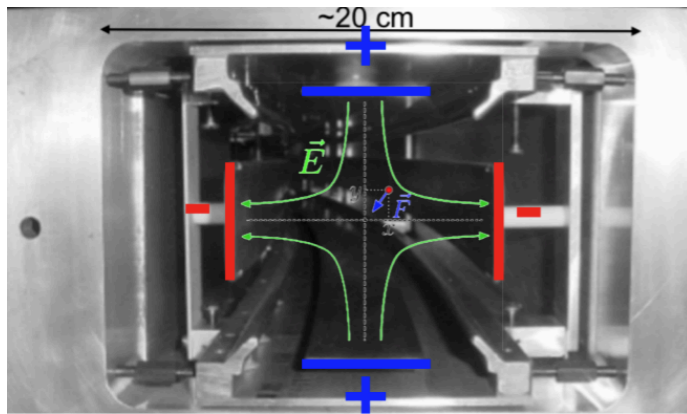
Quads charging and discharging cause mechanical vibration



# ESQ Transients

$$a_{\mu} \propto \frac{f_{\text{clock}} \omega_a^m (1 + C_e + C_p + C_{ml} + C_{pa})}{f_{\text{calib}} \langle \omega'_p(x, y, \phi) \times M(x, y, \phi) \rangle (1 + B_k + B_q)}$$

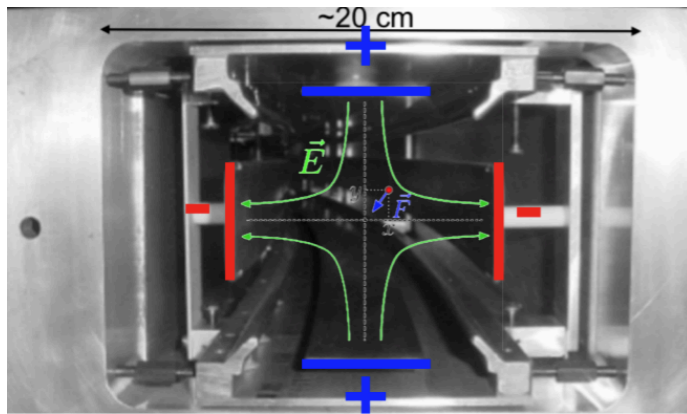
Quads charging and discharging cause mechanical vibration



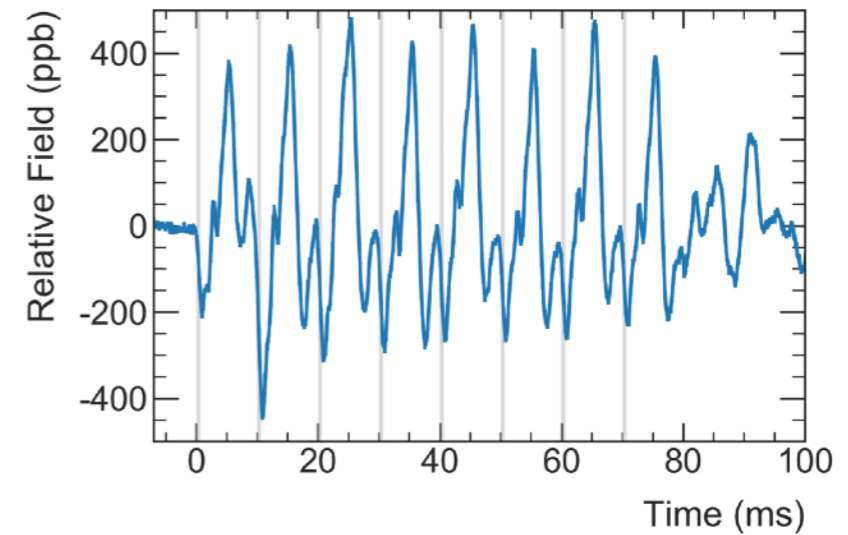
# ESQ Transients

$$a_{\mu} \propto \frac{f_{\text{clock}} \omega_a^m (1 + C_e + C_p + C_{ml} + C_{pa})}{f_{\text{calib}} \langle \omega'_p(x, y, \phi) \times M(x, y, \phi) \rangle (1 + B_k + B_q)}$$

Quads charging and discharging cause mechanical vibration



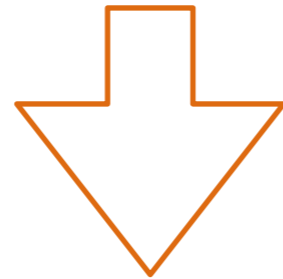
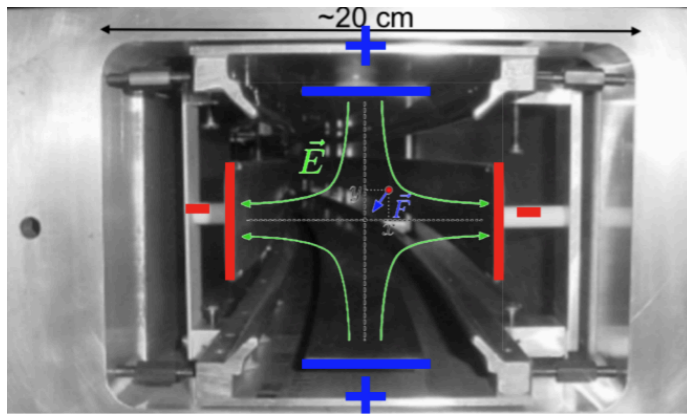
Field Perturbation



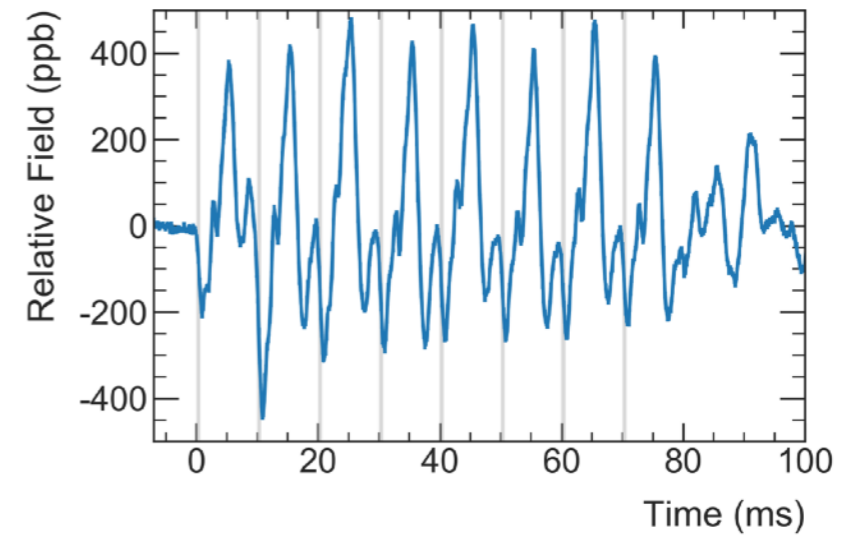
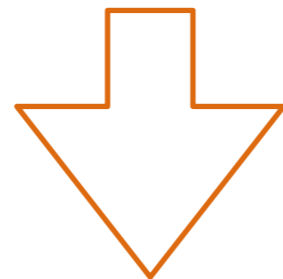
# ESQ Transients

$$a_{\mu} \propto \frac{f_{\text{clock}} \omega_a^m (1 + C_e + C_p + C_{ml} + C_{pa})}{f_{\text{calib}} \langle \omega'_p(x, y, \phi) \times M(x, y, \phi) \rangle (1 + B_k + B_q)}$$

Quads charging and discharging cause mechanical vibration



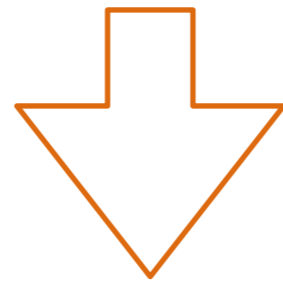
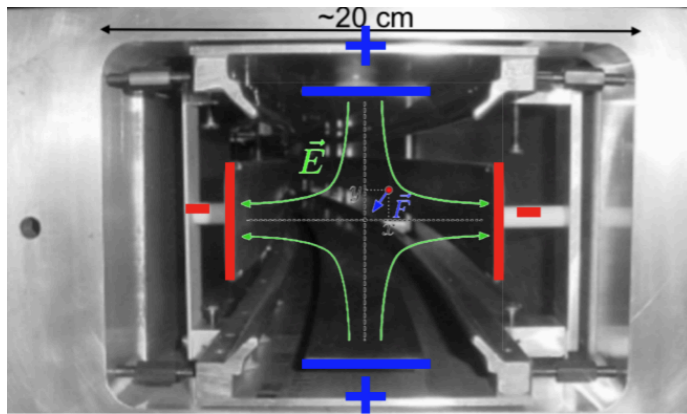
Field Perturbation



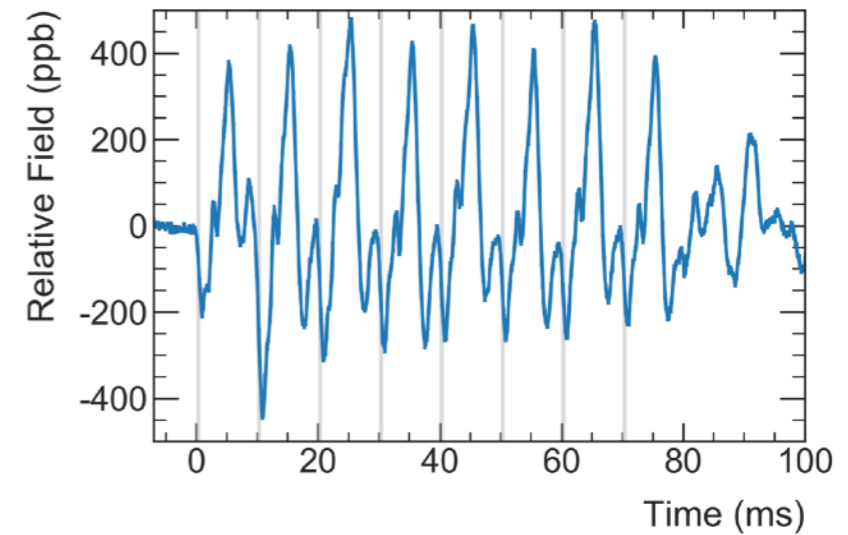
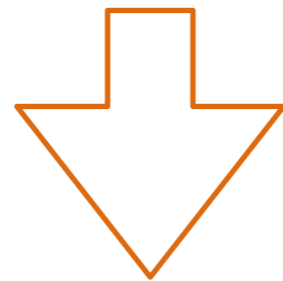
# ESQ Transients

$$a_{\mu} \propto \frac{f_{\text{clock}} \omega_a^m (1 + C_e + C_p + C_{ml} + C_{pa})}{f_{\text{calib}} \langle \omega'_p(x, y, \phi) \times M(x, y, \phi) \rangle (1 + B_k + B_q)}$$

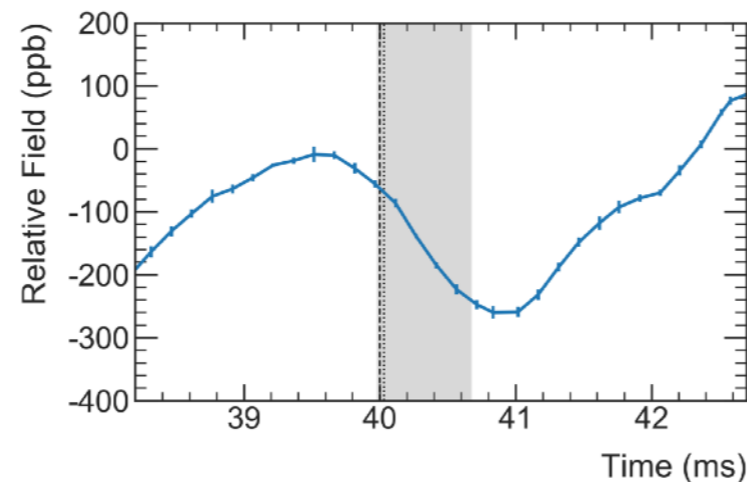
Quads charging and discharging cause mechanical vibration



Field Perturbation



Measure the field with special NMR probes and map the effect!



# E-field and Pitch Correction

$$a_\mu \propto \frac{f_{\text{clock}} \omega_a^m (1 + C_e + C_p + C_{ml} + C_{pa})}{f_{\text{calib}} \langle \omega'_p(x, y, \phi) \times M(x, y, \phi) \rangle (1 + B_k + B_q)}$$

$$\vec{\omega}_a = \frac{e}{m} \left[ a_\mu \vec{B} - a_\mu \frac{\gamma}{\gamma+1} (\vec{\beta} \cdot \vec{B}) \vec{\beta} - \left( a_\mu - \frac{1}{\gamma^2-1} \right) \vec{\beta} \times \vec{E} \right]$$



# E-field and Pitch Correction

$$a_\mu \propto \frac{f_{\text{clock}} \omega_a^m (1 + C_e + C_p + C_{ml} + C_{pa})}{f_{\text{calib}} \langle \omega'_p(x, y, \phi) \times M(x, y, \phi) \rangle (1 + B_k + B_q)}$$

Not all of the muons are at magic momentum!

There is a 0.5% momentum acceptance

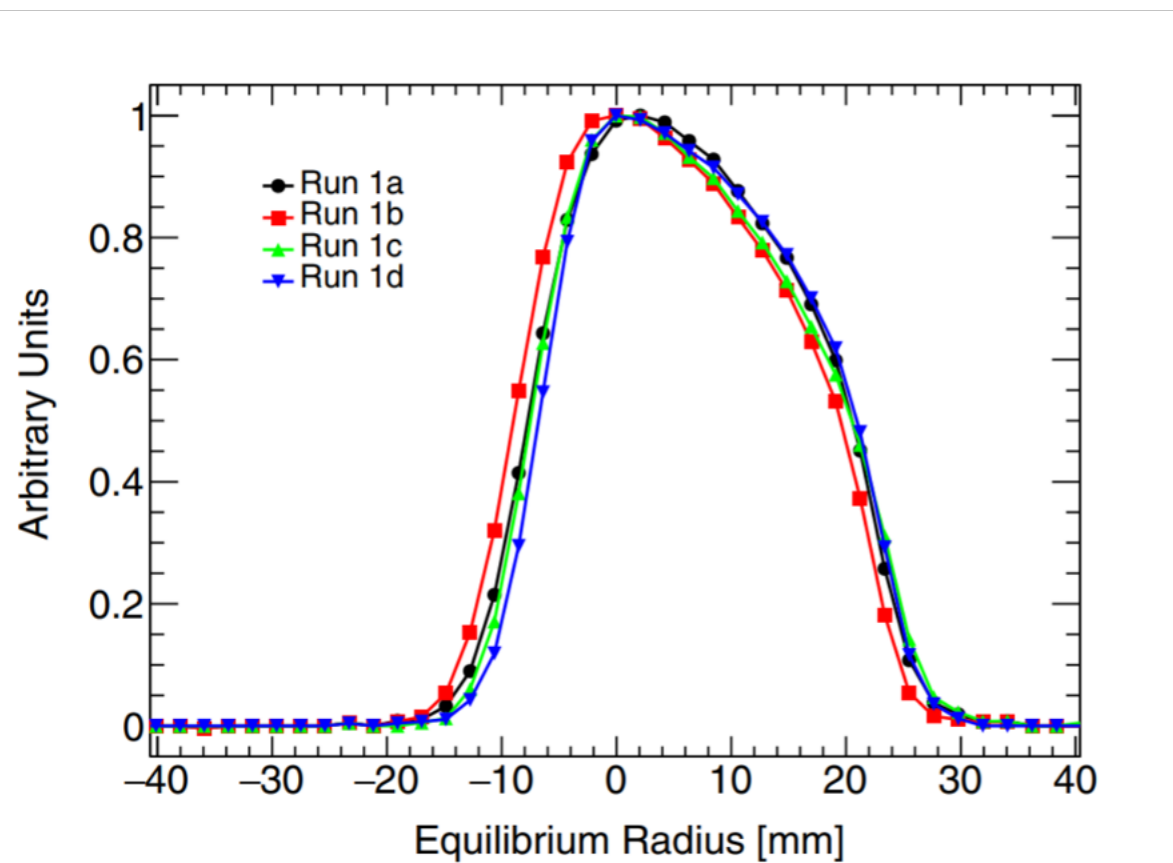
$$\vec{\omega}_a = \frac{e}{m} \left[ a_\mu \vec{B} - a_\mu \frac{\gamma}{\gamma+1} (\vec{\beta} \cdot \vec{B}) \vec{\beta} - \left( a_\mu - \frac{1}{\gamma^2-1} \right) \vec{\beta} \times \vec{E} \right]$$

# E-field and Pitch Correction

$$a_\mu \propto \frac{f_{\text{clock}} \omega_a^m (1 + C_e + C_p + C_{ml} + C_{pa})}{f_{\text{calib}} \langle \omega'_p(x, y, \phi) \times M(x, y, \phi) \rangle (1 + B_k + B_q)}$$

Not all of the muons are at magic momentum!  
There is a 0.5% momentum acceptance

$$\vec{\omega}_a = \frac{e}{m} \left[ a_\mu \vec{B} - a_\mu \frac{\gamma}{\gamma+1} (\vec{\beta} \cdot \vec{B}) \vec{\beta} - \left( a_\mu - \frac{1}{\gamma^2-1} \right) \vec{\beta} \times \vec{E} \right]$$

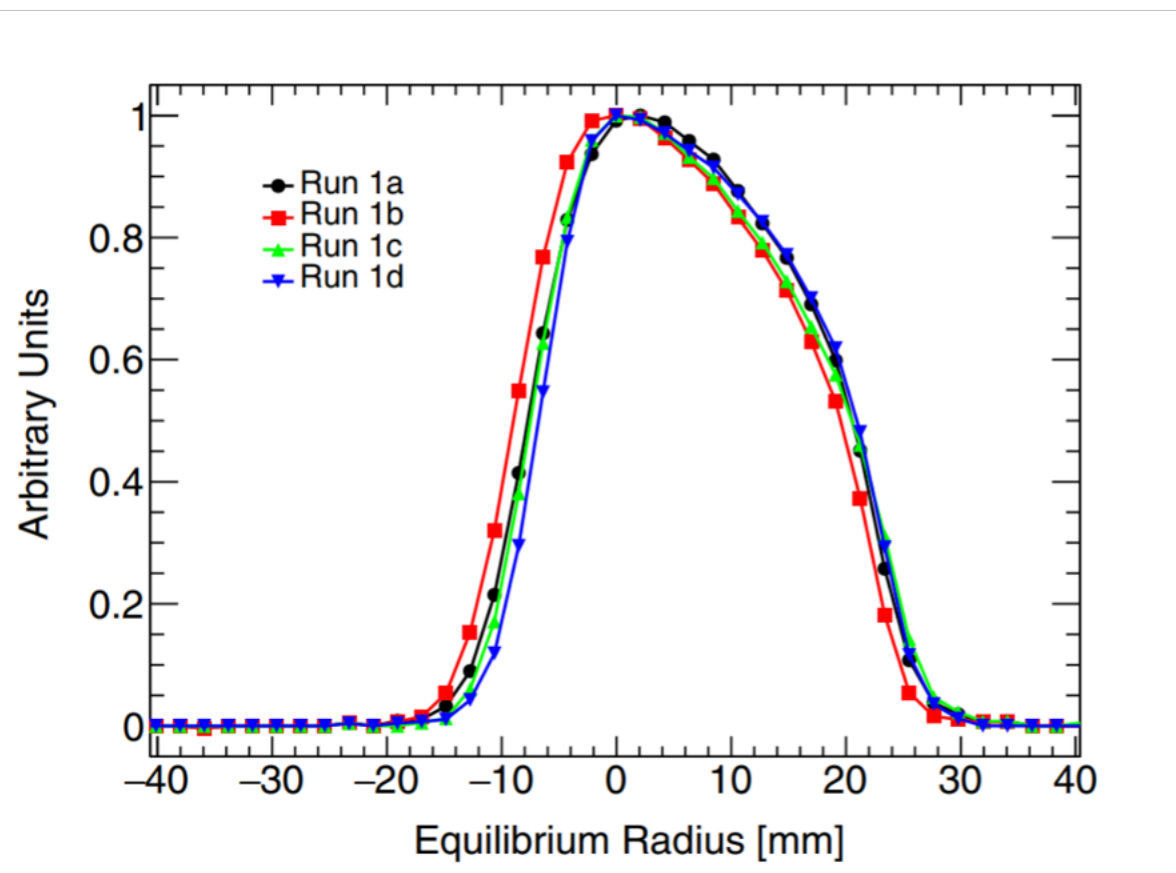


# E-field and Pitch Correction

$$a_\mu \propto \frac{f_{\text{clock}} \omega_a^m (1 + C_e + C_p + C_{ml} + C_{pa})}{f_{\text{calib}} \langle \omega'_p(x, y, \phi) \times M(x, y, \phi) \rangle (1 + B_k + B_q)}$$

Not all of the muons are at magic momentum!  
There is a 0.5% momentum acceptance

~~$$\vec{\omega}_a = \frac{e}{m} \left[ a_\mu \vec{B} - a_\mu \frac{\gamma}{\gamma+1} (\vec{\beta} \cdot \vec{B}) \vec{\beta} - \left( a_\mu - \frac{1}{\gamma^2-1} \right) \vec{\beta} \times \vec{E} \right]$$~~



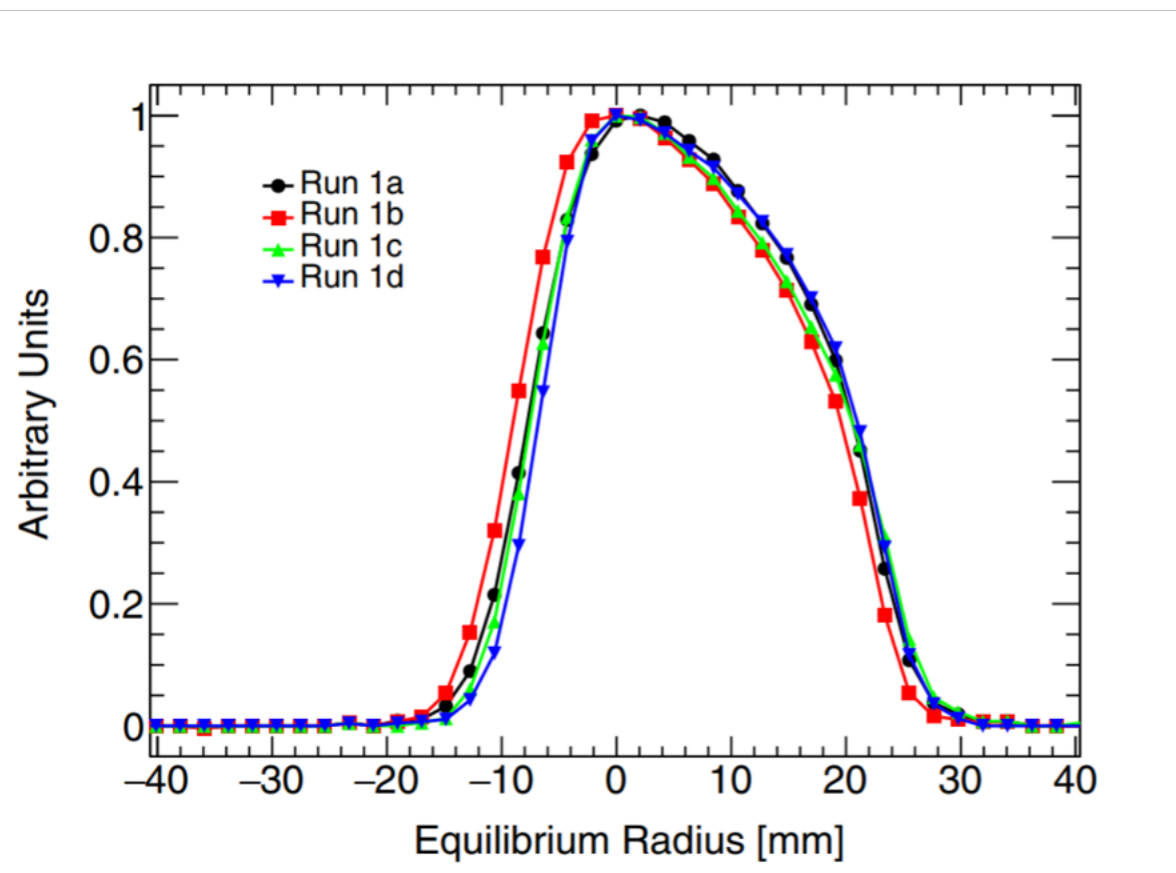
Vertical betatron oscillations cause non-zero average value for  $\vec{\beta} \cdot \vec{B}$

# E-field and Pitch Correction

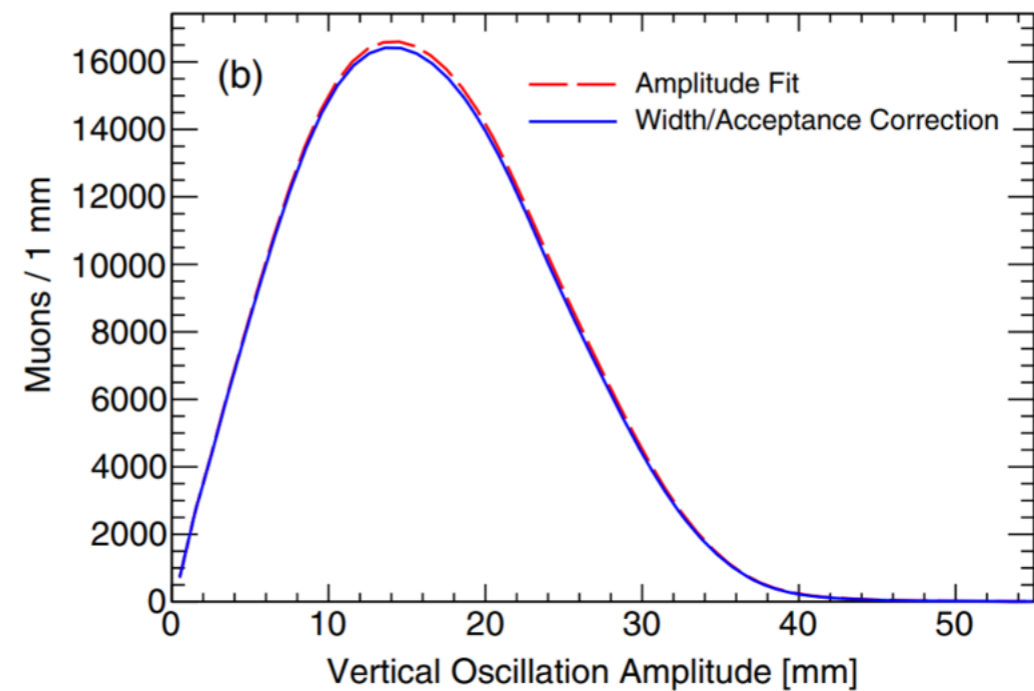
$$a_\mu \propto \frac{f_{\text{clock}} \omega_a^m (1 + C_e + C_p + C_{ml} + C_{pa})}{f_{\text{calib}} \langle \omega'_p(x, y, \phi) \times M(x, y, \phi) \rangle (1 + B_k + B_q)}$$

Not all of the muons are at magic momentum!  
There is a 0.5% momentum acceptance

~~$$\vec{\omega}_a = \frac{e}{m} \left[ a_\mu \vec{B} - a_\mu \frac{\gamma}{\gamma + 1} (\vec{\beta} \cdot \vec{B}) \vec{\beta} - \left( a_\mu - \frac{1}{\gamma^2 - 1} \right) \vec{\beta} \times \vec{E} \right]$$~~



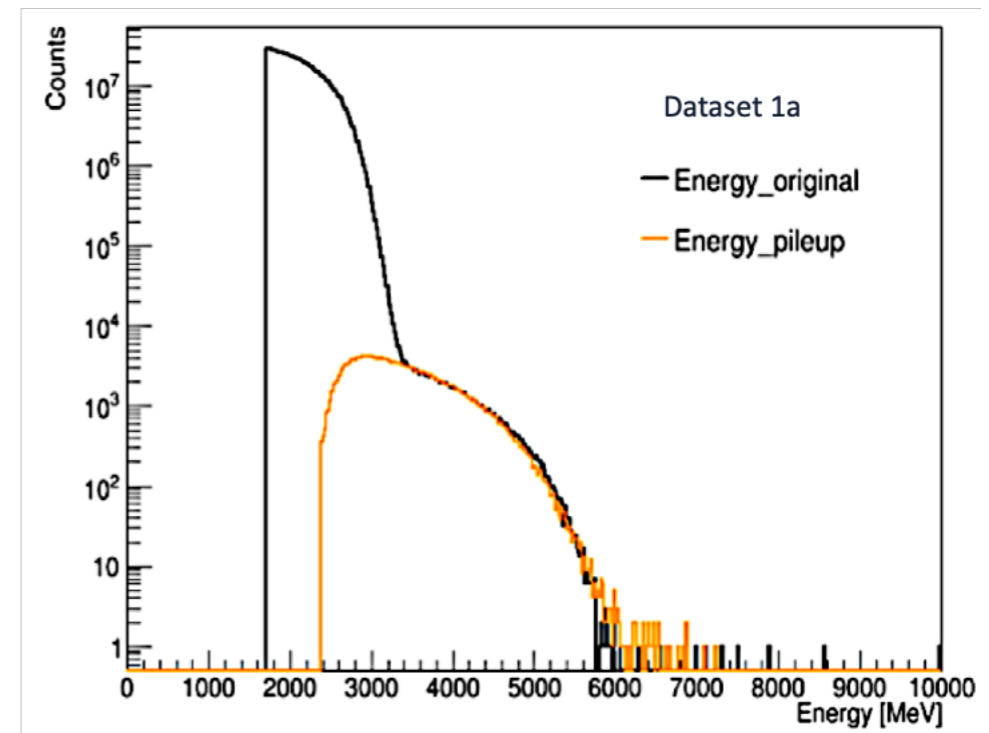
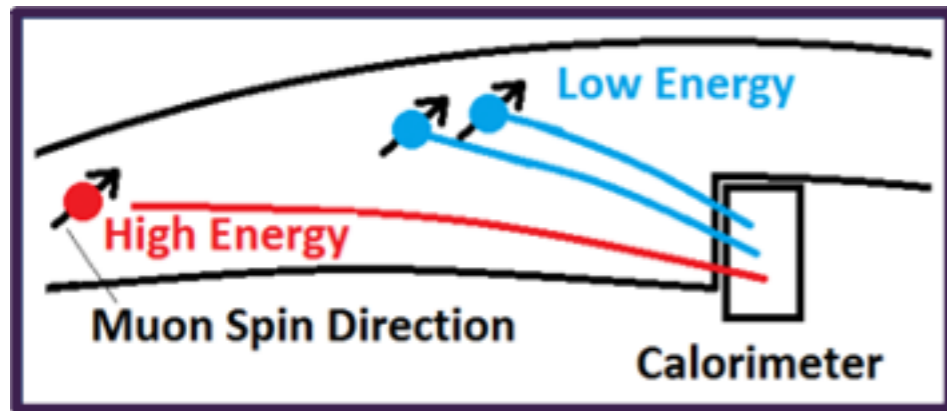
Vertical betatron oscillations cause non-zero average value for  $\vec{\beta} \cdot \vec{B}$



# Pileup

$$a_{\mu} \propto \frac{f_{\text{clock}} \omega_a^m (1 + C_e + C_p + C_{ml} + C_{pa})}{f_{\text{calib}} \langle \omega'_p(x, y, \phi) \times M(x, y, \phi) \rangle (1 + B_k + B_q)}$$

- Pileup is one of the systematics that modulated precession frequency.
- When more than two positrons hit the detector at the same time and place, they could be treated as a single pulse.
- That distorts the time and energy spectrum!



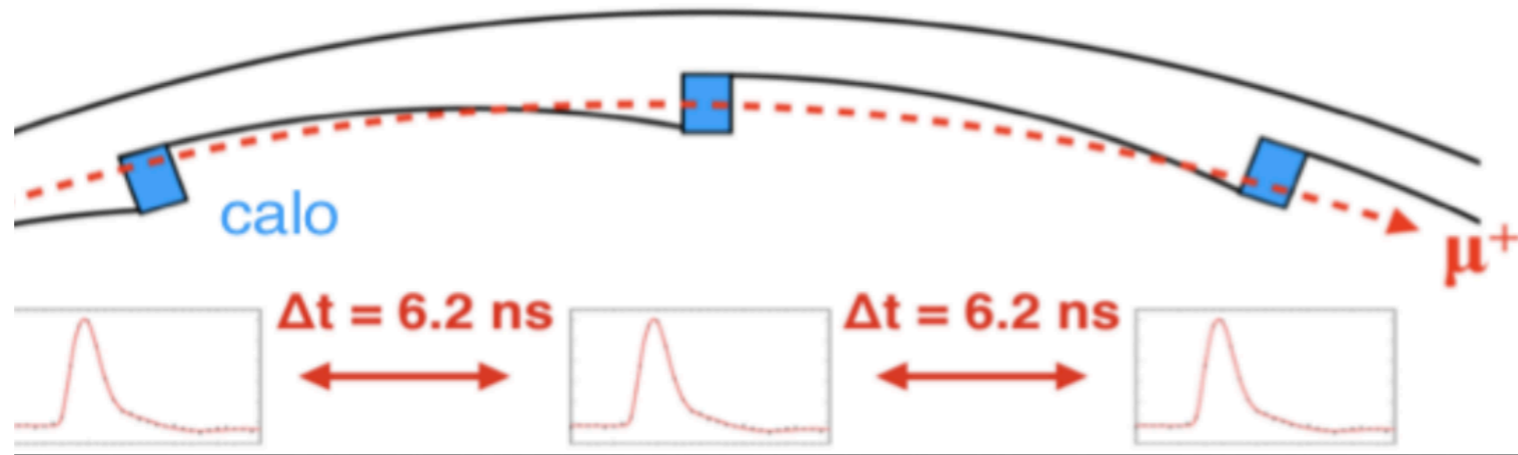
Run-1 data set	1a	1b	1c	1d
Gain changes (ppb)	12	9	9	5
Pileup (ppb)	39	42	35	31
CBO (ppb)	42	49	32	35
Time randomization (ppb)	15	12	9	7
Early-to-late effect (ppb)	21	21	22	10
total systematic uncertainty (ppb)	64	70	54	49

# Muon Loss

$$a_{\mu} \propto \frac{f_{\text{clock}} \omega_a^m (1 + C_e + C_p + C_{ml} + C_{pa})}{f_{\text{calib}} \langle \omega'_p(x, y, \phi) \times M(x, y, \phi) \rangle (1 + B_k + B_q)}$$

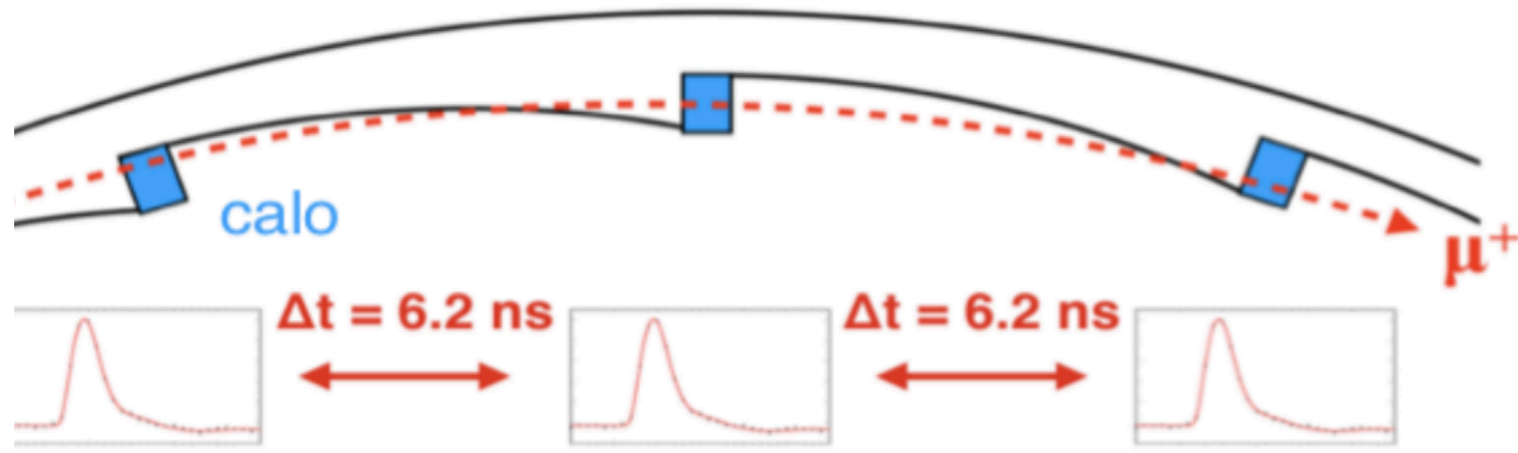
# Muon Loss

$$a_{\mu} \propto \frac{f_{\text{clock}} \omega_a^m (1 + C_e + C_p + C_{ml} + C_{pa})}{f_{\text{calib}} \langle \omega'_p(x, y, \phi) \times M(x, y, \phi) \rangle (1 + B_k + B_q)}$$



# Muon Loss

$$a_{\mu} \propto \frac{f_{\text{clock}} \omega_a^m (1 + C_e + C_p + C_{ml} + C_{pa})}{f_{\text{calib}} \langle \omega'_p(x, y, \phi) \times M(x, y, \phi) \rangle (1 + B_k + B_q)}$$

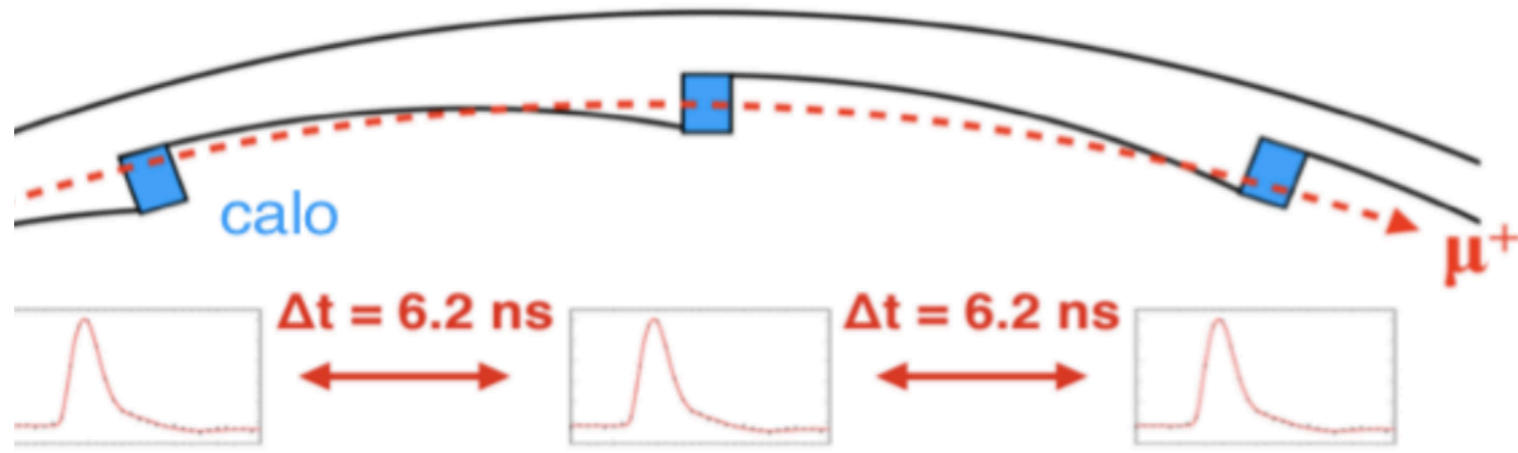


- Muons that were scattered from different materials before decaying and then punch through multiple calorimeters.
- They have different phase than stored muons so they modulate  $\omega_a$ , producing a systematic error.
- We need to identify them in the data!

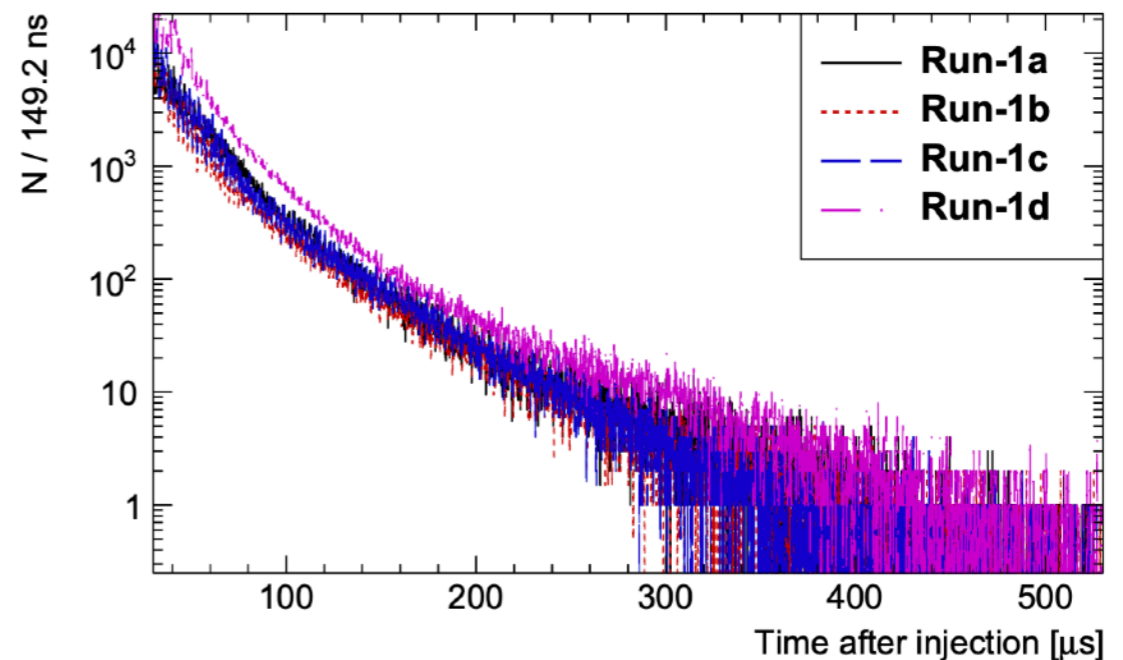


# Muon Loss

$$a_{\mu} \propto \frac{f_{\text{clock}} \omega_a^m (1 + C_e + C_p + C_{ml} + C_{pa})}{f_{\text{calib}} \langle \omega'_p(x, y, \phi) \times M(x, y, \phi) \rangle (1 + B_k + B_q)}$$



- Muons that were scattered from different materials before decaying and then punch through multiple calorimeters.
- They have different phase than stored muons so they modulate  $\omega_a$ , producing a systematic error.
- We need to identify them in the data!



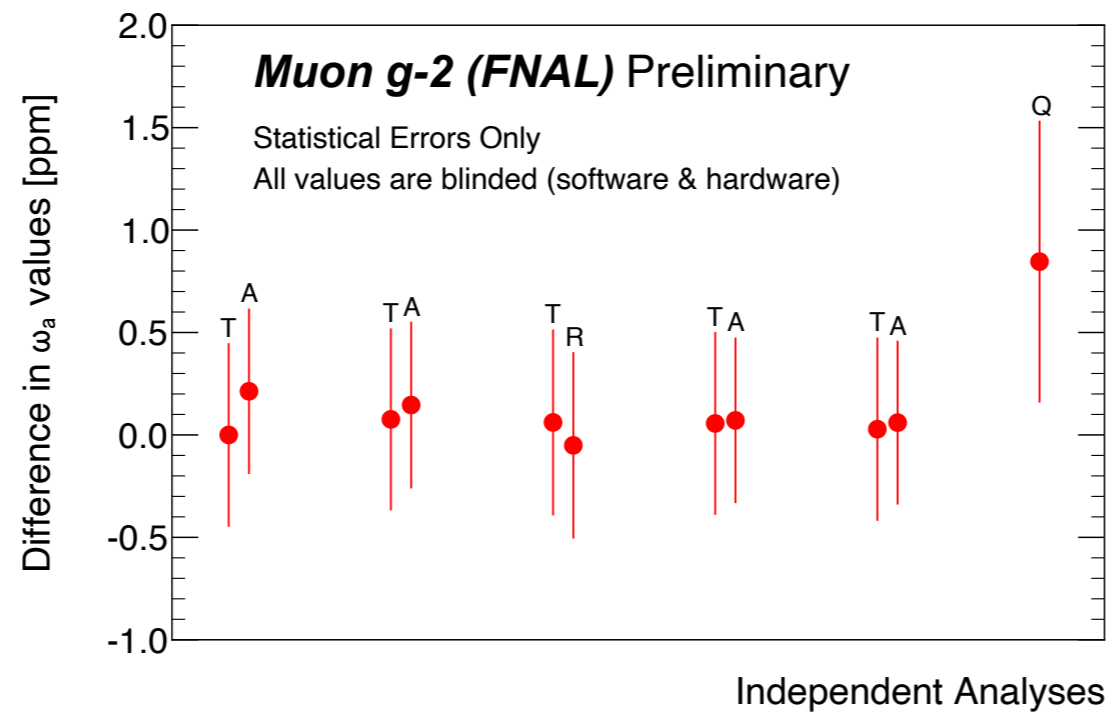
# Calculating $\omega_a$ : Different analysis techniques to reduce systematic errors



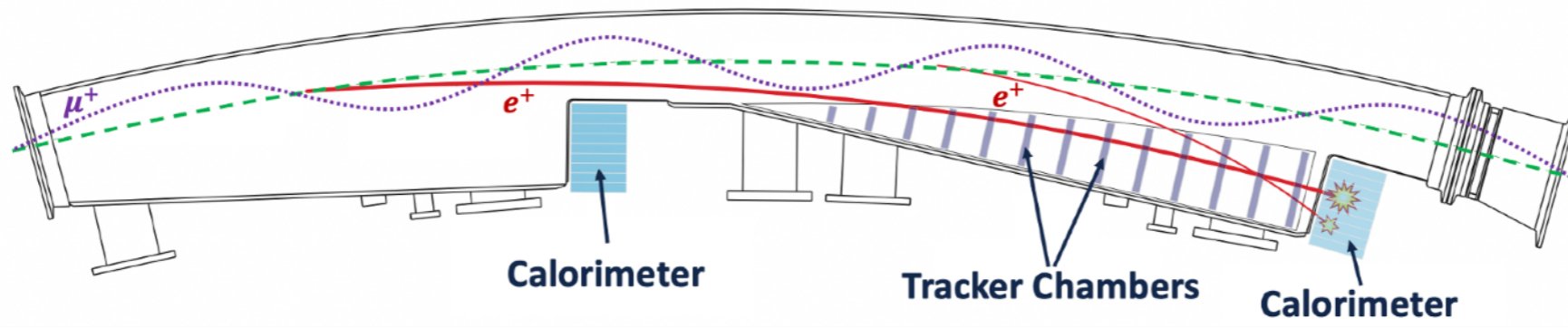
## Fitting Methods

- **T** method:
  - Apply an energy threshold to choose
- **A**symmetry-Weighted Method
  - Apply a smaller energy threshold and weight energy bin by g-2 Asymmetry.
- **R**atio method:
  - Remove the exponential decay of the positron spectrum by sorting the positron time spectra into four equal subsets and then combining them again.
- **Q**-method:
  - A unique energy integrated method where you use sum over digitizer traces above noise level.

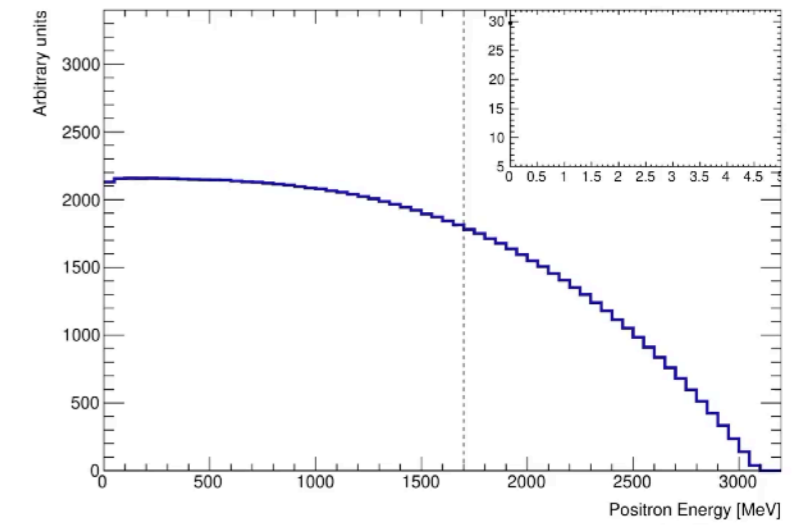
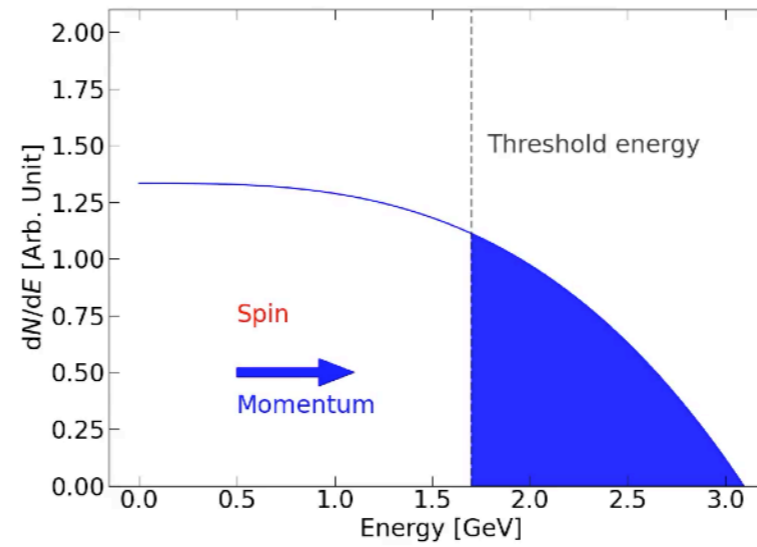
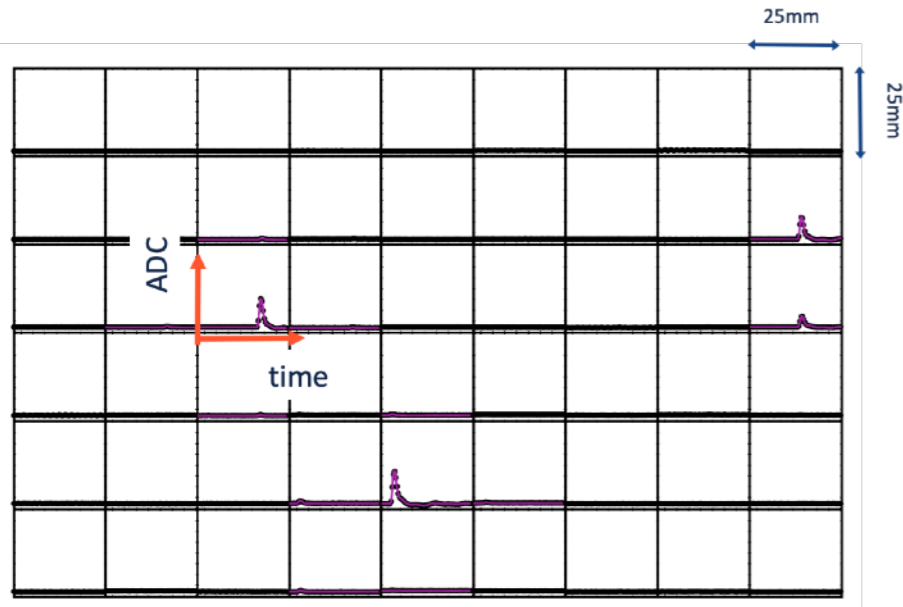
Requires reconstructing the positron time and energy information



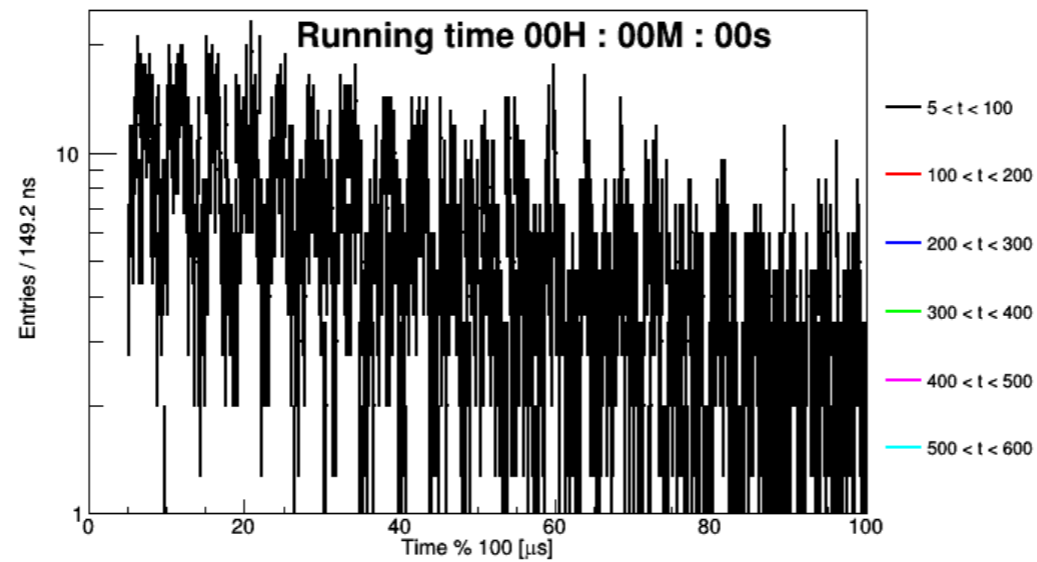
# Calculating $\omega_a$ :



Energy distribution recorded in the calorimeter.

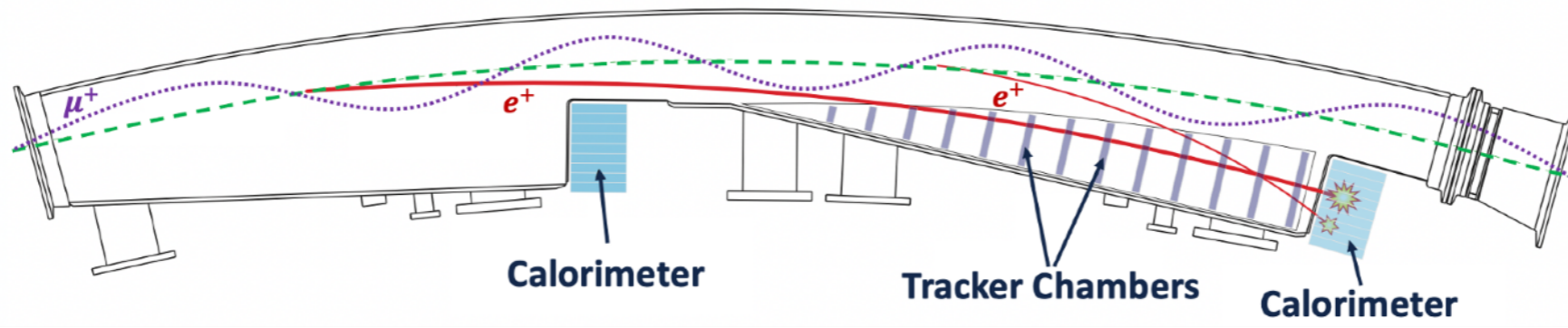


$\omega_a$  blinded by both hardware and software

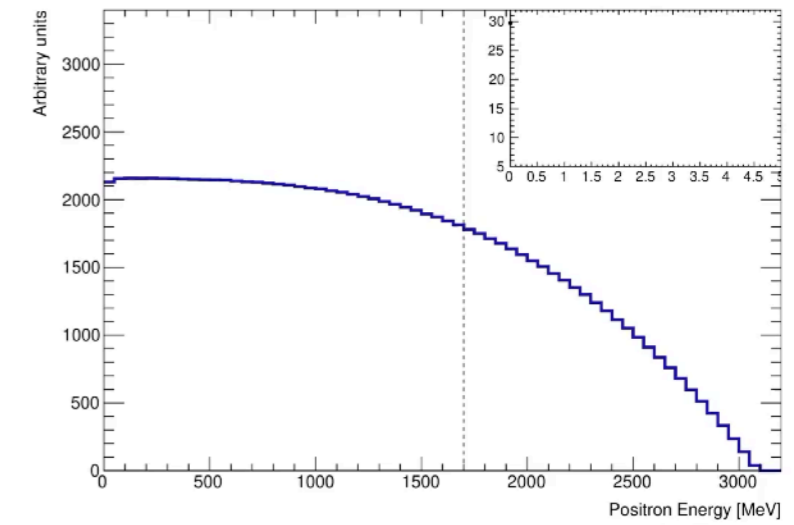
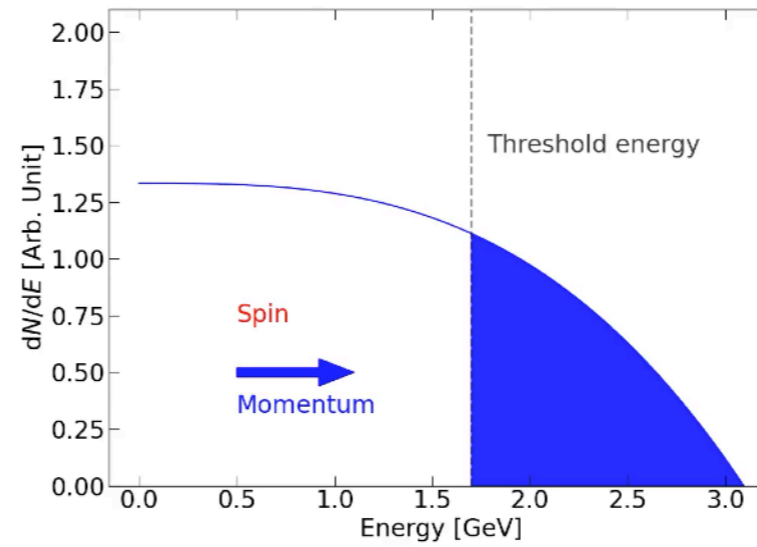
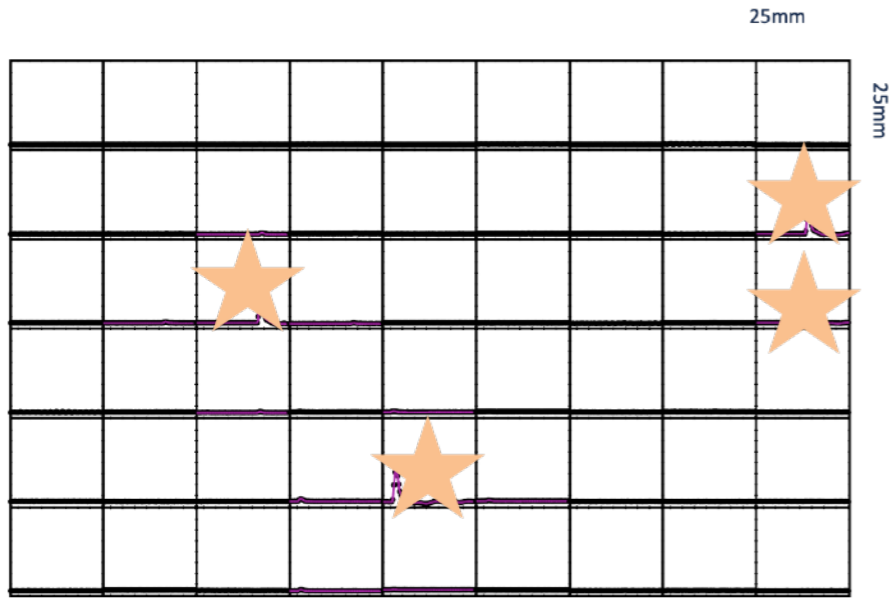


Wiggle plot

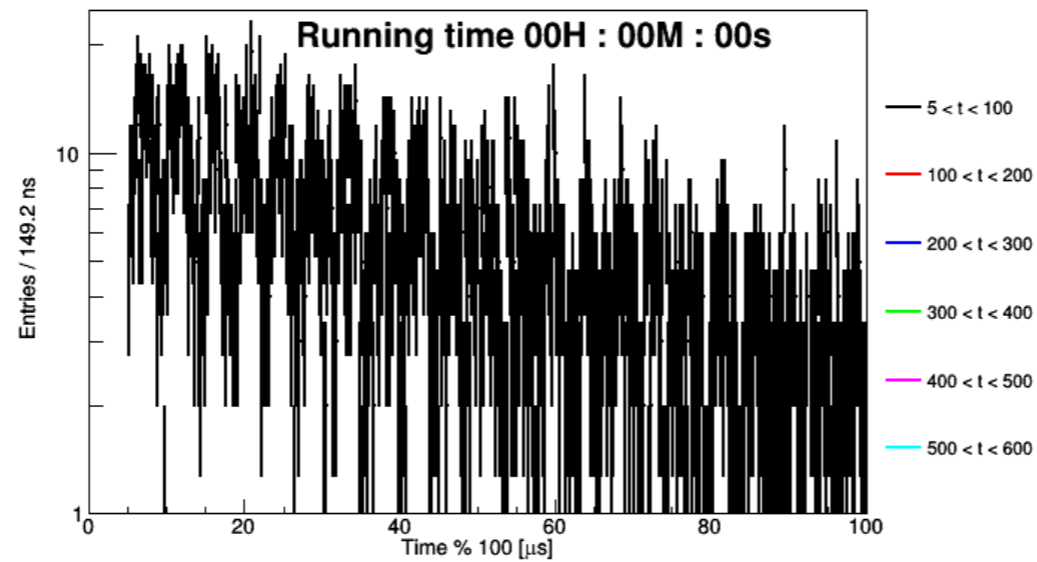
# Calculating $\omega_a$ :



Energy distribution recorded in the calorimeter.

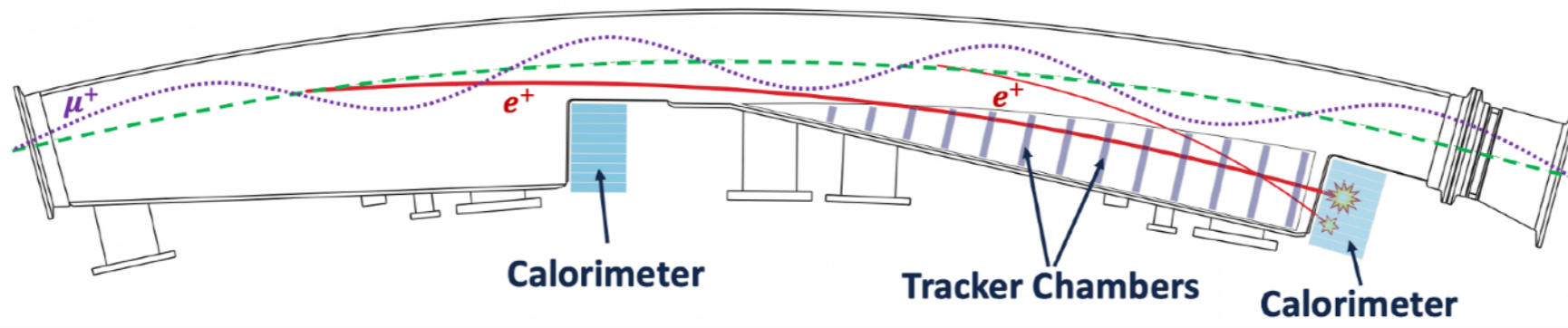


$\omega_a$  blinded by both hardware and software

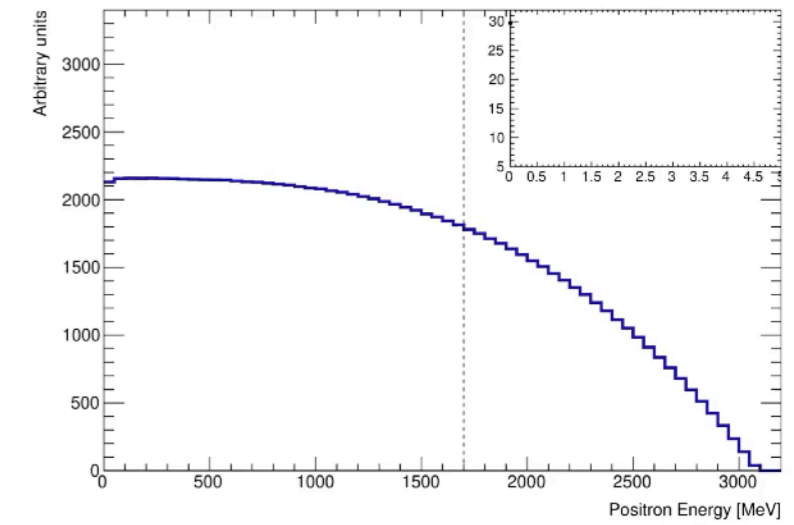
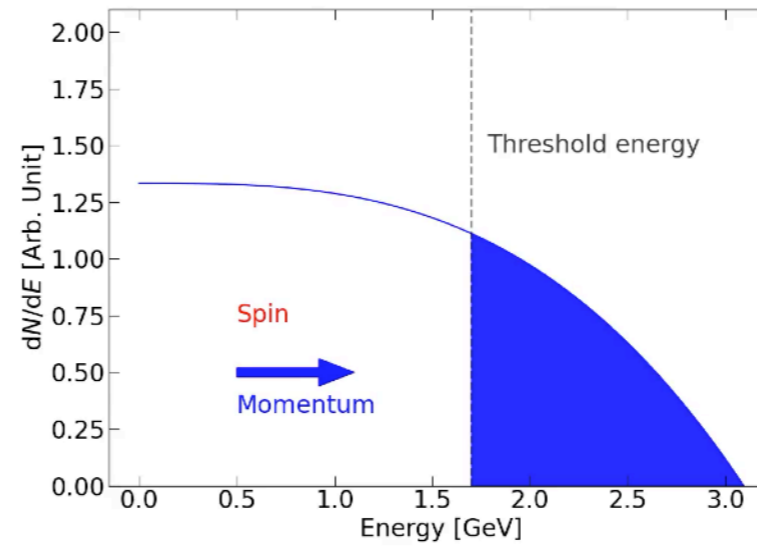
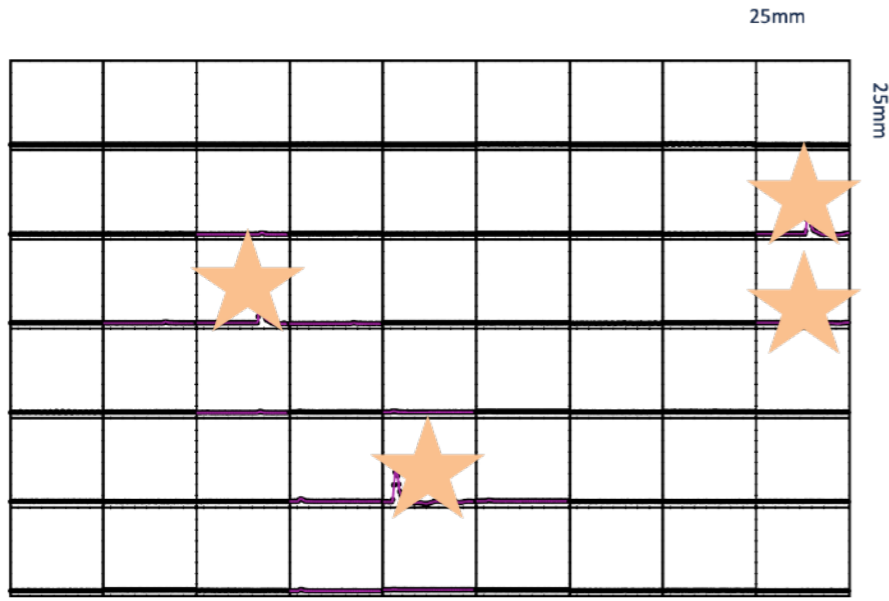


Wobble plot

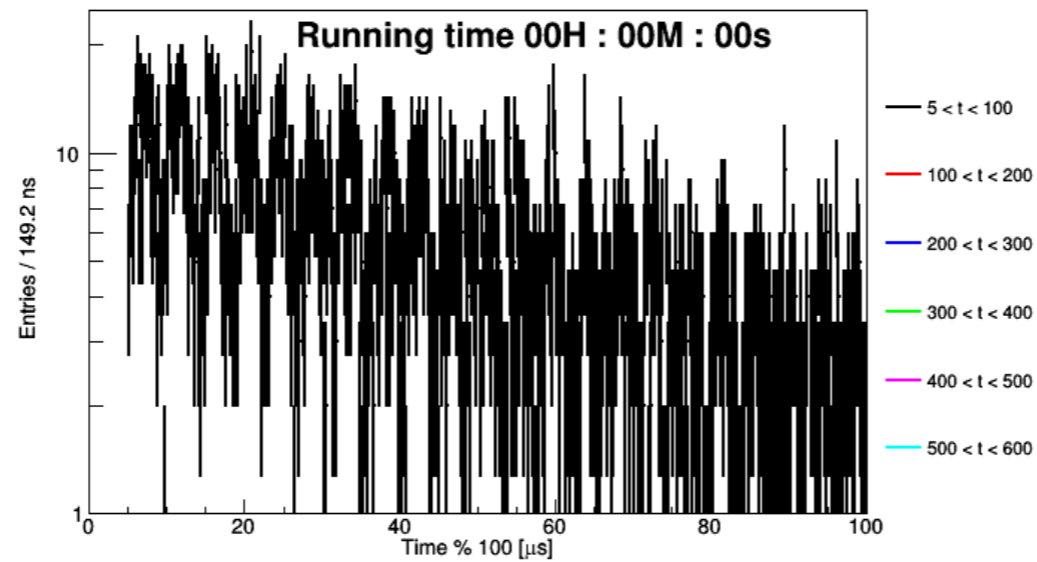
# Calculating $\omega_a$ :



Energy distribution recorded in the calorimeter.

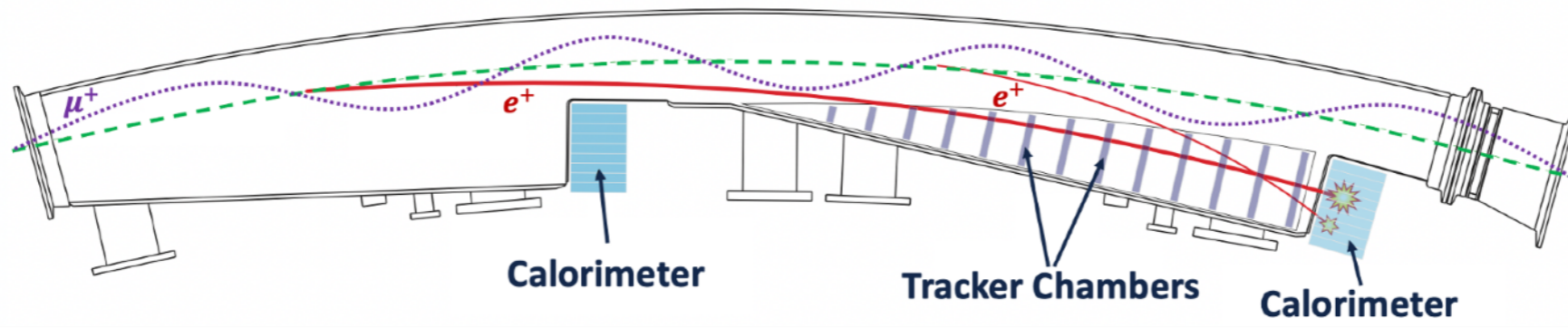


$\omega_a$  blinded by both hardware and software

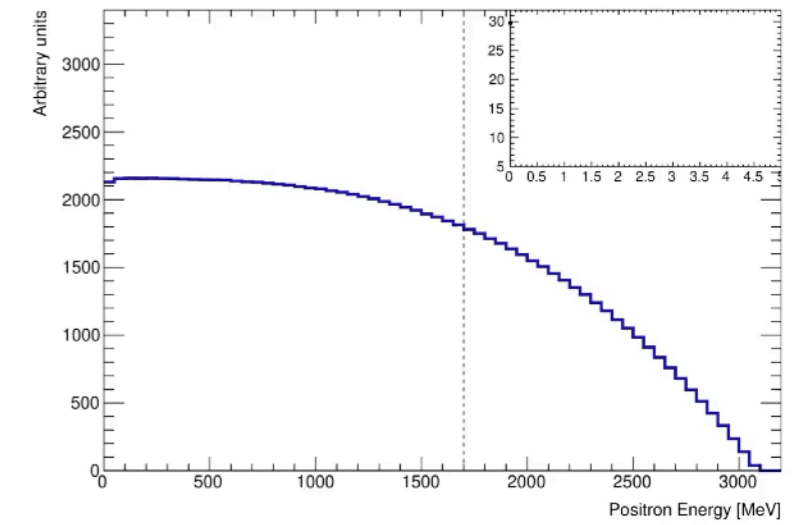
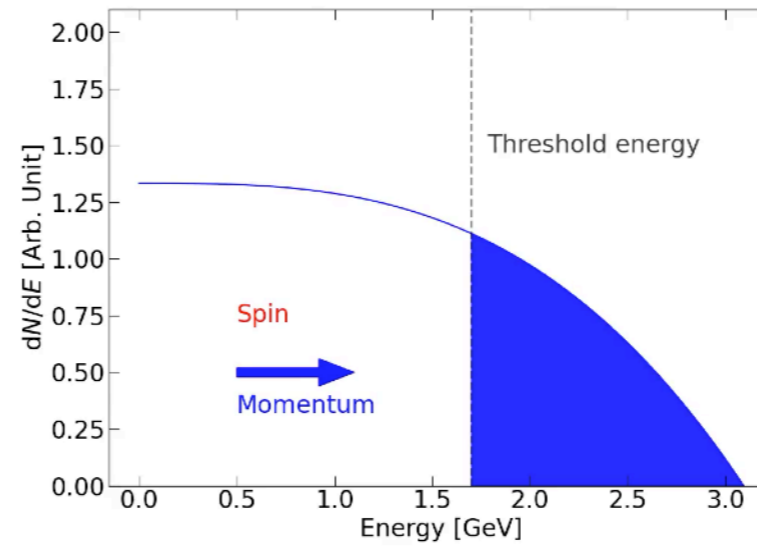
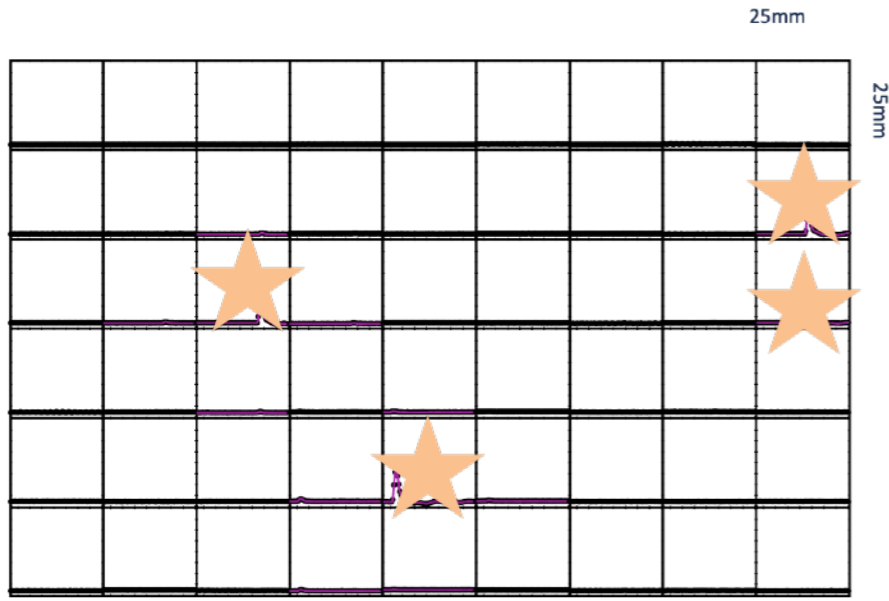


Wiggle plot

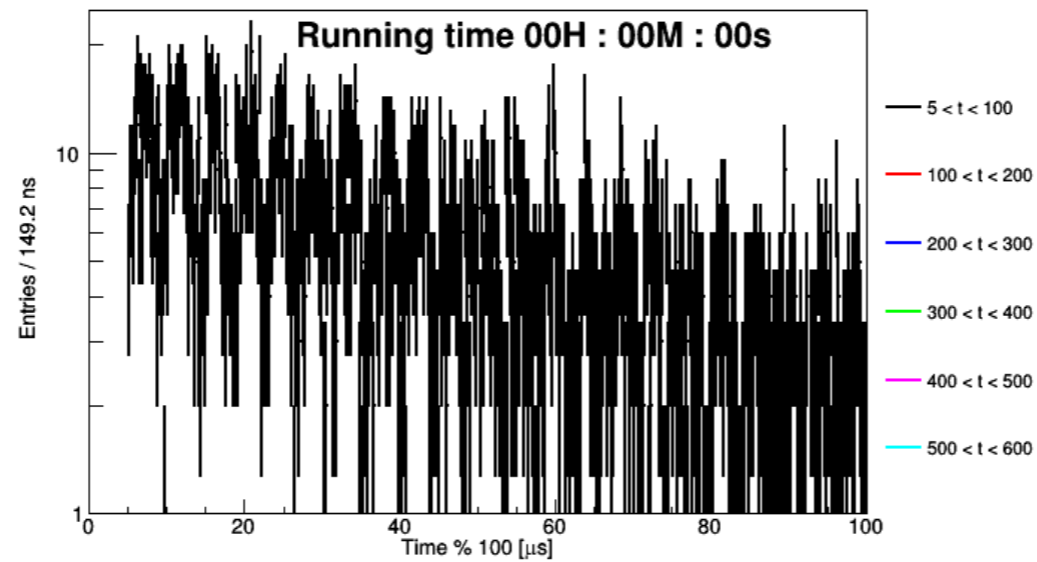
# Calculating $\omega_a$ :



Energy distribution recorded in the calorimeter.



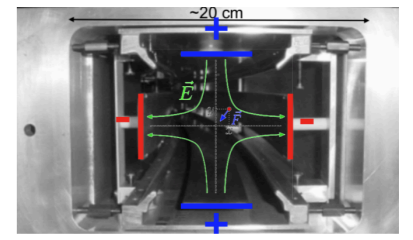
$\omega_a$  blinded by both hardware and software



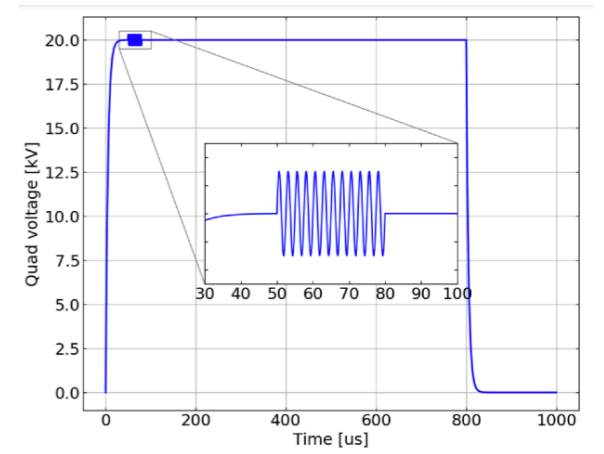
Wobble plot

# RF System Implementation

# RF System Implementation

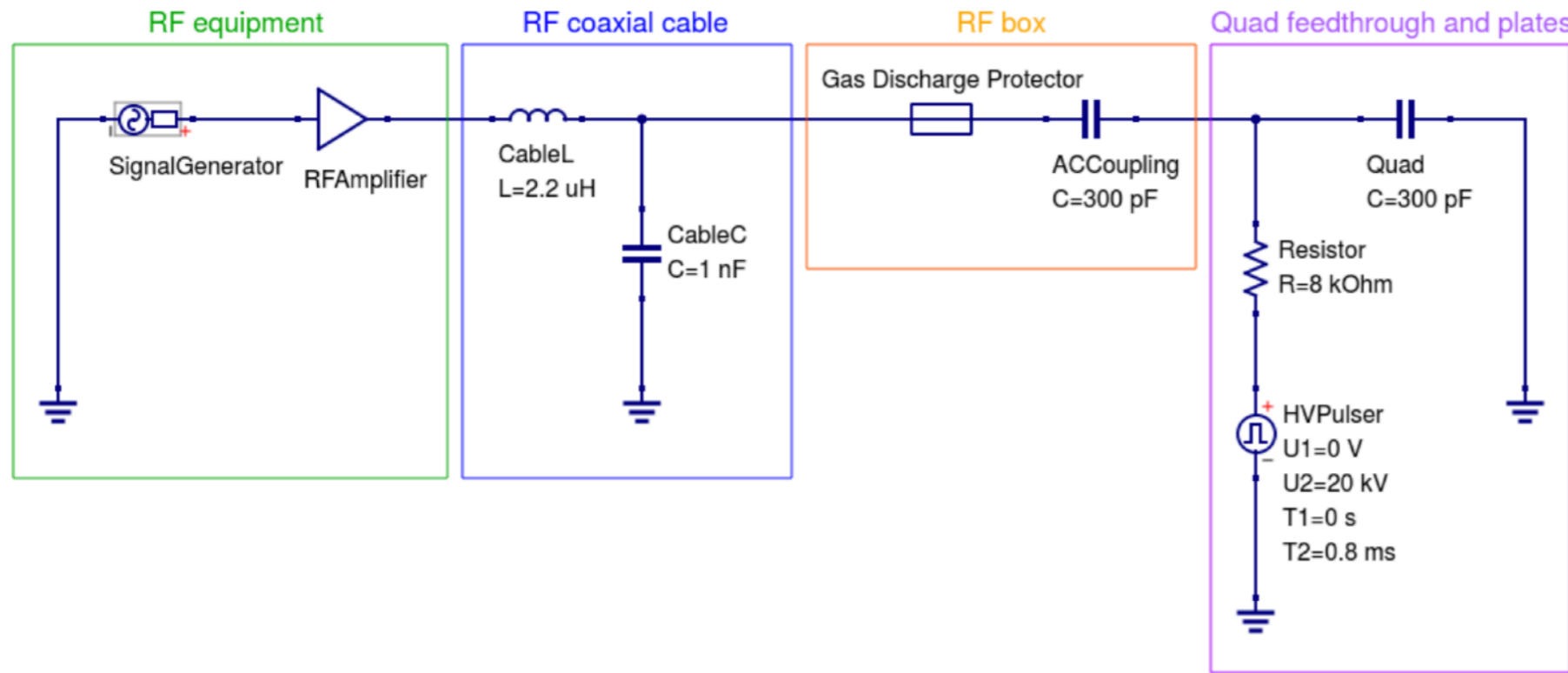
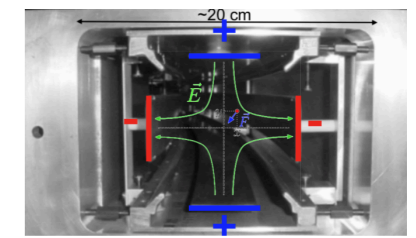


- RF can be applied through the quad plates

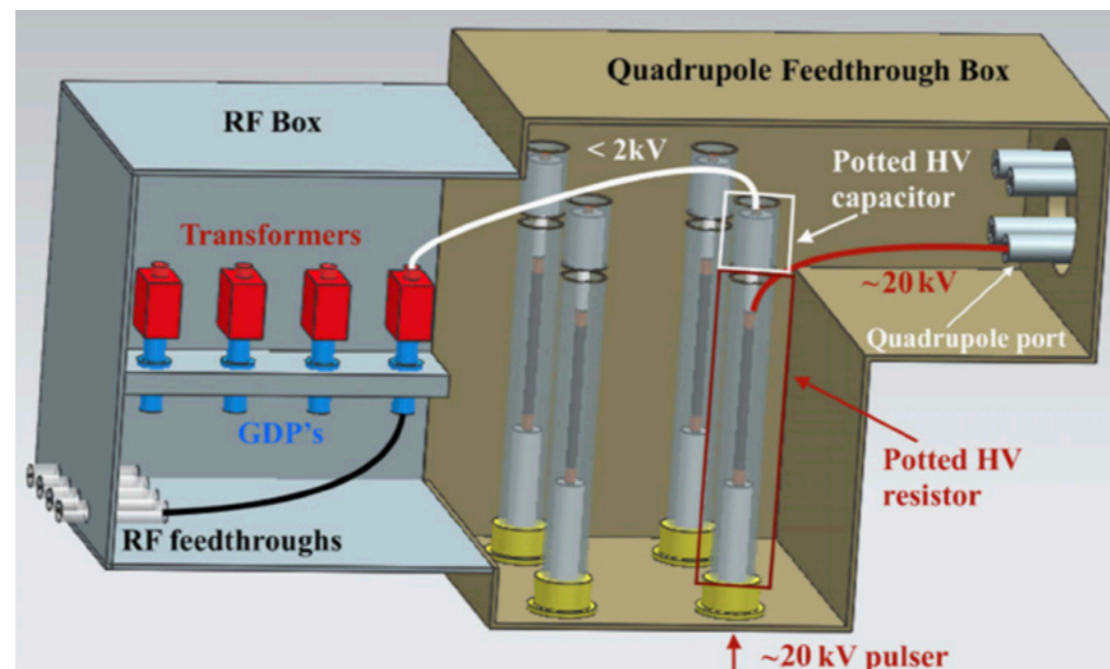
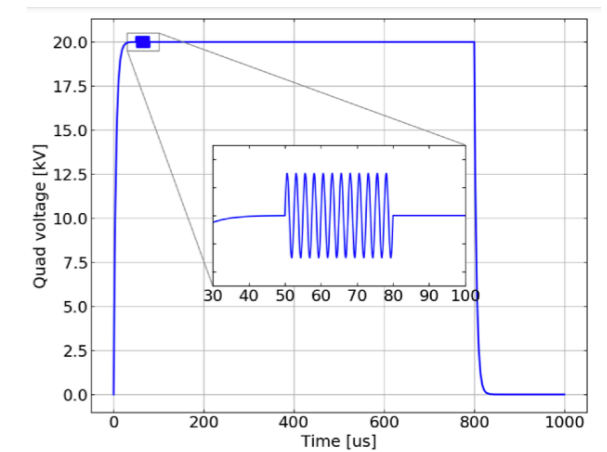




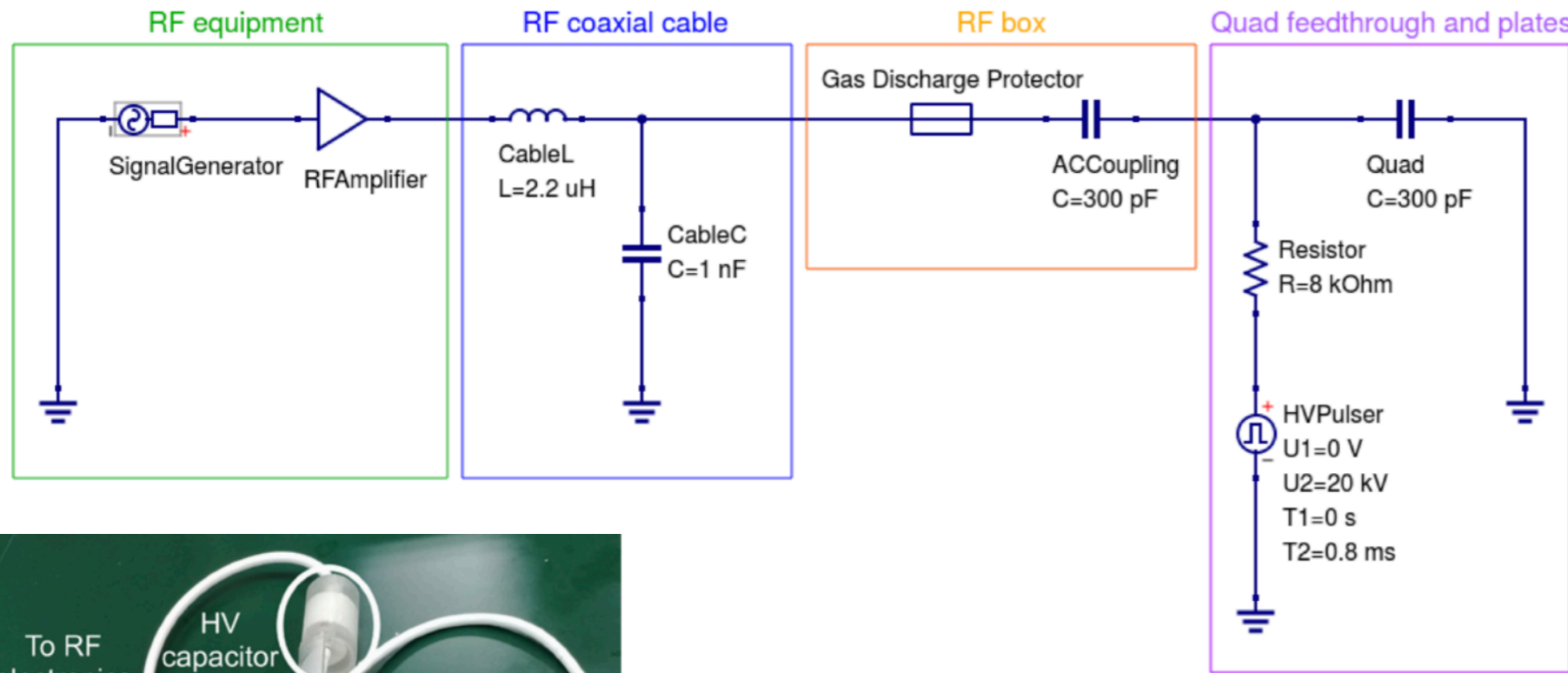
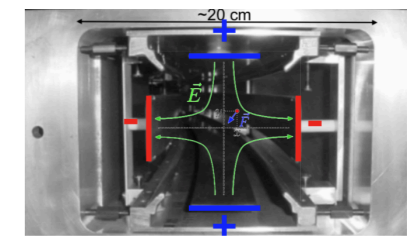
# RF System Implementation



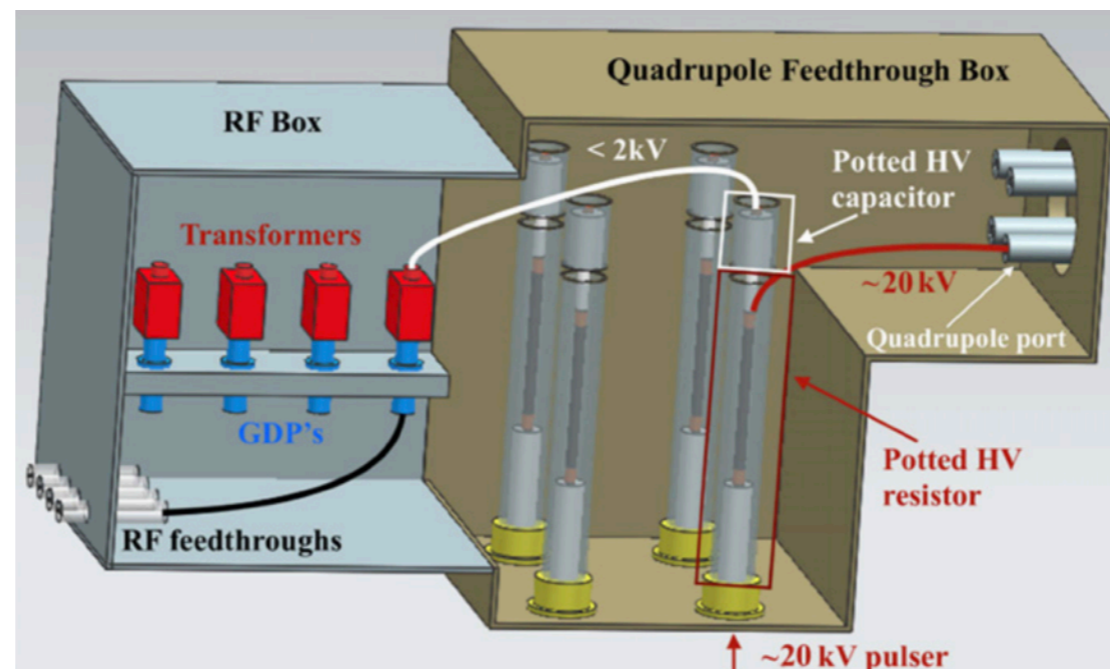
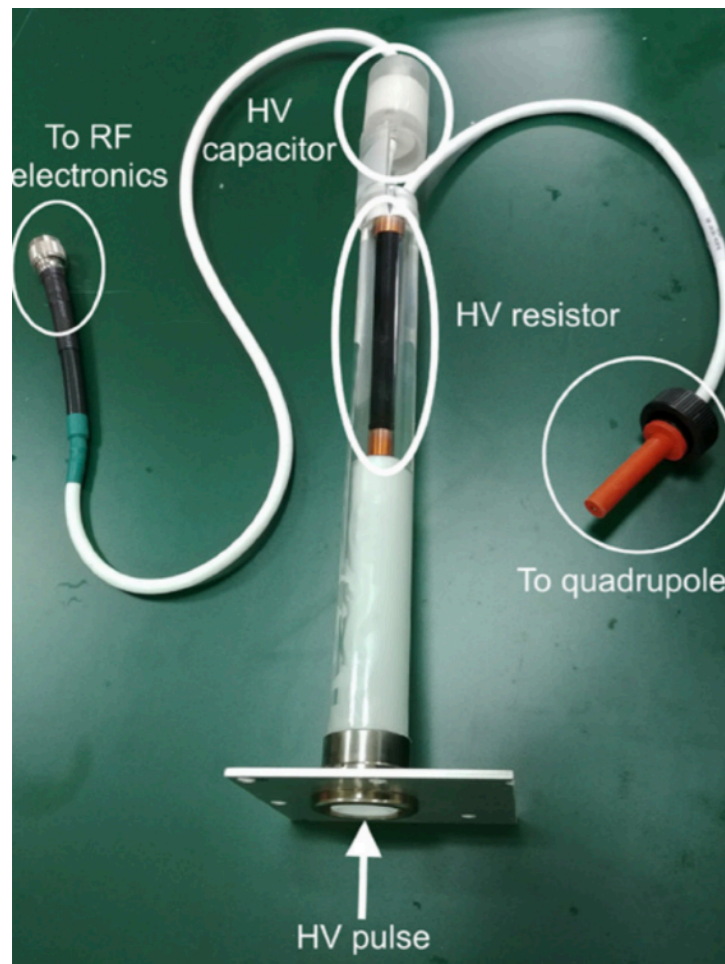
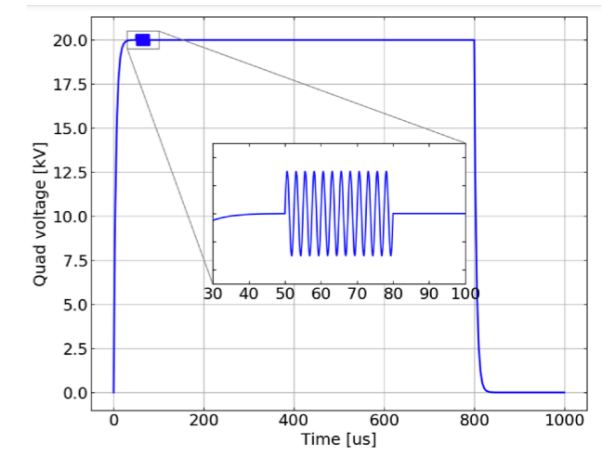
- RF can be applied through the quad plates



# RF System Implementation

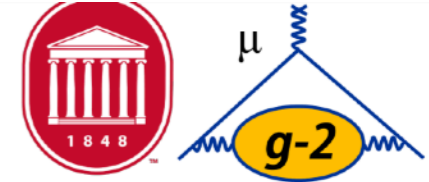


- RF can be applied through the quad plates



# What we gain from negative muon running

## CPTLV: $\mu^+/\mu^- \omega_a$ Difference



- Also note that Muon g-2 with  $\mu^-$  essentially gives you **3** new experimental results here, not just 1!

- What we have:

- BNL ( $\chi = 49.2$ )  $\mu^+/\mu^-$  (700 ppb) & CERN ( $\chi = 43.8$ )  $\mu^+/\mu^-$  (7300 ppb)

$$\Delta \cos \chi = 0.07$$

- What we would get:

- FNAL ( $\chi = 48.2$ )  $\mu^+$  (140 ppb) & BNL  $\mu^-$  (700 ppb)

- FNAL  $\mu^-$  (280 ppb) & BNL  $\mu^+$  (700 ppb)

$$\} \Delta \cos \chi = 0.01$$

- FNAL  $\mu^-$  (280 ppb) & J-PARC ( $\chi = 53.5$ )  $\mu^+$  (450 ppb) - *Dominates*

$$\Delta \cos \chi = 0.07$$

- *Potentially about 15x improvement*

## Comparison of Experiment Parameters

**Table 1.** Comparison of BNL-E821, FNAL-E989, and our experiment.

	BNL-E821	Fermilab-E989	Our experiment ← J-PARC E34
Muon momentum		3.09 GeV/c	300 MeV/c
Lorentz $\gamma$		29.3	3
Polarization	Radius of cyclotron motion: 7.1 m	100%	50% Radius of cyclotron motion: 333 mm
Storage field		$B = 1.45$ T	$B = 3.0$ T
Focusing field		Electric quadrupole	Very weak magnetic
Cyclotron period		149 ns	7.4 ns
Spin precession period		4.37 $\mu$ s	2.11 $\mu$ s
Number of detected $e^+$	$5.0 \times 10^9$	$1.6 \times 10^{11}$	$5.7 \times 10^{11}$
Number of detected $e^-$	$3.6 \times 10^9$	–	–
$a_\mu$ precision (stat.)	460 ppb	100 ppb	450 ppb
(syst.)	280 ppb	100 ppb	<70 ppb
EDM precision (stat.)	$0.2 \times 10^{-19}$ e · cm	–	$1.5 \times 10^{-21}$ e · cm
(syst.)	$0.9 \times 10^{-19}$ e · cm	–	$0.36 \times 10^{-21}$ e · cm

[PTEP 2019 \(2019\), 053C02](#)